MINISTRY OF EDUCATION AND SCIENCE OF UKRAINE

National Mining University

STRESS-STRAIN STATE OF ROCK MASS WHILE MINING FLAT COAL SEAM UNDER PROTECTED OBJECTS

Monograph

Dnipropetrovsk

NMU

2014

УДК 622.831.3:622.834
ББК 33
Н27

Рекомендовано до друку
вченою радою Державного ВНЗ «НГУ»
(протокол № 11 від 27листопада 2013 р.)

Рецензенти:

В.І. Голінько – доктор технічних наук, професор, завідувач кафедри аерології та охорони праці ДВНЗ «Національний гірничий університет» (м. Дніпропетровськ);

М.С. Четверик – доктор технічних наук, професор, завідувач відділу геомеханічних основ технологій розробки родовищ Інституту геотехнічної механіки ім. М.С. Полякова НАН України (м. Дніпропетровськ).

Stress-strain state of rock mass while mining flat coal seam under protected
Н27 objects: monograph/ A.V. Yavorsky, E.A. Yavorskaya, A.G. Koshka, L.A. Tokar, V.P. Serdyuk; Ministry of Education and Science of Ukraine; National Mining University. – D.: NMU, 2014. – 112 p.
ISBN 978-966-350-457-5

The monograph concerns the problems of determining rules of stress-strain state change of two-layer rock mass “washes-carbon” while mining flat coal seam under protected objects by the example of mines in Western Donbass. Rational process parameters of coal seam mining under protected objects are the research result.

The monograph is for engineers, employees of higher educational institutions, research institutes, and engineering companies of coal industry.

Il. 67. Literature reference: 105 titles

УДК 622.831.3:622.834
ББК 33

ISBN 978-966-350-457-5

INTRODUCTION

Coal industry is the key branch for Ukraine as it provides energy independence of the state as well as extraction of valuable raw materials for metallurgy.

Efforts of research teams and production collectives of coal industry are focused on the improvement of technical-economic indicators of the branch. Technical capabilities of domestic mechanized systems of new generation enable to increase significantly load on stopes owing to increase in advance rate; however complicated mining and geological environment and annual increase in mining depth restrain intensification and concentration of mining.

Today, due to heavy investment deficit in the development of Ukrainian mines, reserves under built-up areas and plain floods are progressively involved in mining. For example, about 50% of commercial reserves of Western Donbass productive mines are concentrated under power lines, railway tracks, highways, pipe-lines, and plain floods.

To substantiate methods and parameters of intensive mining providing it without inflicting harm on protected objects one should have clear-cut idea on laws of processes of displacements, deformations, and failure of rocks of mass being undermined. However, lack of adequate data while developing measures to project objects, normative deformation factors of earth's surface, typical for complete undermining are used. In this context, stress-strain state of rocks within a level of a seam under mining as well as parameters of powered support, and a stope advance rate are not considered. Besides, nobody takes into account cap rocks effecting on rate of subsidence and other deformation factors. Rational parameters of powered support and a stope advance rate are identified only basing on analysis of stress-strain state of rocks in the neighbourhood of a stope separately from earth's surface deformation.

As a result, both methods of objects protection and parameters of equipment used often turn out to be ineffective. Hence, it is very important to solve the problem of laws of rock deformation and braking of rock mass being undermined while mining as the problem counts for a great deal for coal industry of the country.

The authors highly appreciate invaluable help and advisory support of L.V. Novikova, Doctor of Engineering Science, Professor of Higher Mathematics and L.I. Zaslavskaya, Senior Lecturer, and colleagues from the Departments of Underground Mining, Mine Surveying, Construction and Rock Mechanics of the National Mining University for their valuable help and comments which have been taken into consideration in the process of working upon the monograph.

The authors extend thanks to the authorities and employees of mines of "Pavlogradugol"OJSC for their comprehensive aid while running of mine experiments, and providing with required materials.

CHAPTER 1. STATE-OF-THE ART OF FLAT SEAMS MINING UNDER PROTECTED OBJECTS

1.1. Common data

Ukraine is first in Europe on coal reserves. Its total resources are 117.2 billion tons, and 45.8 billion tons are prospected ones. Of all prospected reserves 25 billion tons are in Western Donbass.

Ten mines of "Pavlogradugol"OJSC operate in the region. Area of the deposit share under mining is 600 square km. Its great share is accounted for plain floods, industrial facilities, and civilian objects. Under plain floods of such rivers as the Samara, the Ternovka, and the Malaya Ternovka 186.3 million tons of coal occur, and 412 million tons of coal occur under industrial facilities, and civilian objects [1]. Such settlements as Blagodatnoye, Verbki, Ternovka, Rosishki, Samarskoye etc. are within the zones of undermining. In addition, both highway and Kiev-Donetsk railway are partially located at the territory of mine fields.

Table 1.1 covers information on the objects undermined by mines of "Pavlogradugol"OJSC according to surveying statistics.

Coal formation of Western Donbass is associated with Samara series C_1^3 of Mississippian period [11]. The series thickness reaching 470 m covers 64 coal seams. 15-20 seams with C_1 to C_{12} designations are commercial.

Coal seams which prevailing thickness is 0.5 to 1.0 m are lightly pitching, and they are contiguous. Distance between them varies from 4…6 to 40…50 m. their stratification depth is 50 to 1300 m.

Today mines of Western Donbass apply pillar mining system with double faces, and single ones. As a rule, mining is performed in descending order. Mine faces move from a shaft to mine-field boundaries. A roof id controlled by means of complete runoff. As practice shows, in the process considerable earth's surface caving take place to be rather dangerous for objects protected. To prevent undermining effect there were taken shots to make goaf stowing [2, 3]. However, the practice was not naturalized due to increase in labour intensity, a face deloading, and lack of motivations of mined coal improvement.

Minor deformations of earth's surface took place in the process of augering; however, the approach is less productive than that coal cutting [4, 5]. For the same reason a system of shortwall mining turns out to be inefficient.

That is why prospects in gain in coal yield under the conditions should be connected with fully-mechanized faces, with load increase on mining faces owing to mining equipment of new generation providing significant load increase on mining faces through intensity rise.

Table 1.1

Balance reserves within zones of underground works effect on protected objects of “Pavlogradugol”OJSC, thousand tons

A mine	Balance reserves	Objects protected									Reserves within zones of effect	
		Pits and mine sites	Civic buildings	Industrial buildings	Including		Water bodies		Forest cover	Other objects	Total	Including those in proven pillars
					Railways	Pipelines	Gathering ponds	Plain flood				
Ternovskaya	57874	1388	7386	5585	3160	1705	0	26061	15690	4408	60518	2127
Stepnaya	189380	1630	162	6131	5403	0	0	28575	0	150	36648	3990
Yubineinaia	62535	1060	7439	12821	175	0	5796	0	0	0	27116	1060
Pavlogradskaia	39844	619	2239	7611	4803	1846	4202	11096	7328	1527	34622	2222
Samarskaia	74941	1250	8631	2480	194	101	735	33920	7754	0	54770	1250
Dneprovskaia	108776	1767	924	133	75	56	0	0	0	154	2978	1767
N.a. Geroiev Kosmosa	189494	3994	2500	47528	3054	12992	0	0	1703	14553	70278	3994
Zapadno-Donbasskaia	229778	6191	45584	5298	3377	456	293	45332	0	1721	104419	6191
N.A.Stashkova	48907	1060	12716	4556	1821	2735	208	8264	2478	22483	51765	1060
Blagodatnaia	79354	985	36500	3911	1370	1012	106	23622	4520	317	69961	2531
“Pavlogradugol ”OJSC	1080883	19944	124081	96054	23432	20903	11340	176870	39473	45313	513075	26192

Today mines of Western Donbass apply modern powered domestic equipment of KD-99, KD- 90 and DM with such shearers as KA-80, KA-200, RKU-10, GSH-200, and UKD-300. Products of such companies as "Ostroj" and "TMachinery" (Czech Republic), and Bucyrus DBT (Germany) are being successfully commissioned.

Load increment on stopes as well as on their advance rate is seen. Thus, daily output of face 1049 in "Dneprovskaia" mine equipped with powered system "Ostroj" with MB-410E shearer and CZK-190/800 "TMachinery" conveyer is 2500 tons of coal. In a 161 face of "Stepnaia" mine equipped with plow plant by Bucyrus DBT, maximum daily output was 4500 tons. In this context, advance of stopes are 100-150 meters per month.

Under the conditions of Western Donbass, effect of such advance on rock mass, and on earth's face is not studied. The paper tries to solve the problem analytically and numerically. That will help to substantiate rational parameters of safe mining under protected objects.

Hereafter a face advance rate, and powered support parameters at this or that depth will be considered as rational ones if they provide labour safety in the face as well as coal mining efficiency without protected objects damaging.

When such parameters are identified, mine examination data, and recommendations of branch standards are usually applied [7–9, 13, 14, and 17]. However, possibilities of full-scale investigations are restricted, and normative documents can not reflect in full specific mining and geological conditions. As a result, either environment or protected objects suffer, or coal losses in bowels are inflated, production level decreases, investment expenditures of the enterprise increase, and its return on assets drops.

In this context, analytical decision of rock mechanics problem to have qualitative pattern and quantitative estimations of the whole rock mass stress-strain state as part of parameters of coal mining at any stage becomes important. As a face advance rate affects significantly stress-strain state of undermined mass, roof failing character, and earth's surface displacement process intensity, then its possible increase border should be identified taking into account specific mining and geological conditions, and mining depth.

Mining and geological conditions of Western Donbass have their own specificity. Enclosing rocks are interlaid argillites and aleurolites; arenites are less frequent.

Washes consist of layers of clays, adoles of sandy shale and argillaceous slates, fine sands; sometimes they are limestones and bench gravels. Their total thickness is within 90 - 140 m.

Fig. 1.1 shows stratigraphic column of washes typical for mining and geological conditions under consideration; Fig. 1.2 shows summary lithological column on C_6 and C_6^1 coal seams used to develop computed and theoretical model of rock mass undermined. Table 1.2 shows adequate average characteristics of washes, coal, and enclosing rocks on SNiP (Construction Norms & Regulations) [15] and literature [10, 20].

Physical and mechanical characteristics of washes kept in it correspond to weighed average values according to enclosing rocks seam thickness (Fig. 1.1).

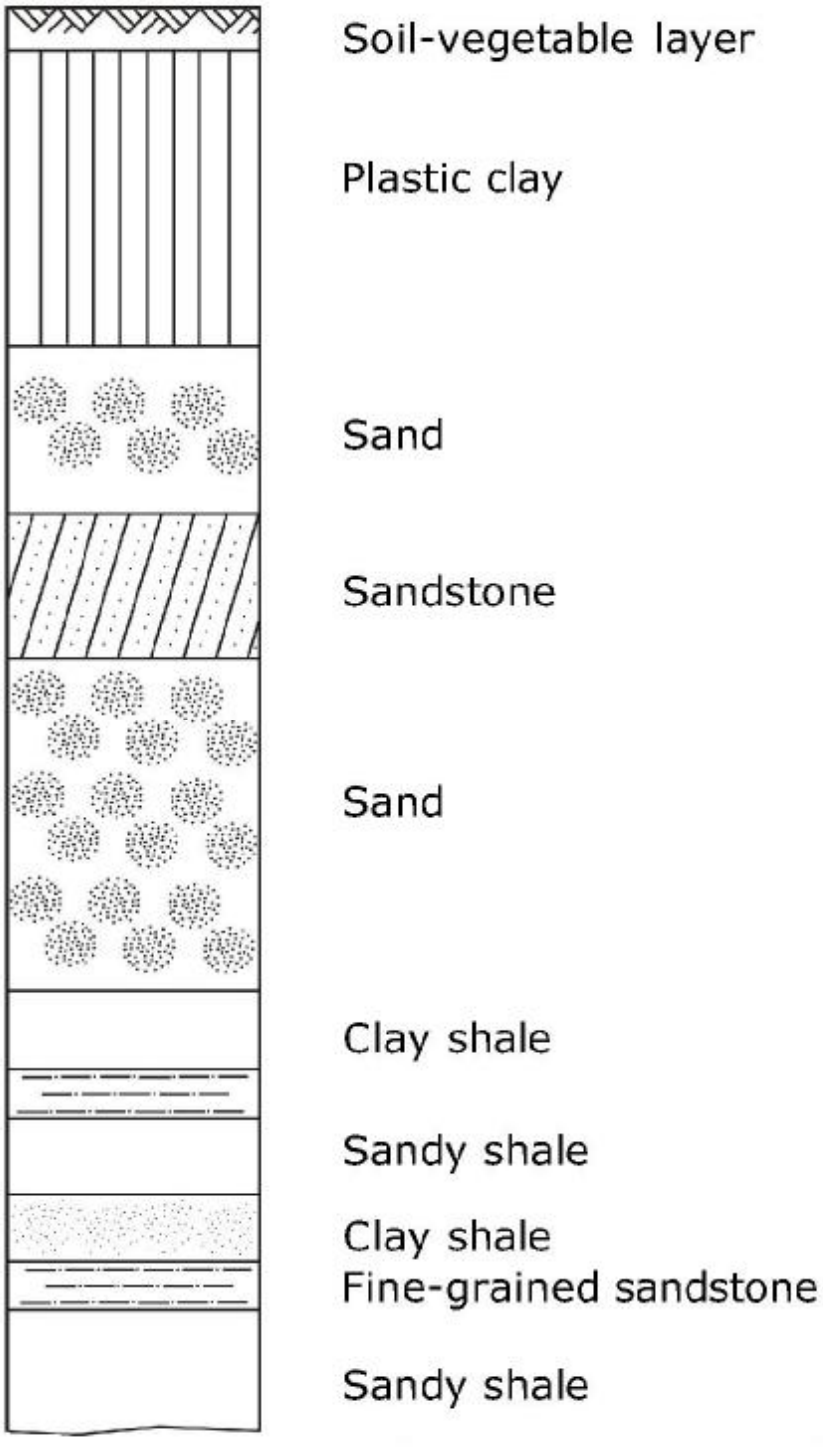

Fig. 1.1.Stratigraphic column of washes typical for mines of Western Donbass

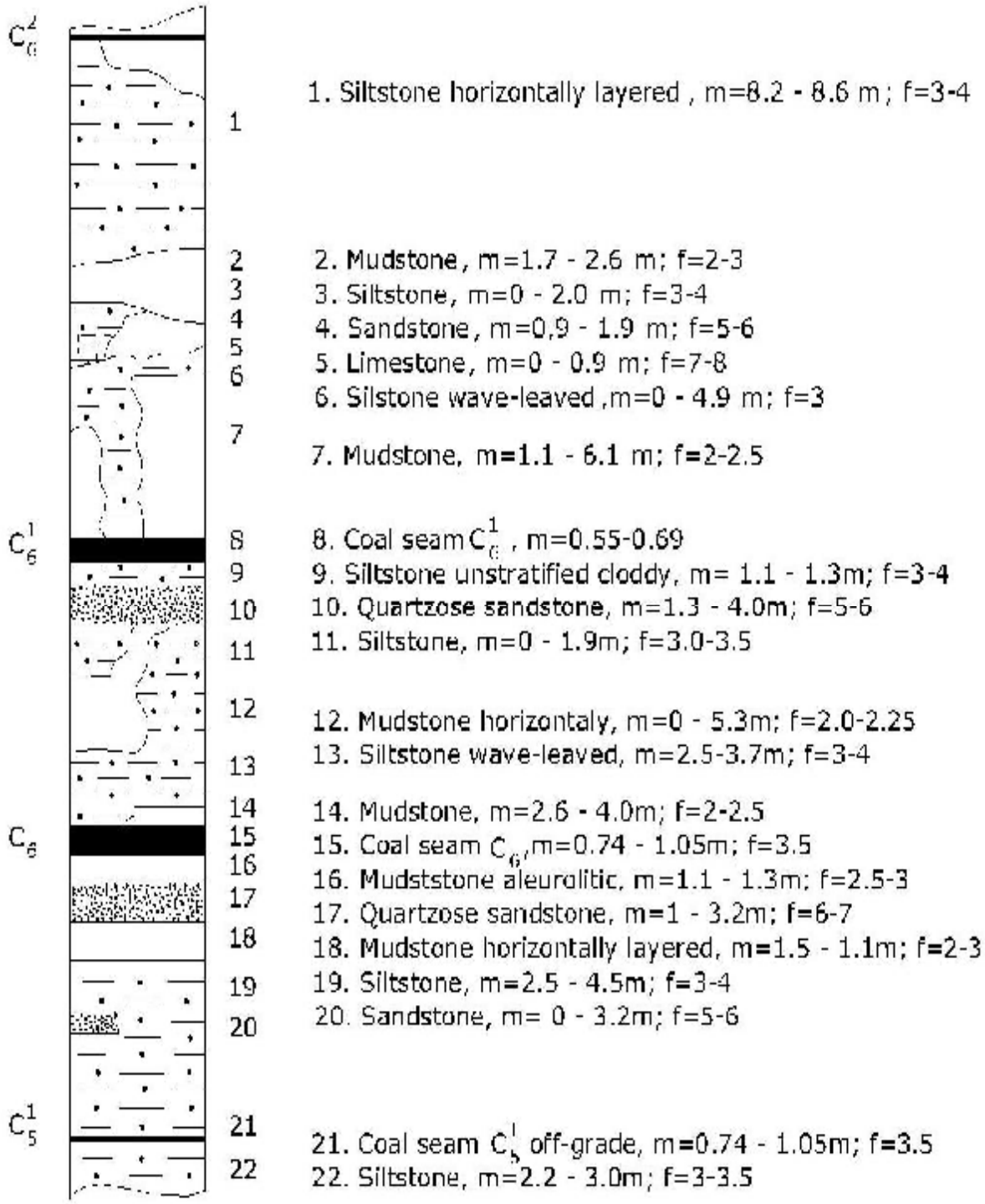

Fig. 1.2. Summary lithological column on C_6 and C_6^1 coal seams

Table 1.2

Rock	Physical and mechanical characteristics			
	σ_c, MPa	γ, tf/m^3	E, MPa	ν
argillites	20	2.65	$2.8 \cdot 10^3$	0.3
aleutites	30	3.0	$2.9 \cdot 10^3$	0.3
sandstone	50	3.1	$2.8 \cdot 10^3$	0.3
limestone	155	2.84	$4.2 \cdot 10^4$	0.3
washes	0.6	1.5	70	0.3
coal	35	1.47	$2 \cdot 10^4$	0.35

As the Table shows, mostly enclosing rocks are less robust than coal. The fact can explain natural soil swelling, and roof rocks running into mine workings [6].

Initially, such hard rocks as sandstone exhibit resistance to displacements; as a result, more or less sizeable spaces with console-hanging rock layers are formed in undermined mass. When worked-out space becomes of certain size, stresses become extreme, falls take place, and deformation process activates. Ultimately, with complete undermining, the latter factors in displacement basin formation. Depending upon rock properties, depth and advance rate of a face, the displacements are more or less intensive. The process is rather long; that's why calculated and theoretical model developing should take into consideration temporal changes in rock properties because such sedimentary rocks as argillites, aleurites, and sandstones having the greatest specific weight in productive stratum of deposits are of pronounced rheological properties. As experiments with the rocks samples show, their rheological properties are even demonstrated when loads are 20…30% of fracture loads and deformation loads are 50…100 % of conditionally transient loads. Moreover, temporal deformation process often takes place in accordance with linear law [20, 88].

On this basis, the work uses a known model of linear congenital environment with creep kernel of Abel type [22].

Deformation law of such environment is:

$$e(t) = \frac{1}{E}\left[s(t) + \int_0^t L(t,t)s(t)dt \right], \qquad (1.1)$$

Where $\varepsilon(t)$ and $s(t)$ are deformation and stress going with considered moment t counting off from initial stress moment; $L(t,t) = d(t-t)^{-a}$ is creep kernel.

Physical and mechanical properties from Table 1.2 are taken as initial data at the research start time while identifying $\varepsilon(t)$ and $s(t)$. Creeping parameters a and d taking into account congenital properties of rocks and coal are taken up according to paper [10] and catalogue [23] data. Values of parameter d are in Table 1.3, and parameter's a value for coal and enclosing rocks is a=0.7, and – 0.862 for washes according to recommendations [16].

Table 1.3

Creeping parameters d for coal and enclosing rocks

Rock	Washes	Sandstone	Aleurite	Argillite	Coal
$d \cdot 10^{-3}, c^{a-1}$	1.39	3.28	5.54	11.7	2.32

In line with a theory of linear and contiguous environment in the process of stress identifying, rock elasticity modules at time t are determined by

$$E_t = \frac{E}{1+\Phi_t}, \tag{1.2}$$

Where E is rock elasticity module on data by Table 1.2;

Φ_t is a creeping function calculated on the $\Phi_t = \frac{d}{1-a} \cdot t^{1-a}$ formula (1.3)

t is time in seconds.

Estimation of stress condition of area under consideration is performed on P.P. Balandyn criterion [21] on the basis of

$$s_{экв} = \frac{1-y}{2}(s_x + s_y) + \\ + \frac{1}{2}\sqrt{(1-y)^2(s_x+s_y)^2 + y\left[(s_x+s_y)^2 + 3(s_x - s_y)^2 + 12t_{xy}^2\right]} \le [s] \tag{1.4}$$

In a condition (1.4) s_p are s_c limits of tension stress and contraction of rocks;

$$y = \frac{s_p}{s_c};$$

Where $[s]$ is tolerated stress.

Results of rock tests by A.N. Stavrotny [89] and H. Cook [90] show that the criterion is rather sufficient to describe their breaking under triaxial compression and compression with extension [92]. Positive practice of criterion (1.4) use in geomechanical problems while estimating rock stress condition in the neighbourhood of mine workings confirms that. Comparison of theoretical results with adequate data of mine monitoring indicates their satisfactory agreement [35, 39, 40, 41, 42, and 85-87].

1.2 Analysis of research results concerning displacement of rock mass and the earth's surface in the process of underground mining

Identification of rules which condition rock mass displacement under the influence of underground mining is one of critical problems. Its solution is very important for science. Its urgency depends on the necessity of coal seams mining under protected natural objects, buildings, towns, cities, and settlements.

Owing to current traditions, certain computational models and methods are used to research rock pressure manifestations; other certain ones are applied in the process of rock displacements research.

Common analytical solutions for the first concept have been obtained on the basis of simplified computational models; they mainly belong to linearly elastic homogeneous media [18, and 24 - 26]. However, real rock mass is often outside of the rules.

Numerical methods of finite and boundary elements help to approximate computational model to a real object. Papers [27 - 35] and many others describe the methods theory as well as their numerous applications for problems of rock mechanics.

The practically proven mathematical tool is efficient in the process of rock mass stress-strain state identifying despite its geometry and structure. Monograph [36] considers a number of statistical problems of rock mechanics confirms that; paper [41] involves probabilistic assessment of rocks breaking zones in the neighbourhood of large interacted workings; and paper [42] is engaged in explanation of parameters of contiguous coal seams mining with the help of powered systems under the conditions of Lvov-Volynsk deposit.

Numerical methods give ability to describe behaviour of physically non-linear rock masses, out-of-limit deformation of rocks, and their parting [37, 38, and 40].

Solutions obtained with the help of the methods are interested both scientifically and practically. Those are, for example, numerical estimations of mining rate effect on a rate of convergence of roof and cavity floor formed in the process of ore augering [39], and on the value of load action on powered support while contiguous coal seams mining by means of powered systems [42]; that is the algorithm of parameters computation for stable roof-caving increment in a face described in a paper [43].

However, due to consideration of limited area of mass within neighbourhood of a stope, neither analytical solution method nor numerical one can link earth's surface deformations with determined stresses, deformation, and deformation rate.

By contrast, problems concerning displacements discuss behaviour of mass having infinite boundaries; that helps to identify deformed condition of earth's surface. Graphical methods, analytical and experimental methods, and analytical ones are used.

The majority of researches combine deformation of earth's surface with angled parameters; as a rule, they consider conditions of terminated displacement process, and seam depth as well as a stope dimensions are basic influencing factors. In this context survey measurement data are used; hence, results obtained have not sufficient similarity.

S.G. Avershin and M.A. Kuznetsov have developed one of the most well-known analytical and experimental methods of parameters computation within displacement basin at the earth's surface [44, 45]. The method is still employed. According to it, basing upon analysis of curves of vertical failure h, curving K, horizontal component of displacements x, and horizontal deformations e, along principle profile of the basin linear dependence between horizontal component of displacement vector, and first derivation of horizontal component of displacement vector with second derivation of vertical component are established. As a result, maximum values of basic elements of deformed surface along principle profiles of

displacement basin on extension and across the strike (horizontal displacements, falls, horizontal deformations of expansion-compression, and curving) are determined. Paper [45] describes a method to develop first-approximation curve of failure rate distribution along a line coinciding with a face advance rate. However, the curves developing needs experimental determination of maximum failure, abscissas of points of failure curve bend, proportionality factor between horizontal component of displacement vector, and first derivative on vertical component.

In paper [46] D.A. Kazakovski proposes to make preliminary computations of relative failure values on average for specific mining and geological conditions values of displacement angle d . In this context real observations should determine relative value of maximum failure, and coefficient characterizing mining depth at which transition of plate-like form of deflection curve to dished one takes place. In papers [47 and 48] that very author provides empiric formulae which help to determine a value of maximum surface failure depending upon a seam depth and a stope dimensions for different types of flat-lying deposits. The formulae hypothesize tentative short-time field studies.

None of the above papers studies effect of physical and mechanical properties of enclosing rocks on a displacement process. Meanwhile as field studies performed in different regions show, parameters of displacement basin depend heavily on their properties and mass structure. In this regard a paper by R.A. Muller is of practical interest [55]. According to available procedures, compensation factors are introduced while analyzing earth's surface. The factors take into account variableness of mechanical properties of rocks and operation conditions. The compensation factors refer to the conditions of Karaganda coal field.

Most of all failures are not illustrative from the viewpoint of protection of facilities. If edges of basin are important, even serious failures may cause deformation being absolutely undamaging for protected objects. Horizontal deformations and slope change are more dangerous. The former are accompanied by considerable tensile stresses, and the latter – by formation of console chocking-up favouring the decay of buildings under gravity. Hence, availability of flat-lying basins under the conditions of great mining depth stipulates displacement angle detection taking into account changes in falls and horizontal deformations. That is done in papers [56 and 57] in the context of mining and geological conditions of Donetsk coal field.

The author of paper [58] insists that shift angles should be determined in such a way to make deformations of earth's surface within boundaries of protected area equal to admissible deformations for protected objects referring to tables of corrections to measured angles values. Summing up considered results of research as for the basin parameters performed with the help of empiric method, one may specify that all of them belong to these or those specific mining and geological conditions, and have no sufficient similarity. Even within one and the same basin in different regions, dependence of horizontal and vertical failures on maximum failure is manifested differently. This points to the fact that it is required to take into account at least hardness of enclosing rocks [59]. Nevertheless the fact is not taken into consideration in prescriptive guidances [12, 17, 18, and 19]. In this context, paper

[60] is interesting as it considers different mining and geological conditions, and capping thickness. While determining a point of maximum convergence, in addition to value amount of inclination a , cross-strike dimensions of a working, and mining depth, the authors introduce coefficient depending on enclosing rocks strength varying within 0.4…2.0. The harder rocks are, the higher is the coefficient. Computation results for Kuznetsk, Donetsk, and Karaganda coal basins are compared with in-situ measurements.

From the viewpoint of description of basin displacement parameters and its form, it is expedient to regard a standard curve method, so-called source function [44, 61, and 62]. The analytical and experimental method is: the surface point displacement is considered as a total of separate elementary units of a working. If we find a value of surface displacements under the effect of the working unit depending upon mutual location of the latter and surface points, then total effect can be identified as well. Determined in such a way dependence contains invariables to be identified on the results of in-situ measurements. Many hypotheses have been developed as for the dependence. Hence, basing on differential relation between horizontal displacements and falls in basin displacement, and conditions for continuity of rock mass deformations in the context of two-dimensional computational model, R.A. Muller has developed differential equation as for convergence function. Exponential influence function is its solution [63]. The influence function expression involves a coefficient taking into account availability of washes. Deduced from experiments values of the coefficient for a number of coal basins are in paper [64].

Exponential function involving three coefficients obtained empirically is used in paper [65] as analytical form of influence curve.

However, the idea concerning influence of each elementary unit may be described with the help of probability distribution, i.e. Gaussian distribution curve.

So, considering Gaussian distribution curve as a settling curve in a semi-basin, V.I. Cherniaev finds maximum fall angles. Estimated values of convergences and falls have insignificant differences to compare with those measured under adequate conditions [66].

Papers [67 and 68] also use Gaussian distribution curve which coefficients are maximum falls in semi-basin, and maximum curvature. The empiric dependences characterizing deformations of basin mirror mining and geological conditions of Donetsk coal basin, and Lvov-Volynsk coal basin.

M.I. Iofis developed a technique of earth's surface deformations computation also based on standard curves procedure [69]. Recommendations formulated on the paper concern Lvov-Volynsk coal basin. For the conditions, the author developed a formula for a total period of displacement process depending upon mining depth and a face advance rate. Besides, the paper gives a formula to determine a maximum rate of earth's surface fall.

Foreign researches also refer to Gaussian function. For example, having expressed a profile graph of a basin by means of Gaussian curve and determined experimentally a rate of change to a profile of semi-basin displacement in a flex, S. Knotte obtained its curve equation, and determined the curve maximum as well as

the point position in which the value took place. As a result, possibility reveals itself which provides assumption concerning effect of projected coal-seam mining on earth's surface, and on objects located within [70].

In paper [71] influence curve being Gaussian curve is replaced with influence triangle. It is hypnotized that displacement rate of earth's surface is proportional to a difference of terminal fall, and to a fall value within time concerned. It is regarded that a stope has constant rate.

On the basis of such assumptions as time functions, a profile of displacement basin, falls, and curve are determined. The dependences help to conclude that increase in a face rate may sizably decrease deformations of earth's surface. The formulae make it possible to identify curve maximum which will affect surface object in the process of two-way mining, and to estimate reduction range of the curve depending on a stope advance. However, it should be noted that geometry of influence triangle is to be identified with the help of real experiment.

Polish researcher E. Litvinishin used another technique to establish the equation of rock displacement. He applied a model of loose (bondless) environment, a rule on mass conservation, and hypothesis of S.G. Avershin concerning proportionality of horizontal displacements of first derivative of vertical displacements. As for earth's surface deformations, the theory by E. Litvinishin conforms fully to conclusions by Knotte. Besides, research of E. Litvinishin helps to conclude that there is mathematical parallel between displacement process of rocks and thermal conductivity [72].

Under boundary conditions specified in a roof plane by paper [72], the equation solution identifies both vertical and horizontal components of rock displacement as a function of function spatial coordinates. Dependence taking into account a face advance is recognized for vertical displacements. Again, the formula covers observed parameter. Polish researcher A. Salustovich developed another analytical solution. The solution is based on the idea that within inflection zone, mass is homogeneous flexed platform on elastic foundation. On one side that is coal pillar; on the other side that is broken-down rock or backfill. Plane elasticity is being solved. Formulae determining a value of profile curvature of displacement basin, falls, and horizontal deformations within any its point is its result. Maximum settlement of ground, displacement angles, and mining depth are key parameters. Besides, the formulae involve coefficients characterizing rock properties being determined experimentally [73].

Representative of that very Polish school V. Budryk obtained analytical expression for horizontal deformations of earth's surface basing upon hypothesis by S.G. Avershin as for availability of zero line at certain distance from earth's surface. Besides, he used an assumption that horizontal displacements are distributed according to parabolic law.

To calculate parameters of basin displacement on the dependences obtained, it is required to know maximum convergence of earth's surface, mining depth, and tangent of displacement critical angle. Mining practice obtain them on the basis of survey data [74].

All-Union Research Institute of Mine Surveying also investigated in the line of

analytical solutions (papers by R.A. Muller, S.G. Avershin, A.G. Akimov etc.). In this context, mass was considered as an averaged homogeneous weightless structure [75]. With the help of transformation of differential equations of plasticity theory in displacement, author developed continuity equation expressing zero volume deformation. Real changes in rocks were taken into account by means of a value of maximum fall in the process of complete undermining-seam thickness ratio. Hence, paper [75] develops resulting differential equation which form coincides with thermal-conductivity equation. Fourier method was applied for different boundary conditions. As a result, there are developed expressions of convergence functions, horizontal displacements, falls, curve, and deformations of tensile (compression). Also there are developed formulae for maximum values of all parameters of basin of displacements at the surface. Length of semi-basin and characteristic of rock hardness having different values under different mining and geological conditions are their coefficients. Those, shown in the article belong to Karaganda coal basin, and Moscow region coal basin.

Papers [76, 77] apply mathematical analogy of displacements distributing caused by underground mining with Brownian movement. In such a way, the problem solution is to solve differential equation in local derivatives of parabolic type (thermal-conductivity equation). In both directions average size of particles is different; owing to that internal stratification within rock bed is taken into consideration. The author points to possibility in principle to take into account external stratification by means of introducing of independent sizes of particles for each bed. However, the aspect stays to be uninvestigated.

It should be noted that differential equation of displacement process (equation of thermal conductivity and diffusion) by E. Litvinishin [72] on the basis of bondless structure model, by S.G. Avershin [44] on the basis of geometrical dependences between mass displacements on cross stratification and on normal to cross stratification, and by R.A. Muller with the use differential equations of plasticity [75] and on the basis of stochastic theory are identical.

That gives ground to consider equation of thermal conductivity and diffusion as fundamental for the process of displacements in rock mass under the influence of underground mining. Therefore, by means of solving it for two-layered “washes-carbon” earth with regard to a face advance, mining depth, and stope geometry, one can develop analytical relationships for components of rock strata stress-strain state and earth’s surface at any stage of coal seam mining. In addition, it is required to know hardening parameters of coal and enclosing rocks. Numerical solution of rock mechanics problem may be applied. It is clear that the method of boundary elements with adequate basic analytical solution for semi-infinite area is suitable [30].

Authors of paper [78] identify nature of distributing of displacements and deformations within selvedges of displacement basin applying a model of linear and deformable medium. In this context maximum dimensions of bearing pressure zone within the bed, over it, and under it are set as equal to dimension of selvedges of displacement basin at the surface. Values of fall and maximum convergence of a basin within a point having limit curve value developed by means of field studies data compilation are applied as boundary conditions. Rock mass is considered as

homogenous with effective elasticity modulus, and Poisson ratio is counted to be 0.5. Despite the fact that the latter can not correspond to reality in full, calculated displacements and deformations on the brink of the basin are in keeping with records under the conditions of Lvov-Volynsk and Kuznetsk coal basins.

Paper by G.I. Cherny [79] identifies falls and deformations of earth's surface relying on a model of viscous flow by Bingham-Shvedov. Potential of such an approach to a displacement process is limited as it needs laboratory tests of rock samples.

Papers [80 and 81] consider problems of deformation processes control while underground mining. Relying upon field data of Western Donbass mines the authors assert that metamorphism intensity of enclosing rocks, and two caving steps of upper roof-a stope advance ratio are two determinants for compression-extension deformations.

In addition to papers [80 and 81], papers [49] and [82] may be used for calculation and theoretical models developing to be applied for mining and geological conditions of mines in Western Donbass.

The former describes slope angles of lines connecting earth's surface points in which maximum falls, maximum horizontal displacements, and maximum extensions with boundaries of mining operations. The measurements were performed in mines.

Paper [82] includes dependence diagrams of curves and horizontal deformations of earth's surfaces in terms of D/H parameter (D is geometry of a stope on the strike, and H is mining depth) constructed in accordance with instruction [12]. In-situ measurements are plotted. Satisfactory coincidence of results is registered.

A report on research [86] involves analysis of overseeing deformations of earth's surface and facilities in "Stepnaia" mine under the conditions of Krasnoarmeisk – Pavlograd electric railway undermining. It covers profiles of fall basin at different stages of mining as well as curves of slopes and curvature developed on the data of ground reference measurements on railheads. Real maximums of earth's surface deformations are compared with nominal ones.

Paper [84] describes results on strata movements within bearing pressure zone obtained with the help of equivalent material models. The experiments were made to estimate effect of mined stratum thickness. That helps to conclude that there is definite value of thickness mined for any specific conditions. With this value maximum convergence at the surface takes place within bearing pressure zone. Unfortunately, the paper has neither resumptive ratios nor data of movement calculations within area under study.

Generalizing results of the most interesting and available research concerning earth's surface movements as a result of underground mining, we would like to single out the following:

1) Hypothesis of structure homogeneous underlies developed analytical solutions; they don't take into consideration availability of washes which effect greatly rate of subsidence, and other factors of earth's surface deformations; as a rule they belong to complete undermining conditions.

2) Each solution obtained with the help of analytical and experimental methods needs real experiments. It is often far from being possible at a planning stage.

3) Certain analytical solutions as well as solutions resulting from analytical and experimental methods are not connected with stress-strain state of rocks within a layer mined and stress-strain state of rock strata.

4) The solutions ignore parameters of powered support; the majority of them also ignore a stope advance.

5) No solution takes into consideration redistribution of stress-strain state of rock strata in the process of coal mining.

We can conclude that:

- Owing to available mathematical analogy between displacement of rocks and thermal conductivity, analytical ratios for displacements and deformations of earth's surface and rock strata may be developed by means of solution of differential equation of thermal conductivity type for two-layered "washes-carbon" earth.

- To identify rules of rock deformation and fragmentation in the process of flat coal seam mining with the help of complex powered faces under protected objects, deformations obtained should be associated with stresses. Judging by enclosing rocks lithology and their physical and mechanical properties, for mining and geological conditions of Western Donbass that can be done with the help of a model of linear and congenital structure with creep kernel of Abel.

- Target analytical solution should provide determining of displacements, deformations, and stresses within any point of undermined rock mass at any coal mining stage taking into account a stope advance, mining depth, and rheological properties of rock.

- Criterion of rock braking by P.P. Balandyn is the most expedient for mining and geological conditions under consideration.

- Identifying rational parameters of powered support and a stope advance at certain depth and when the coal seam is being mined under protected objects, one should rely upon analysis of stress-strain state of rocks in the neighbourhood of the stope, earth's surface deformations, and upon limits by the branch standards as for load acting on roof support canopy, upon appropriate response and hydraulic props yield as well as upon earth's surface deformation factors.

1.3 Objects of the research

The analysis of the current state of concerned general technological problem shows that to deliver on the target (to determine rules of changes in stress-strain state of rock mass while mining coal seam under protected objects) following peripheral problems should be solved:

1. To solve analytically a plane problem of rock mechanics for two-layered "washes-carbon" earth taking into account a stope advance, mining depth, and lithology of rocks which help to determine stress-strain state in any point of rock mass and earth's surface at any stage of coal seam mining.

2. To develop algorithm of numerical solution of a plane problem of rock mechanics in terms of boundary-element method. That should be done to identify

stiffening parameters of stratified rock mass required for analytical solution of the research basic problem.

3. To identify rules of rock mass deformation and breakage in the process of coal seam mining, use the analytical ratios to determine and analyze stress-strain state of rocks in the neighbourhood of a stope in the initial phase, and earth's surface under the conditions of complete and partial undermining.

4. To determine possible roof-caving step and load acting on a roof support canopy in the case of the most dangerous stress in terms of analysis of the stress-strain state.

5. To use general ratios for developing of formulae to calculate maximums of earth's surface deformations required to be compared with standard reasonable factors for different protected objects.

6. To formulate methods for coal-mining rational parameters determination. The parameters should provide mining without doing harm to protected objects (power and stiffening parameters of powered support, a stope advance); to identify the parameters for mines in Western Donbass.

7. To make comparative analysis of estimated values of earth's surface deformation factors and adequate data of survey measurements as well as data obtained for similar conditions through normative technique to substantiate certainty of rules, conclusions, and recommendations.

1.4 General technique of the research

Theoretical, applied, and experimental research of stress-strain state of stratified heterogeneous mass and earth's surface were performed in the context of flat coal seams mining under protected objects under the conditions of Western Donbass mines. Structural schematic of the research technique is in Fig. 1.3.

Theoretical research involved analysis of coal reserves under protected objects within productive mines of "Pavlogradugol" OJSC; studies of mining and geological conditions and reasons for flat coal seams mining by means of integrated and powered faces; analysis of available approaches to related problems solving; and mathematical formulation of general technological problem, and related partial problems of rock mechanics.

The main result of theoretical research is a new analytical solution of differential equation of thermal-conductivity type for two-layered "washes-carbon" earth with creep kernel of Abel.

The analytical solution helps to identify displacements, deformations, and stresses in any point of undermined mass at any stage of coal seam mining taking into account a stope advance, a face geometry, mining depth, and lithology of rocks.

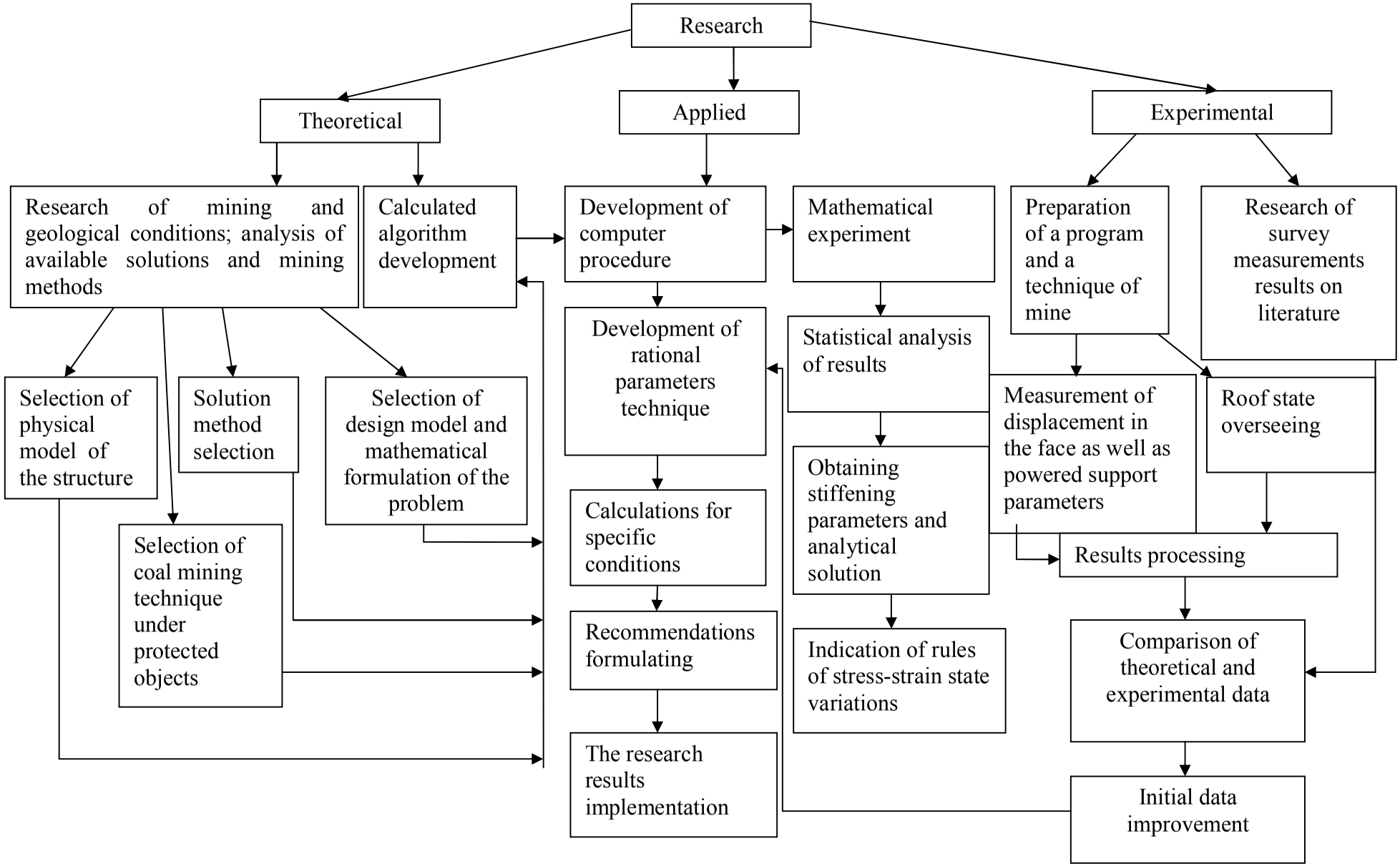

Figure 1.3.Structural schematic of the research

Rules of changes in stress-strain state of earth's surface and rock mass in the process of flat coal seam mining have been specified with the help of developed analytical expressions for displacements, deformations, and stresses.

General analytical ratios have been used for formulae to calculate maximums of earth's surface deformations to compare with standard nominal factors for different protected objects.

The developed algorithm to solve flat problem of rock mechanics through boundary-element method is another result of the theoretical research.

The algorithm is meant for determination of stiffening parameters of stratified undermined mass. The parameters are included in considered differential equation of thermal-conductivity type. As a rule, the parameters have been determined experimentally.

Owing to application of ratios of Crouch problem being true for semiplane, boundary conditions at the earth's surface are fulfilled automatically; only internal boundaries of considered area are digitized (contours o the stope). That is the algorithm advantage to compare with available ones.

Applied research involves programming which implements the developed algorithm of geomechanical problem solving with the help of boundary-element method, and numerical experiment performing (calculations at various values of key parameters).

Statistical analysis of the numerical experiment results helps to develop piecewise-linear function characterizing hardness of heterogeneous rock mass beds, and to associate earth's surface deformations with stress-strain state of rocks within coal seam mined.

"Technique of rational coal mining parameters determining under protected objects" has been developed with the use of identified rules of rock mass stress-strain state changes while undermining.

Data calculated concerning earth's surface displacements were compared with survey measurements data taken from literature.

Besides, comparison of data obtained for similar conditions on standard technique as well as on analytical ratios was performed. As a result, there were formulated recommendations as for powered support parameters and a stope advance at certain mining depth under protected objects under the conditions of Western Donbass mines; in addition they were applied in "Stepnaia" mine of "Pavlogradugol" OJSC.

CHAPTER 2. THE ALGORITHM OF ANALYTICAL AND NUMERICAL DETERMINATION OF UNDERMINED ROCK MASS STRAIN STATE

2.1 Characterization of the problem analytical solution algorithm

Consider homogenous undermined rock mass as ponderable homogenous medium with averaged properties.

As it is known, for flat problem, balance Navier equation being sum of projections on vertical intense axis OY acting on surface element with $dx \cdot dy$ square (Fig. 2.1) is:

$$\frac{\partial s_y}{\partial x} + \frac{\partial t_{xy}}{\partial y} - g = 0, \tag{2.1}$$

Where g is specific weight of the medium.

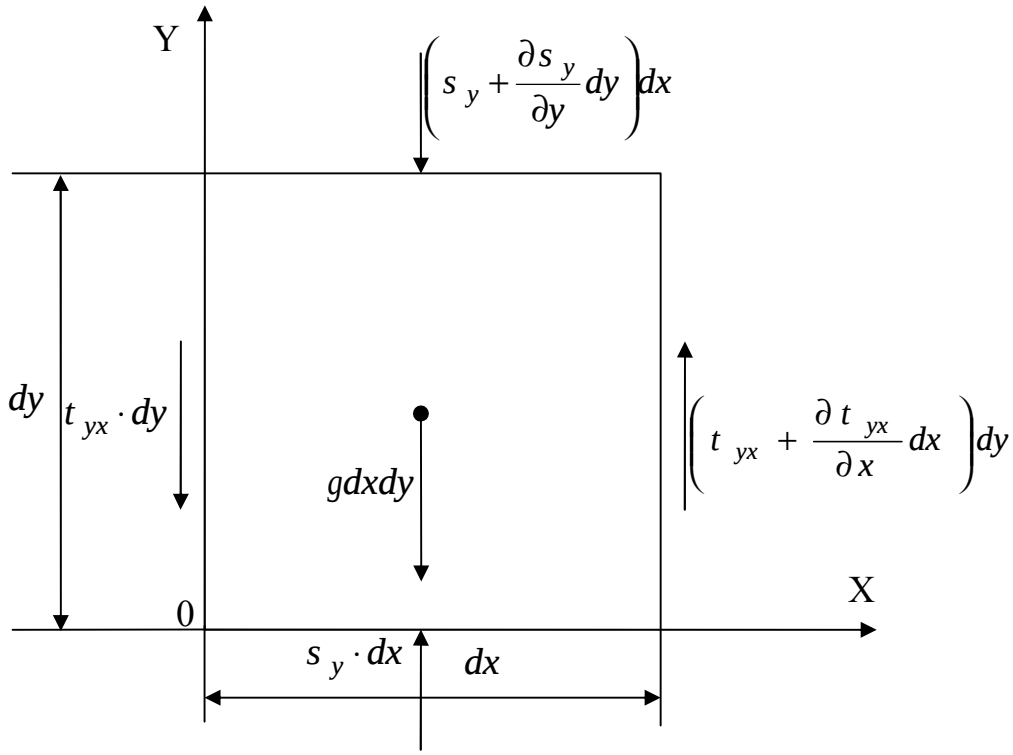

Fig. 2.1. Forces acting towards OY axis on surface element of the medium

Use a model of less-connected medium [64] in which intensity of vertical bearing reaction of rock s_y with its slump h is associated by means of

$$s_y = -c_1 h, \tag{2.2}$$

ratio, and the vertical intensity of displacement t_{yx} is related to vertical convergence derivative $\frac{\partial h}{\partial x}$ through the ratio

$$t_{yx} = c_2 \frac{\partial h}{\partial x} \tag{2.3}$$

Values c_1 and c_2 in ratios (2.2) and (2.3) are coefficients of rock compressive and shear stiffness depending on mechanical properties of enclosing rocks. The latter is measured in kg/cm^3 or t/m^3, and the former in kg/cm or t/m.

If rock mass is homogeneous, then stiffness coefficient c_1 does not depend on coordinates, and c_2 is a function of y coordinate as any working places certain restrictions on a displacement value.

To develop difference balance equation of low-cohesive medium in displacement components, we insert ratios (2.2) and (2.3) in equation (2.1).

We obtain

$$-\frac{\partial}{\partial y} c_1 h + \frac{\partial}{\partial x} c_2(y) \frac{\partial h}{\partial x} - g = 0,$$

or

$$\frac{\partial h}{\partial y} = K(y) \frac{\partial^2 h}{\partial x^2} - \frac{g}{c_1}, \tag{2.4}$$

where

$$K(y) = \frac{c_2(y)}{c_1} \tag{2.5}$$

Forgetting body forces, we arrive at the equation

$$\frac{\partial h}{\partial y} = K(y) \frac{\partial^2 h}{\partial x^2} \tag{2.6}$$

Function (2.5), being a part of differential equation (2.6), may be expressed as

$$K(y) = \frac{c_2(y)}{c_1} = c^2 y, \tag{2.7}$$

where c^2 is dimensionless parameter depending on shear stiffness-compressive stiffness ratio determined by the formula

$$c^2 = \frac{E}{6(1+n)c_1 Dl} \tag{2.8}$$

Dl is singular horizontal displacement at the surface of separated vertical column which basis is at the working; with its unit area section and height $y = H$, and unit angle turn $\frac{\partial h}{\partial x}$ under the effect of shear forces (Fig. 2.2).

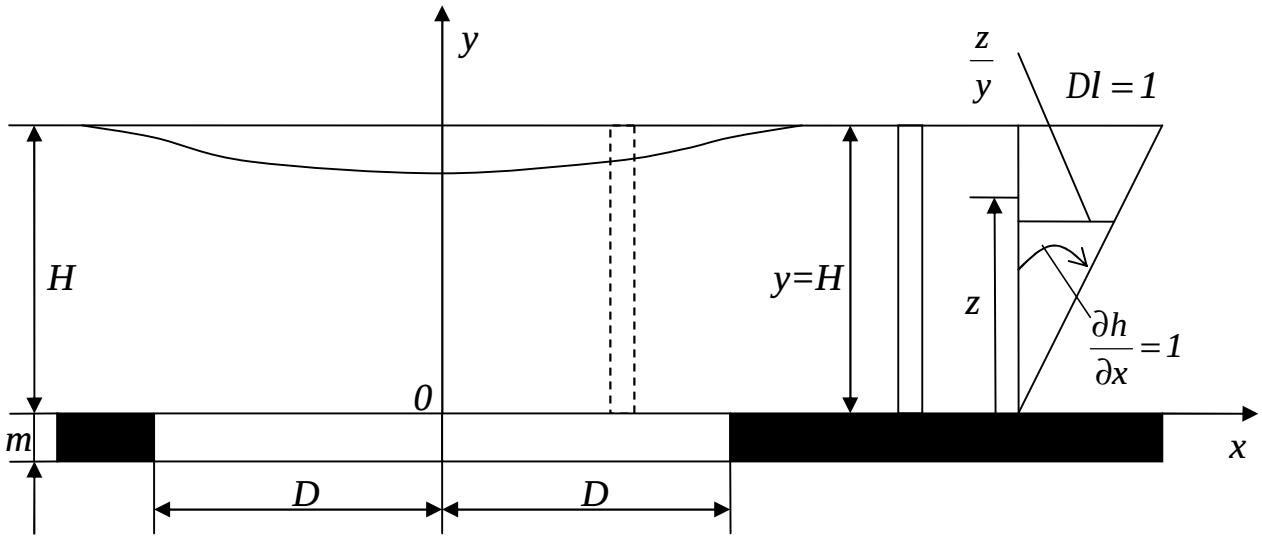

Fig. 2.2. Formulating rock shear stiffness coefficient

Equation (2.6) has similar form with the known thermal-conductivity equation. It makes analogy between vertical displacements of weightless rock mass and rules of warm transport within infinitely homogeneous medium.

Use Fourier method [93], and show the integral of differential equation (2.6) as

$$h(x,y) = X(x)Y(y) \tag{2.9}$$

After function (2.9) has been inserted into initial equation (2.6) we obtain:

$$Y'(y)X(x) = K(y)Y(y)X''(x) \tag{2.10}$$

From (2.10) one gets

$$\frac{Y'}{K(y)Y} = \frac{X''}{X} = -n^2,$$

where n is an arbitrary parameter.

We have ordinary differential equations:

$$X'' + n^2 X = 0 \qquad \text{and} \qquad \frac{Y'}{Y} = -n^2 K(y)$$

From the former one gets

$$X(x) = A\cos nx + B\sin nx, \tag{2.11}$$

And from the latter one gets

$$\ln|Y| = -n^2 K(y)dy \text{ or}$$

$$Y(y) = \exp\left(-n^2 \int K(y)dy\right) \tag{2.12}$$

Taking into account (2.11) and (2.12), partial solution of a differential equation (2.6) after (2.9) may be

$$h_n(x,y) = (A_n \cos nx + B_n \sin nx)\exp\left(-n^2 \int K(y)dy\right)$$

As the differential equation (2.6) is linear and homogeneous equation, then its general solution is developed as

$$h(x,y)=\sum_n exp\left(-n^2\int K(y)dy\right)(A_n\cos nx+B_n\sin nx)$$

Or, as all arbitrary parameters *n* are equal, it is shown in the form of

$$h(x,y)=\int_{-\infty}^{\infty} exp\left(-n^2\int K(y)dy\right)[A(n)\cos nx+B(n)\sin nx]dn \qquad (2.13)$$

If *y=0,* then it follows from (2.13) that

$$h(x,y)\big|_{y=0}=f(x)=h(x,\,0)=\int_{-\infty}^{\infty}[A(n)\cos nx+B(n)\sin nx]dn \qquad (2.14)$$

For function *f(x)*, Fourier integral is

$$f(x)=\frac{1}{2p}\int_{-\infty}^{\infty}[\cos nx\int_{-\infty}^{\infty}f(x)\cos nx\cdot dx+\sin nx\int_{-\infty}^{\infty}f(x)\sin nx\cdot dx\,]dn \qquad (2.15)$$

Comparing (2.14) and (2.15), we obtain

$$A(n)=\frac{1}{2p}\int_{-\infty}^{\infty}f(x)\cos nx\cdot dx\,;\quad B(n)=\frac{1}{2p}\int_{-\infty}^{\infty}f(x)\sin nx\cdot dx$$

Hence,

$$h(x,y)=\frac{1}{2p}\int_{-\infty}^{\infty}f(x)dx\int_{-\infty}^{\infty}exp\left(-n^2\int K(y)dy\right)(\cos nx\cos nx+\sin nx\sin nx)dn=$$

$$=\frac{1}{2p}\int_{-\infty}^{\infty}f(x)dx\int_{-\infty}^{\infty}exp\left(-n^2\int K(y)dy\right)\cos n(x-x)dn=$$

$$=\frac{1}{p}\int_{-\infty}^{\infty}f(x)dx\int_{0}^{\infty}exp\left(-n^2\int K(y)dy\right)\cos n(x-x)dn \qquad (2.16)$$

Inserting

$$\int K(y)dy=j(y) \qquad (2.17)$$

And taking into account that

$$\int_0^{\infty}exp\left(-j(y)n^2\right)\cos bn\cdot dn=\frac{1}{2}\sqrt{\frac{p}{j(y)}}\,exp\left(-\frac{b^2}{4j(y)}\right),$$

We get from (2.16)

$$h(x,y)=\frac{1}{p}\int_{-\infty}^{\infty}f(x)dx\,\frac{\sqrt{p}}{2\sqrt{j(y)}}exp\left(-\frac{(x-x)^2}{4j(y)}\right)=$$

$$=\frac{1}{2\sqrt{pj(y)}}\int_{-\infty}^{\infty}f(x)exp\left(-\frac{(x-x)^2}{4j(y)}\right)dx \qquad (2.18)$$

Partial solution we find out under boundary conditions which describe a state of complete undermining:

$$h(x,y)\big|_{y=0}=f(x)=\begin{cases}0, & -\infty<x<-D,\quad D<x<\infty\\ -h_0, & -D<x<D,\end{cases} \qquad (2.19)$$

Where h_0 is maximum convergence of rock roof taking place in the process of complete undermining; and

$2D$ is a working length when under considered mining and geological conditions, deformation reaches surface.

Assuming (2.19) $h_0 = m$ (where m is mined seam thickness), one can roughly take into consideration effect on vertical displacements of body forces.

In fact, $q = \frac{h_0}{m}$ parameter characterizing a rock change while its displacing depending on mining and geological conditions is 0.6…0.9 [14]. Hence, in terms of (2.19), $h_0 = m$ $(q = 1)$ congruence means extra vertical displacements consideration at the expense of rock weight.

Including (2.19), the integral of a differential equation (2.6) will be

$$h(x,y) = -\frac{h_0}{2\sqrt{pj(y)}} \int_{-D}^{D} exp\left(-\frac{(x-x)^2}{4j(y)}\right) dx \left\{ \begin{array}{l} \frac{x-x}{\sqrt{2j(y)}} = t \\ dt = \frac{dx}{\sqrt{2j(y)}} \end{array} \right\} =$$

$$= -\frac{h_0\sqrt{2j(y)}}{2\sqrt{pj(y)}} \int_{\frac{-D+x}{\sqrt{2j(y)}}}^{\frac{D-x}{\sqrt{2j(y)}}} exp\left(-\frac{t^2}{2}\right) dt = -\frac{h_0}{\sqrt{2p}} \int_{\frac{-D+x}{\sqrt{2j(y)}}}^{\frac{D-x}{\sqrt{2j(y)}}} exp\left(-\frac{t^2}{2}\right) dt \qquad (2.20)$$

Considering (2.17), from (2.7) ratio we obtain an expression for function $j(y)$

$$j(y) = \int K(y)dy = \frac{c^2 y^2}{2}.$$

Taking into account (2.20), the expression is

$$h(x,y) = -\frac{h_0}{\sqrt{2p}} \int_{-\frac{D+x}{cy}}^{\frac{D-x}{cy}} exp\left(-\frac{t^2}{2}\right) dt \qquad (2.21)$$

Introduce Gaussian function

$$\Phi(z) = \frac{2}{\sqrt{2p}} \int_{0}^{z} exp\left(-\frac{t^2}{2}\right) dt \qquad (2.22)$$

And reduce partial solution (2.21) of differential equation (2.6) to the form

$$h(x,y) = -\frac{h_0}{2}\left[\Phi\left(-\frac{D+x}{cy}\right) - \Phi\left(\frac{D-x}{cy}\right)\right], \qquad (2.23)$$

Where $h_0 = m$.

Hence, there is obtained an expression which will help to identify convergence value within any section of a mass and earth's surface in the direction which is perpendicular to layering. Making its differentiation, we obtain falls and flexions of mass settling curves:

$$i(x,y)=\frac{\partial h}{\partial x}=-\frac{h_0}{2cy}\left[\Phi'\left(\frac{D+x}{cy}\right)-\Phi'\left(\frac{D-x}{cy}\right)\right] \quad (2.24)$$

$$k(x,y)=\frac{\partial^2 h}{\partial x^2}=-\frac{h_0}{2c^2y^2}\left[\Phi''\left(\frac{D+x}{cy}\right)+\Phi''\left(\frac{D-x}{cy}\right)\right] \quad (2.25)$$

2.2 Determination of horizontal displacements and deformations within homogeneous small-cohesive medium

To determine displacements in the direction being parallel to layering, use continuity condition (or incompressibility condition for considered small-cohesive medium) in the form of

$$\frac{\partial h}{\partial y}+\frac{\partial x}{\partial x}=0, \quad (2.26)$$

Where x is a displacement in the direction being parallel to layering.

Substituting (2.26) to differential equation (2.6) and integrating it, we obtain:

$$x=-c^2y\frac{\partial h}{\partial x}+Y(y),$$

Where $Y(y)$ is arbitrary integrating function.

If horizontal bedding takes place under $x=0$ from symmetry condition (рис. 2.2) we have

$$\frac{\partial h}{\partial x}=0 \quad \text{and} \quad x=0$$

Hence, function $Y(y)\equiv 0$.

Therefore, dependence to determine horizontal displacements in the directions being parallel to layering, is

$$x=-c^2y\frac{\partial h}{\partial x} \quad (2.27)$$

This is that very dependence developed differently by S.G.Avershin, and such Polish researchers as E. Litvinishin, S. Knotte, and V. Budryk.

Thus, if we know convergence function $h(x,y)$, it is possible to find horizontal displacements from equation (2.27) with regard to (2.23):

$$x(x,y)=h_0\frac{c}{2}\left[\Phi'\left(\frac{D+x}{cy}\right)-\Phi'\left(\frac{D-x}{cy}\right)\right] \quad (2.28)$$

Derivative with respect to x from function (2.28) is horizontal compressive deformation (tensile deformation) (in the direction of OX axis):

$$e(x,y)=\frac{\partial x}{\partial x}=\frac{h_0}{2y}\left[\Phi''\left(\frac{D+x}{cy}\right)+\Phi''\left(\frac{D-x}{cy}\right)\right] \quad (2.29)$$

Such ratios as (2.23), (2.24), (2.25), (2.28), and (2.29) help to determine comprehensive idea of displacements and deformations within homogenous massive and in superficial convergence basin under the conditions of complete undermining when a stope dimension L reaches $2D$ value.

Parameter c being a part of the ratios and characterizing the medium hardness as follows from (2.8) formula, depends on rock elasticity modulus E which varies with time according to adopted model of linear and congenital medium. If we know a longwall advance V, we can determine time t during which $L = 2D$ stope had been formed. Substituting the t value в формулу (1.3) find creep function F_t; determine rock elasticity modulus E_t at considered moment t using formula (1.2) according to a known value F_t. Taking into account value E_t developed in such a way according to formula (2.8), determine c^2, and then c; hence, according to ratios (2.23) - (2.25), (2.28) and (2.29) we can specify displacements and deformations with regard to the medium rheology as well.

However, to make adequate description of rock mass displacements and earth's surface deformations, it is required to give up on the hypothesis of mass homogeneity in the process of undermining, and to introduce a stope advance in an algorithm of scheme analytical solution. That is done in this work. In several, following paragraph considers layered medium.

2.3 Consideration of layerage and heterogeneity of medium

If a mass is of layer type, then function $K(y)$ will be piecewise linear (each layer is small-cohesive homogeneous medium with own physical and mechanical properties); that is:

$$K(y) = \begin{cases} c_1^2 y, \ 0 \le y \le y_1 \\ c_2^2 y + b_2, \ y_1 \le y \le y_2 \\ \ldots\ldots\ldots\ldots\ldots\ldots \\ c_i^2 y + b_i, \ y_{i-1} \le y \le y_i \\ \ldots\ldots\ldots\ldots\ldots\ldots \\ c_n^2 y + b_n, \ y_{n-1} \le y \le y_n, \end{cases} \qquad (2.30)$$

Where $y_i = \sum_{k=1}^{i} h_k$;

$y_n = H$ is mining depth;

h_k is thickness of k^{th} rock layer; and

b_i are parameters identified by the rock strata geometry.

In this context, approach to initial difference equation solution of problem considered stays unchangeable. One should basically know c_i^2, $i=1,2,\ldots,n$ parameters characterizing hardness of layers, and depending on physical and mechanical properties of rocks.

For such two-layered medium as “cappings-carbon” which will be used in the following to make analytical solution of the problem, $K(y)$ function is

$$K(y)=\begin{cases} c_1^2 y, & y < y_1, \\ c_2^2 y + (c_1^2 - c_2^2) y_1, & y > y_1, \end{cases} \qquad (2.31)$$

Where $y_1 = H - h$;

h is washes thickness;

c_1 and c_2 are hardness parameters of carbon and washes correspondingly.

Graph of the function is in Fig. 2.3.

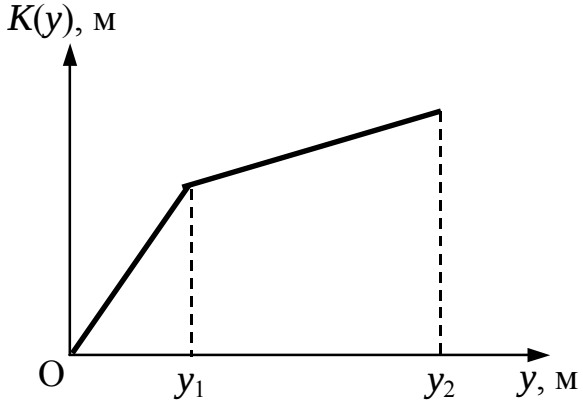

Fig. 2.3. Hardness function of two-layered mass

Hence, $j(y)$ function is:

$$j(y)=\int_0^y c_1^2 y dy = \frac{c_1^2 y^2}{2}, \text{ for } y < y_1;$$

$$j(y)=\int_0^{y_1} c_1^2 y dy + \int_{y_1}^{y} \left[c_1^2 y + \left(c_1^2 - c_2^2\right) y_1\right] dy =$$

$$= \frac{c_2^2 y^2}{2} + \frac{c_1^2 - c_2^2}{2} y_1 \left(2y - y_1\right) \text{ for } y > y_1 \qquad (2.32)$$

Basing on the boundary-element method in the form of troubles [31], the work develops calculated algorithm of numerical solution of plane geomechanical problem. The algorithm provides identifying the parameters for layered flaky heterogeneous mass together with rock weight.

Following paragraph describes the algorithm.

2.4 Determination of hardness parameters of rock layers with the help of boundary-element method

To determine c_i^2 hardness of i^{th} layer, plane problem of rock mechanics is solved for elastic mass with physical and mechanical properties of the layer. The mass encompasses coal layer, a stope, and worked-out space with decomposed rocks. Actual road is rock weight (Fig. 2.4).

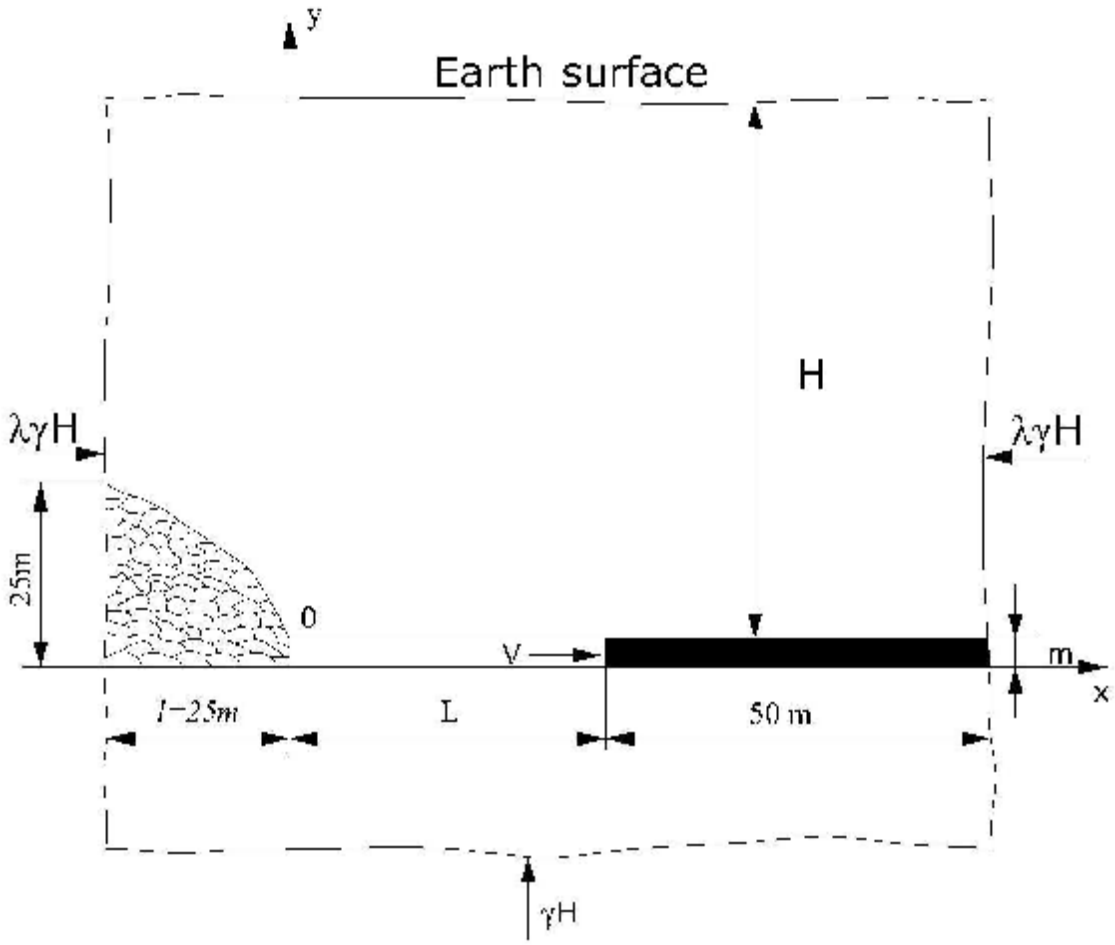

Fig. 2.4. Calculation model of current problem

From mathematical viewpoint, considered problem is a problem of stress-strain state of semiplane; earth's surface is its border. The latter, as any other border of considered area should be divided into boundary elements; it is required for each that their stresses and displacements meet the conditions. However, quite a number of elements are required for satisfactory introduction of surface effects. But if the development of calculated algorithm of boundary element method is based on analytical solution automatically meeting boundary conditions set at the surface, then only internal contours of considered area (boundaries of workings) should be sampled.

The work uses such a solution of permanent displacement discontinuity within arbitrary oriented finite segment $|\bar{x}| \le a$, $\bar{y} = 0$ in semi-infinite area (Fig. 2.5). The solution was obtained by S. Crouch [31].

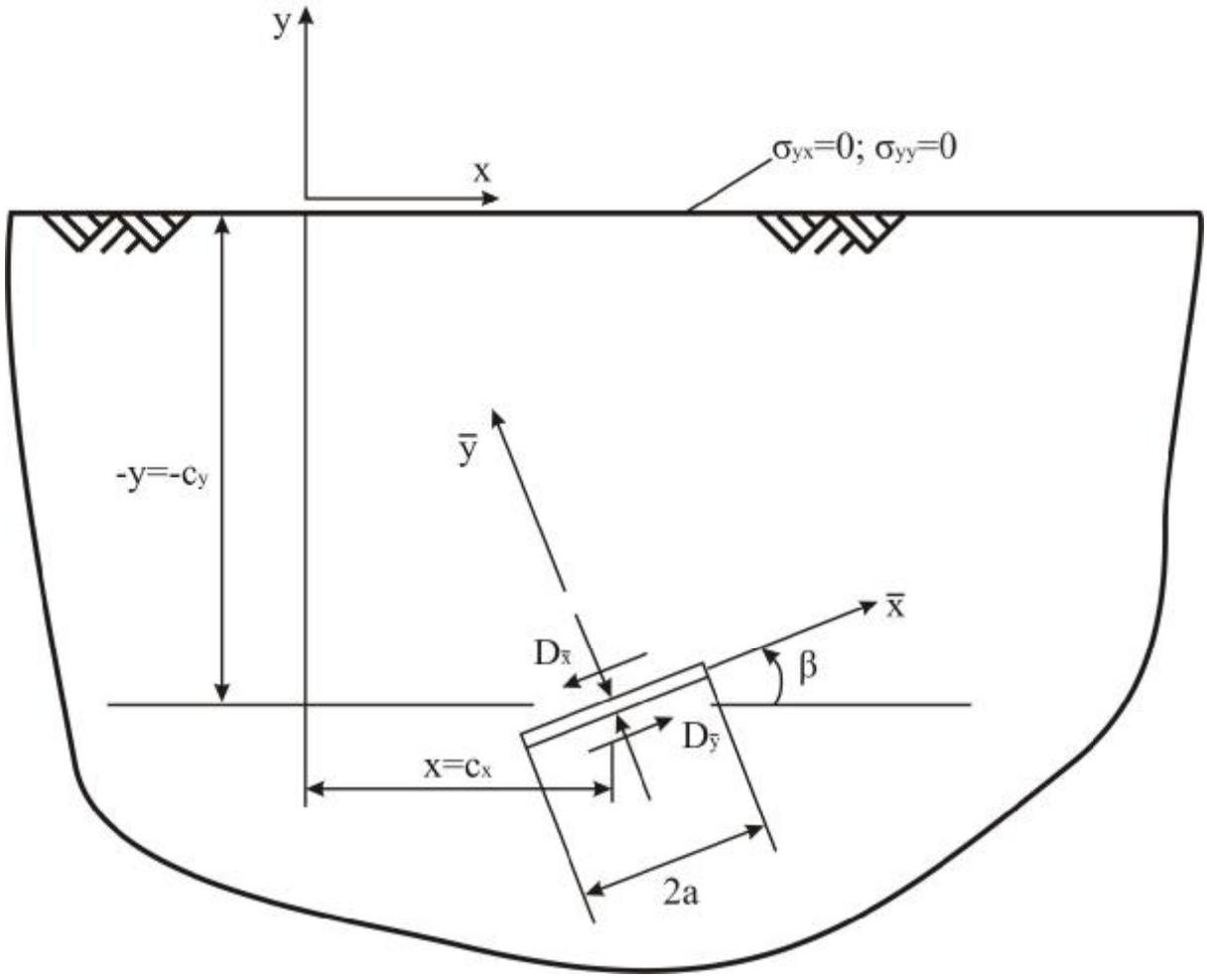

Fig. 2.5. Displacement discontinuity in $y \le 0$ semiplane

In this context the two stages are performed according to reflection method on the superposition principle.

First, unlimited area covering two segments with constant displacement discontinuities $D_{\bar{x}}$ and $D_{\bar{y}}$ is considered. One of them is within $y < 0$ area being real discontinuity; another is within $y > 0$ area being "reflected" and located symmetrically related to $y = 0$ line (Fig. 2.6).

By the data of symmetry, tangential forces are not available on $y = 0$ line. However, normal forces are not equal to zero; then stage two of the analysis is to specify complementary solution making them cut.

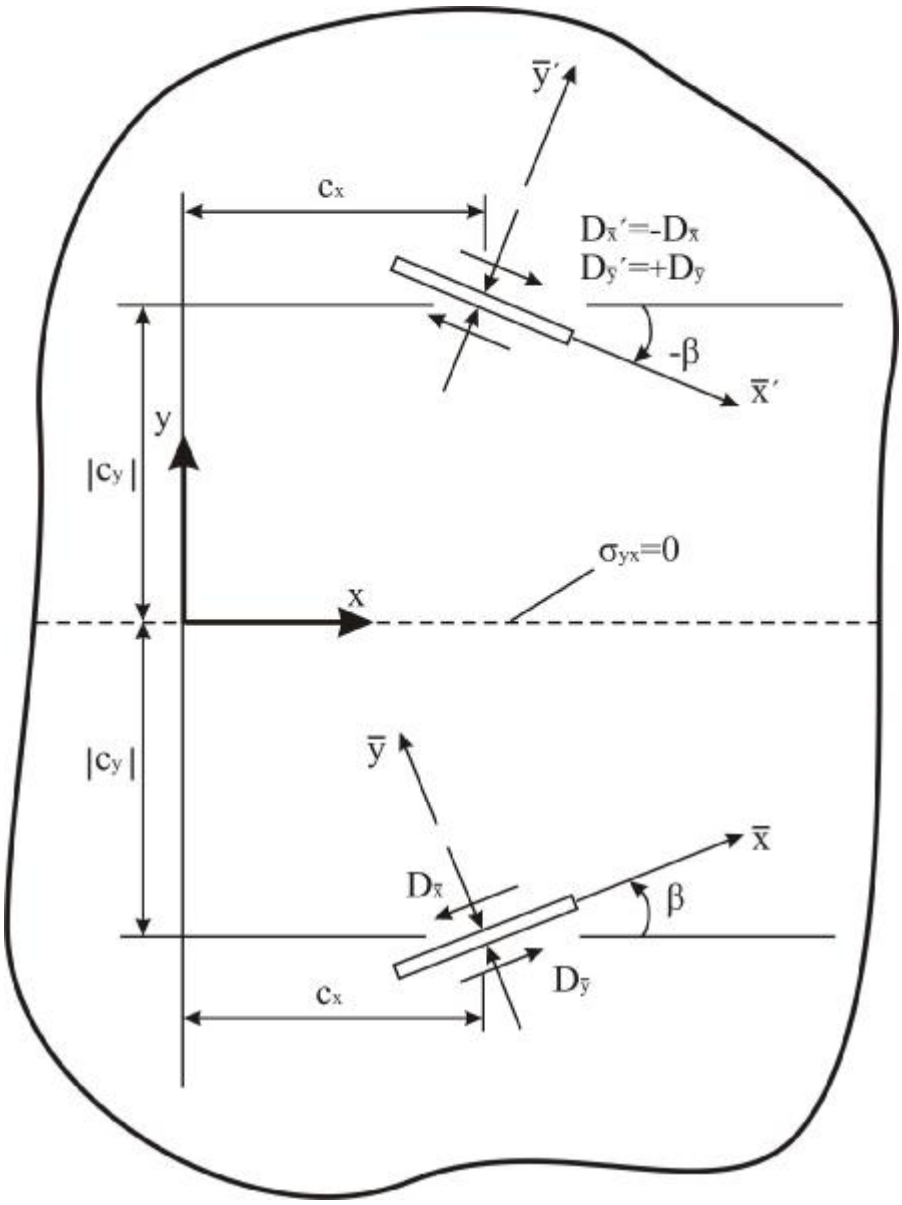

Fig. 2.6. Actual displacement discontinuity and conceptual one

Final summary solution in index notations within x, y plane is:

$$U_i = U_i^A + U_i^I + U_i^S,$$
$$s_{ij} = s_{ij}^A + s_{ij}^I + s_{ij}^S. \qquad (2.33)$$

Index A shows displacements and stresses resulting from actual displacement discontinuity; index I shows those resulting from reflection; and index S shows those developed as a result of complementary solution.

Formulae for displacements and stresses being a part of solution (2.33) are [31]:

$$U_x^A = D_{\bar{x}}[-(1-2n)F_2^A \sin b + 2(1-n)F_3^A \cos b + \bar{y}(F_4^A \sin b - F_5^A \cos b)] +$$
$$+ D_{\bar{y}}[-(1-2n)F_2^A \cos b - 2(1-n)F_3^A \sin b - \bar{y}(F_4^A \cos b + F_5^A \sin b)],$$
$$U_y^A = D_{\bar{x}}[(1-2n)F_2^A \cos b + 2(1-n)F_3^A \sin b - \bar{y}(F_4^A \cos b + F_5^A \sin b)] + \qquad (2.34)$$
$$+ D_{\bar{y}}[-(1-2n)F_2^A \sin b + 2(1-n)F_3^A \cos b - \bar{y}(F_4^A \sin b - F_5^A \cos b)].$$

$$
\begin{aligned}
&s_{xx}^{A} = 2GD_{\bar{x}}[\,2F_4^A \cos^2 b - F_5^A \sin^2 b - \bar{y}(\,F_6^A \cos 2b - F_7^A \sin 2b\,)] + \\
&+ 2GD_{\bar{y}}[-F_5^A - \bar{y}(\,F_6^A \sin 2b + F_7^A \cos 2b\,)], \\
&s_{yy}^{A} = 2GD_{\bar{x}}[\,2F_4^A \sin^2 b - F_5^A \sin 2b - \bar{y}(\,F_6^A \cos 2b - F_7^A \sin 2b\,)] + \\
&+ 2GD_{\bar{y}}[-F_5^A - \bar{y}(\,F_6^A \sin 2b + F_7^A \cos 2b\,)], \\
&s_{xy}^{A} = 2GD_{\bar{x}}[\,F_4^A \sin 2b - F_5^A \cos 2b + \bar{y}(\,F_6^A \sin 2b + F_7^A \cos 2b\,)] + \\
&+ 2GD_{\bar{y}}[-\bar{y}(\,F_6^A \cos 2b - F_7^A \sin 2b\,)].
\end{aligned}
\qquad (2.35)
$$

Where $D_{\bar{x}}$ and $D_{\bar{y}}$ components of displacement discontinuity; and

$2a$ is length of a segment within which displacements are subject to constant in value discontinuity;

$$
F_2^A(\bar{x},\bar{y}) = \frac{\partial f^A(\bar{x},\bar{y})}{\partial \bar{x}}; \qquad F_3^A(\bar{x},\bar{y}) = \frac{\partial f^A(\bar{x},\bar{y})}{\partial \bar{y}};
$$

$$
F_4^A(\bar{x},\bar{y}) = \frac{\partial^2 f^A(\bar{x},\bar{y})}{\partial \bar{x}\partial \bar{y}}; \qquad F_5^A(\bar{x},\bar{y}) = \frac{\partial^2 f^A(\bar{x},\bar{y})}{\partial \bar{x}^2};
$$

$$
F_6^A(\bar{x},\bar{y}) = \frac{\partial^3 f^A(\bar{x},\bar{y})}{\partial \bar{x}\partial \bar{y}^2}; \qquad F_7^A(\bar{x},\bar{y}) = \frac{\partial^3 f^A(\bar{x},\bar{y})}{\partial \bar{x}\partial \bar{y}^3};
$$

$$
\begin{aligned}
f^A(\bar{x},\bar{y}) = F_1(\bar{x},\bar{y}) = -\frac{1}{4p(1-n)}[\,\bar{y}(\,arctg\frac{\bar{y}}{\bar{x}-a} - arctg\frac{\bar{y}}{\bar{x}+a}\,) - \\
-(\bar{x}-a)\ln\sqrt{(\bar{x}-a)^2+\bar{y}^2} + (\bar{x}+a)\ln\sqrt{(\bar{x}+a)^2+\bar{y}^2}
\end{aligned}
$$

Local coordinates $\bar{x}$ and $\bar{y}$ are related to global x and y transformation formulae:

$$
\begin{aligned}
\bar{x} &= (x - c_x)\cos b + (y - c_y)\sin b, \\
\bar{y} &= -(x - c_x)\sin b + (y - c_y)\cos b
\end{aligned}
\qquad (2.36)
$$

Analytic expressions for displacements and stresses caused by reflected displacement discontinuity are similar. They were obtained as a result of complementary solution. Within global coordinate system their total is:

$$
\begin{aligned}
&U_x^I + U_x^S = D_{\bar{x}}\{(1-2n)F_2^I \sin b - 2(1-n)F_3^I \cos b + [(3-4n)(y\sin 2b - \bar{y}\sin b) + \\
&+ 2y\sin 2b\,]F_4^I + [(3-4n)(y\cos 2b - \bar{y}\cos b) - y(1-2\cos 2b)]F_5^I + \\
&+ 2y(y\sin 3b - \bar{y}\sin 2b)F_6^I - 2y(y\cos 3b - \bar{y}\cos 2b)F_7^I\} + D_{\bar{y}}\{(1-2n)F_2^I \cos b + \\
&+ 2(1-n)F_3^I \sin b - [(3-4n)(y\cos 2b - \bar{y}\cos b) - y]F_4^I + \\
&+ (3-4n)(y\sin 2b - \bar{y}\sin b)F_5^I - 2y(y\cos 3b - \bar{y}\cos 2b)F_6^I - \\
&- 2y(y\sin 3b - \bar{y}\sin 2b)F_7^I\};
\end{aligned}
$$

$$U_y^I + U_y^S = D_{\bar{x}}\{-(1-2n)F_2^I \cos b - 2(1-n)F_3^I \sin b - [(3-4n)(y\cos 2b - \bar{y}\cos b) +$$
$$+ y(1-2\cos 2b)]F_4^I + [(3-4n)(y\sin 2b - \bar{y}\sin b) - 2y\sin 2b]F_5^I +$$
$$+ 2y(y\cos 3b - \bar{y}\cos 2b)F_6^I + 2y(y\sin 3b - \bar{y}\sin 2b)F_7^I\} +$$
$$+ D_{\bar{y}}\{(1-2n)F_2^I \sin b - 2(1-n)F_3^I \cos b - (3-4n)(y\sin 2b - \bar{y}\sin b)F_4^I -$$
$$- [(3-4n)(y\cos 2b - \bar{y}\cos b) + y]F_5^I + 2y(y\sin 3b - \bar{y}\sin 2b)F_6^I -$$
$$- 2y(y\cos 3b - \bar{y}\cos 2b)F_7^I\}$$

(2.37)

$$s_{xx}^I + s_{xx}^S = 2GD_{\bar{x}}\{F_4^I - 3(F_4^I \cos 2b - F_5^I \sin 2b) +$$
$$+ [2y(\cos b - 3\cos 3b) + 3\bar{y}\cos 2b]F_6^I + [2y(\sin b - 3\cos 3b) +$$
$$+ 3\bar{y}\sin 2b]F_7^I - 2y(y\cos 4b - \bar{y}\cos 3b)F_8^I - 2y(y\sin 4b - \bar{y}\sin 3b)F_9^I\} +$$
$$+ 2GD_{\bar{y}}\{F_5^I + [2y(\sin b - 2\sin 3b) + 3\bar{y}\sin 2b]F_6^I -$$
$$- [2y(\cos b - 2\cos 3b) + 3\bar{y}\cos 2b]F_7^I -$$
$$- 2y(y\sin 4b - \bar{y}\sin 3b)F_8^I + 2y(y\cos 4b - \bar{y}\cos 3b)F_9^I\};$$

$$s_{yy}^I + s_{yy}^S = 2GD_{\bar{x}}[F_4^I - (F_4^I \cos 2b - F_5^I \sin 2b) -$$
$$(4y\sin b \sin 2b - \bar{y}\cos 2b)F_6^I +$$
$$+ (4y\sin b \cos 2b + \bar{y}\sin 2b)F_7^I + 2y(y\cos 4b - \bar{y}\cos 3b)F_8^I +$$
$$+ 2y(y\sin 4b - \bar{y}\sin 3b)F_9^I] + 2GD_{\bar{y}}[F_5^I - (2y\sin b - \bar{y}\sin 2b)F_6^I +$$
$$+ (2y\cos b - \bar{y}\cos 2b)F_7^I +$$
$$+ 2y(y\sin 4b - \bar{y}\sin 3b)F_8^I - 2y(y\cos 4b - \bar{y}\cos 3b)F_9^I];$$

$$s_{yy}^I + s_{yy}^S = 2GD_{\bar{x}}[F_4^I - (F_4^I \cos 2b - F_5^I \sin 2b) -$$
$$- (4y\sin b \sin 2b - \bar{y}\cos 2b)F_6^I + (4y\sin b \cos 2b - \bar{y}\sin 2b)F_7^I +$$
$$+ 2y(y\cos 4b - \bar{y}\cos 3b)F_8^I + 2y(y\sin 4b - \bar{y}\sin 3b)F_9^I] +$$
$$+ 2GD_{\bar{y}}[F_5^I - (2y\sin b - \bar{y}\sin 2b)F_6^I + (2y\cos b - \bar{y}\cos 2b)F_7^I +$$
$$+ 2y(y\sin 4b - \bar{y}\sin 3b)F_8^I - 2y(y\cos 4b - \bar{y}\cos 3b)F_9^I];$$

$$s_{xy}^{I} + s_{xy}^{S} = 2GD_{\bar{x}}\{ F_4^I \sin 2b + F_5^I \cos 2b + [2y \sin b(1+4\cos 2b) -$$
$$- \bar{y} \sin 2b] F_6^I + [2y \cos b(3-4\cos 2b) + \bar{y} \cos 2b] F_7^I +$$
$$+ 2y(y \sin 4b - \bar{y} \sin 3b) F_8^I - 2y(y \cos 4b - \bar{y} \cos 3b) F_9^I \} +$$
$$+ 2GD_{\bar{y}} [(4y \sin b \sin 2b + \bar{y} \cos 2b) F_6^I - (4y \sin 2b \cos 2b - \bar{y} \sin 2b) F_7^I -$$
$$- 2y(y \cos 4b - \bar{y} \cos 3b) F_8^I - 2y(y \sin 4b - \bar{y} \sin 3b) F_9^I]; \qquad (2.38)$$

In formulae (2.36) - (2.38), the notations are agreed:

$$F_2^I(\bar{x}',\bar{y}') = \frac{\partial f^I(\bar{x}',\bar{y}')}{\partial \bar{x}'}; \qquad F_3^I(\bar{x}',\bar{y}') = \frac{\partial f^I(\bar{x}',\bar{y}')}{\partial \bar{y}'};$$

$$F_4^I(\bar{x}',\bar{y}') = \frac{\partial^2 f^I(\bar{x}',\bar{y}')}{\partial \bar{x}' \partial \bar{y}'}; \qquad F_5^I(\bar{x}',\bar{y}') = \frac{\partial^2 f^I(\bar{x}',\bar{y}')}{\partial \bar{x}'^2} = -\frac{\partial^2 f^I(\bar{x}',\bar{y}')}{\partial \bar{x}'^2};$$

$$F_6^I(\bar{x}',\bar{y}') = \frac{\partial^3 f^I(\bar{x}',\bar{y}')}{\partial \bar{x}' \partial \bar{y}'^2}; \qquad F_7^I(\bar{x}',\bar{y}') = \frac{\partial^3 f^I(\bar{x}',\bar{y}')}{\partial \bar{y}'^3};$$

$$F_8^I(\bar{x}',\bar{y}') = \frac{\partial^4 f^I(\bar{x}',\bar{y}')}{\partial \bar{x}' \partial \bar{y}'^3}; \qquad F_9^I(\bar{x}',\bar{y}') = \frac{\partial^4 f^I(\bar{x}',\bar{y}')}{\partial \bar{y}'^4};$$

$$f^I(\bar{x}',\bar{y}') = -\frac{1}{4p(1-n)} [\bar{y}'(arctg \frac{\bar{y}'}{\bar{x}'-a} - arctg \frac{\bar{y}'}{\bar{x}'+a}) -$$
$$-(\bar{x}'-a) ln\sqrt{(\bar{x}'-a)^2 + (\bar{y}')^2} + (\bar{x}'+a) ln\sqrt{(\bar{x}'+a)^2 + \bar{y}'^2}]$$

$\bar{x}', \bar{y}'$ and x, y coordinates are related with the help of following transformation formulae:

$$\bar{x}' = (x - c_x)\cos b - (y + c_y)\sin b,$$
$$\bar{y}' = (x - c_x)\sin b + (y + c_y)\cos b \qquad (2.39)$$

Summing (2.34) with (2.37), and (2.35) with (2.38) according to (2.33) definition, we obtain formulae of basic solution required to form a source system of equations of considered geomechanical problem.

Divide internal border of considered area (Fig. 2.4) into N elements; compare each j^{th} element with displacement discontinuity components $D_{\bar{x}}^j$ and $D_{\bar{y}}^j$ which provide prescribed boundary displacements and stresses, or conditions of displacement compatibility at joint surfaces within considered area.

Initial set of equations to identify unknown “fictional” displacements is:

$$\left.\begin{aligned}\sum_{j=1}^{N} C_{\bar{x}\,\bar{x}}^{ij} D_{\bar{x}}^{j} + \sum_{j=1}^{N} C_{\bar{x}\,\bar{y}}^{ij} D_{\bar{y}}^{j} = b_{x}^{i} \\ \sum_{j=1}^{N} C_{\bar{y}\,\bar{x}}^{ij} D_{\bar{x}}^{j} + \sum_{j=1}^{N} C_{\bar{y}\,\bar{y}}^{ij} D_{\bar{y}}^{j} = b_{\bar{y}}^{i}\end{aligned}\right\}, i=1, 2,\ldots, N \qquad (2.40)$$

Where $C_{\bar{x}\,\bar{x}}^{ij}, C_{\bar{x}\,\bar{y}}^{ij}$, $C_{\bar{y}\,\bar{x}}^{ij}, C_{\bar{y}\,\bar{y}}^{ij}$ are influence coefficients for displacements or stresses (depending on those prescribed at the boundaries of conditions) determined according to previously mentioned formulae of basic solution.

Physically influence coefficient of stresses $C_{\bar{y}\,\bar{x}}^{ij} = A_{\bar{y}\,\bar{x}}^{ij}$ is stress in i^{th} element in the line of $\bar{y}$, resulting from a singular displacement discontinuity $D_{\bar{x}}^{j} = 1$ of j^{th} element in the line of $\bar{x}$. Similar use belongs to all other coefficients of stress effect.

Thereafter, coefficient of displacement effect $C_{\bar{y}\,\bar{x}}^{ij} = B_{\bar{y}\,\bar{x}}^{ij}$ is a displacement in i^{th} element in the line of $\bar{y}$, resulting from singular displacement discontinuity $D_{\bar{x}}^{j} = 1$ of j^{th} element in the line of $\bar{x}$. The rest coefficients of displacement effect have similar context.

The problem is solved in secondary stresses. It means that composite stresses are equal to a sum of initial ones taking place in a virgin mass, and secondary stresses stipulated by availability of worked-out hole. As within a contour of a stope total stresses are equal to zero, then vertical and horizontal secondary stresses within it are $s_{yy} = -gH$, and $s_{xx} = -lgH$ (g is rock density, t/m^3; $l = \dfrac{n}{1-n}$ is a coefficient of lateral bearing reaction; and n is Poisson ratio of a rock). Hence, right sides in equations of (2.39) set for elements within a working contour are $b_{\bar{x}}^{i} = -lgH$, $b_{\bar{y}}^{i} = -gH$.

There are adequate equations for contact surface of coal bed with a rock, and broken rock with virgin mass. The equations are a part of (2.40) set having a meaning of displacement compatibility conditions.

If i and i^* are numbers of contacting elements belonging to different areas, then in the process of establishing displacement compatibility conditions within stresses on a joint contour C_{κ}, and in displacements on a joint contour C_l the conditions are:

$$\left.\begin{aligned} s_{\bar{x}}^{i} = s_{\bar{x}}^{i[k]} - s_{\bar{x}}^{i^*[1]} = 0, \quad s_{\bar{y}}^{i} = s_{\bar{y}}^{i[k]} - s_{\bar{y}}^{i^*[1]} = 0 \\ b_{\bar{x}}^{i} = u_{\bar{x}}^{i[1]} + u_{\bar{x}}^{i^*[k]} = 0, \qquad b_{\bar{y}}^{i} = u_{\bar{y}}^{i[1]} + u_{\bar{y}}^{i^*[k]} = 0 \end{aligned}\right\} \qquad (2.41)$$

Gauss method is applied to solve (2.37) equations set. As a result, displacement discontinuities $D_{\bar{x}}^{j}$ and $D_{\bar{y}}^{j}$ are determined; according to formulae of analytical solution (2.34), (2.35), (2.37), and (2.38) by means of summing up scores of each obtained $D_{\bar{x}}^{j}$ and $D_{\bar{y}}^{j}$, stresses and displacements are determined in any point of considered mass including those at the surface.

To identify hardness parameters of enclosing rocks of layered mass, the algorithm involves ability to make mathematical experiment being a solution of a number of problems for weighty homogeneous mass with various physical and mechanical characteristics. Relying on stratigraphic column being typical for considered conditions, properties of parent rocks (argillite, aleurite, sandstone etc.) were alternately ascribed to the mass. $\frac{L}{H}=\frac{2D}{H}$ parameter is varied from 0.3 to 1.1.

Each time, calculation regarding stress-strain state of considered area of the mass was performed up to such $\frac{L}{H}(L=2D)$ values at which maximum convergence at earth's surface-maximum roof closure of mineable layer ratio $\frac{h_{max}}{h_0}$ becomes close to 1 (up to the state of complete undermining). Then c_i parameter is determined with the help of Gauss function table (2.22) of ratio

$$\frac{h_{max}}{h_0}=-F\left(\frac{L}{c_i H}\right), \tag{2.42}$$

obtained from (2.23) if $x=0$, and $y=H$.

Such a calculation for mining and geological conditions of mines in Western Donbass was performed with regard to generalized lithological column according to C_6 and C_6^1 coal layers shown in Fig. 1.2.

Such physical and mechanical characteristics as elastic moduli E, MPa, unit weights g, t/m^3, and Poisson ratios n, washes, coal, and enclosing rocks used as initial data are in Table 1.2.

For decomposed rocks, characteristics were taken according to paper [29] data; they were E_p =10 MPa, n_p =0.499, and g =1.5 t/m^3.

Creep parameters taken into account in the process of calculating elastic moduli at the t moment being that of complete undermining are in Table 1.3.

Results of calculations performed are in Table 2.1. Values of hardness parameters c_i are obtained without taking into account rheologic processes, and c_{ti} - with taking into account rock creep. The latter were obtained for a case when mining depth is H =400 m, and average stope advance is V =60 meters per month.

Table 2.1

Hardness parameters of coal and enclosing rocks

Rock	Argillite	Aleurolite	Sandstone	Coal
c_i^2	0.056	0.066	0.108	0.073
c_i	0.236	0.257	0.329	0.270
c_{ti}^2	0.008	0.017	0.040	0.033
c_{ti}	0.088	0.130	0.200	0.181

If two-layered medium "washes-carbon", we have: C_{κ}^2 =0.075, C_{κ} =0.275 and $C_{t\kappa}^2$ =0.019, and $C_{t\kappa}$ =0.137 for carbon (determined as average values according to Table 2.1), and C_H^2 =0.0011, C_H =0.033 and C_{tH}^2 =0.00062, and C_{tH} =0.0249 for washes (determined according to recommendations of All-Union Institute of Mine Surveying [16]).

Hence, the algorithm is useful while performing mathematical experiment; that is while solving a number of problems for homogeneous mass. However, its abilities are broader. It also proves determining stress-strain state of rock mass and earth's surface taking into account layering in calculation model.

Following problem of earth's surface convergence with the use of a model of "washes-carbon" two-layered medium is an example. Basically, greater number of layers is possible.

2.5 Calculation of earth's surface convergence depending upon a distance of a stope from face entry

To develop displacement basins at earth's surface of layered homogenous mass depending upon a distance of a stope from face entry apply calculation model shown in Fig. 2.7. It covers a layer of washes, carbon (single layer with averaged properties of enclosing rocks), coal bed, a stope, and worked-out space with decomposed rocks. Weight of rocks is actual load.

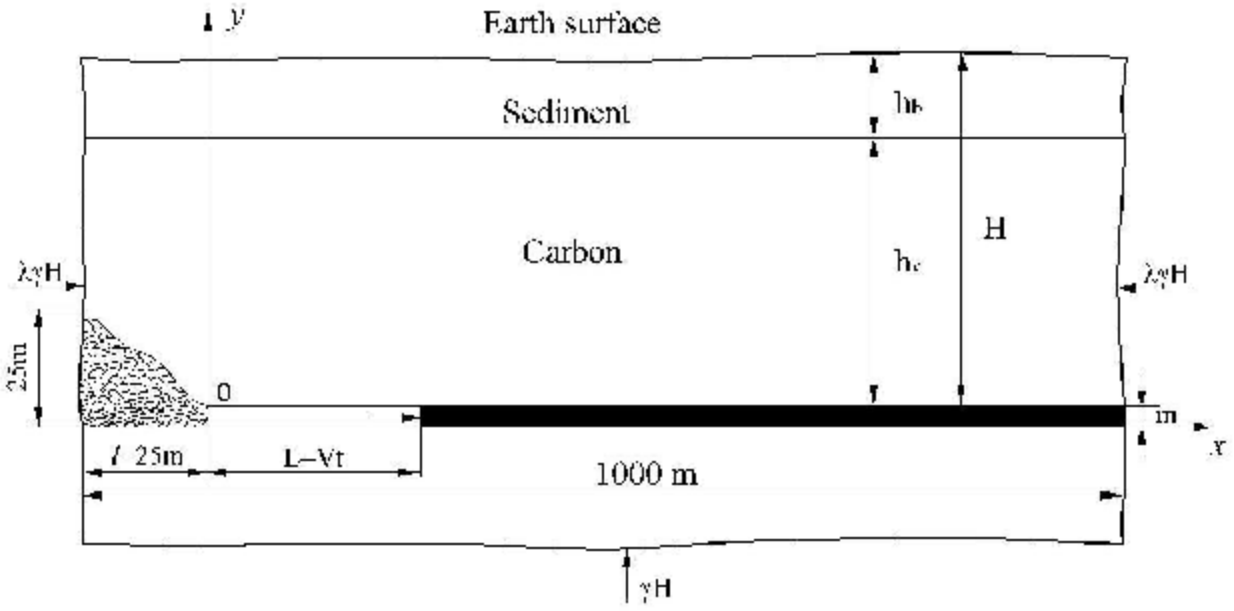

Fig. 2.7. Calculation model

Perform calculation for mining and geological conditions of mines in Western Donbass if initial data are:

h_H =140 m;

H=400 m;
Mineable layer thickness is m =1.0 m; and
Average stope advance is V =60 meters per month.
Properties of coal and enclosing rocks are in Table 2.2.

Table 2.2

Properties of coal and enclosing rocks

Rock	Unit weight, g, t/m^3	Elasticity modulus, $E \cdot 10^{-3}$, MPa	Poisson ratio, n	Creep parameters	
				$d \cdot 10^3$, c^{a-1}	a
Washes	1.5	0.07	0.3	13.9	0.862
Carbon	2.76	3.18	0.3	6.84	0.7
Decomposed rocks	1.5	0.01	0.499	-	-
Coal	1.47	20	0.35	2.32	0.7

Data for carbon shown in Table 2.2 are determined as average values of adequate characteristics of enclosing rocks (argillite, aleurolite, sandstone, and limestone).

Developing displacement basin at the earth's surface being formed above advancing front of mining was performed according to superposition principle. What this means is that the surface point displacement was determined as a total of certain "elementary" mined components effect. Length of such a component was assumed as that equal to a caving step of the main roof. It is 10 to 22 mm under considered conditions [86].

Fig. 2.8 shows displacement basins developed according to calculation data.

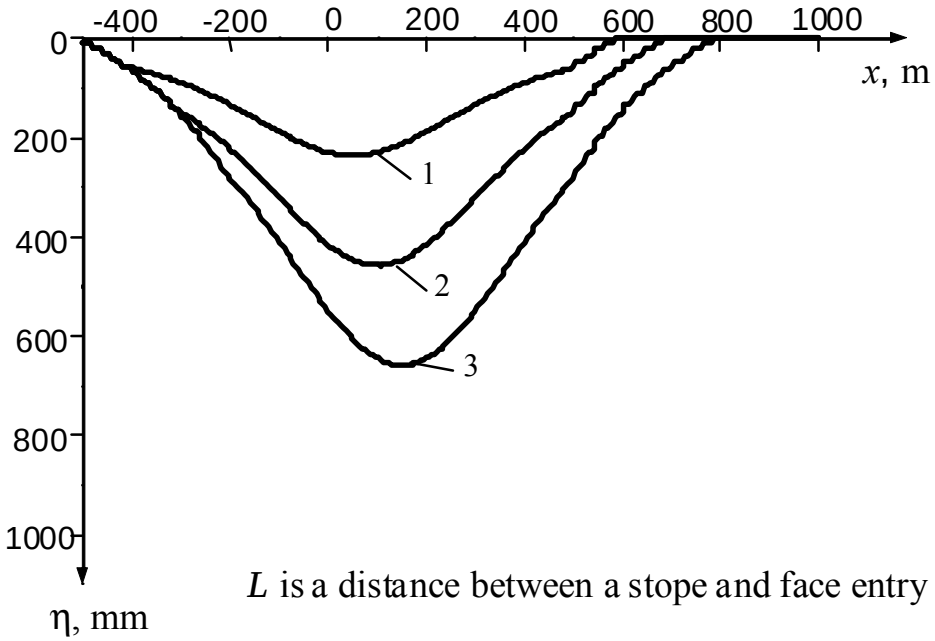

Fig. 2.8. Displacement basins at different locations of a stope:1 – L/H=0.25; 2 - L /H=0.5; 3 - L /H=0.75.

Figs 2.9 a) and b) show curves of calculated convergences and horizontal displacements within principal cross-section of a basin at the surface when complete undermining under considered conditions. Full lines are data of calculation performed without rock creep consideration; dashed lines take the factor into consideration.

Fig. 2.9 a) shows that in time convergence line is smoothed out; in this context, displacement values become 10 to 25% more to compare with calculation data which don't take into account rheological properties of rocks; within basin salvages they become similarly less.

It is possible to note the following in relation to horizontal displacements. In time, a form of curve $x(x)$ stays unchangeable. Only scale varies: $x(x)$ values become 2.1 less.

a)

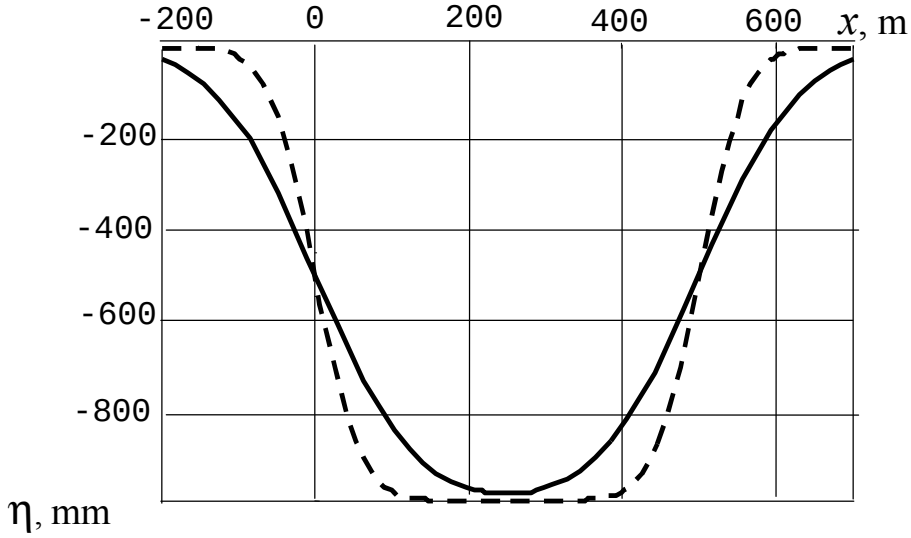

b)

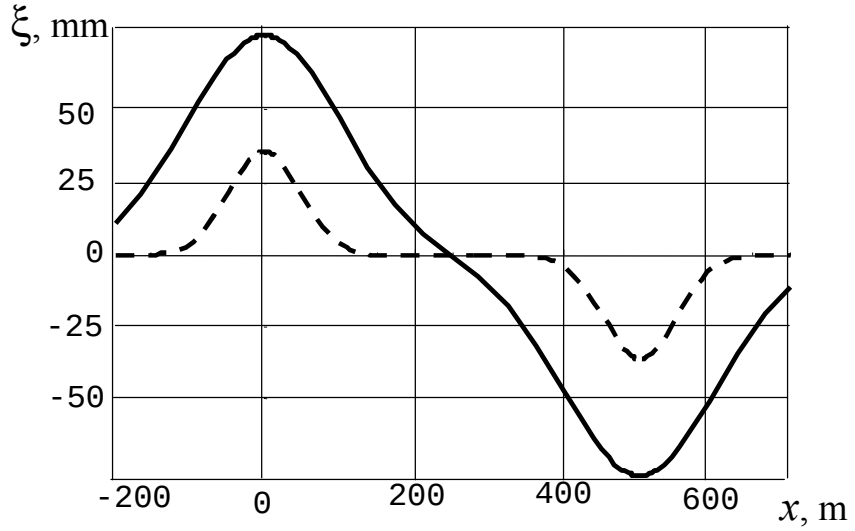

Fig. 2.9. Displacements within a principal cross-section of a basin of the earth's surface: a) – convergences; b) – horizontal displacements

Basing upon data statistic analysis of the calculation, there is defined correlation dependence of maximum convergences on $z = \frac{L}{H}$ parameter characterizing distance of a stope from a face entry:

$$\frac{h_{max}(z)}{h_0} = -5{,}021z^3 - 9{,}271z^2 + 97{,}72z - 0{,}2284, \qquad (2.43)$$

Where h_0 is maximum roof sag when complete undermining;

$z = \frac{L}{H} \in [0{,}05...1{,}25]$.

R=0.99 is correlation parameter of the dependence.

Fig. 2.10 shows $\frac{h_{max}(z)}{h_0}$ curve developed on (2.43) ratio. Points mean data of adequate calculation variations.

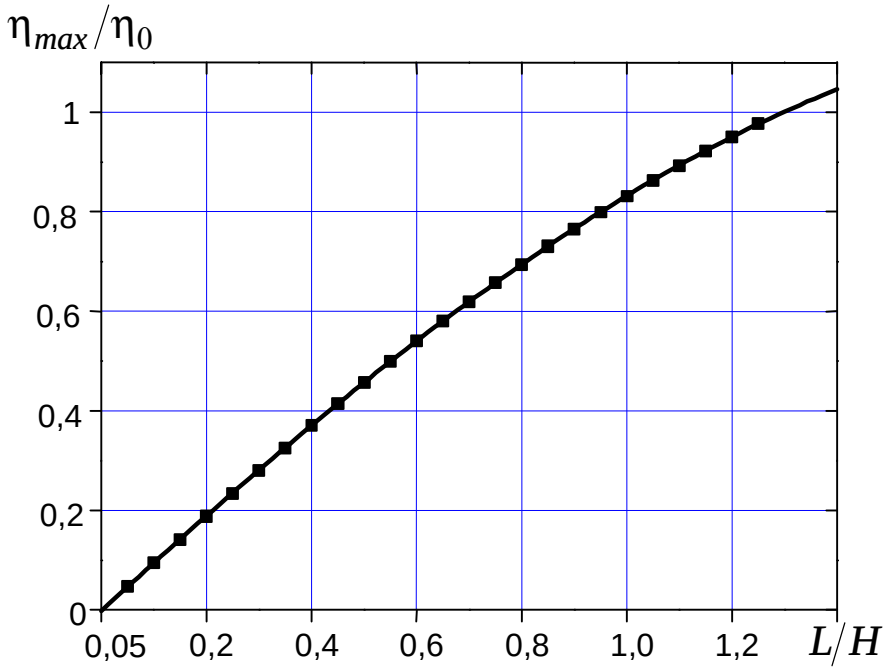

Fig. 2.10. Maximum basin convergences depending upon different locations of a stope

2.6 Analytical solution for two-layer mass taking into account a store advance

While researching displacement processes it is important to know distribution of earth's surface points convergence rate in the process of a stope displacement.

One of the methods to obtain quantitative assessment is to solve plane problem of rock mechanics for "washes-carbon" two-layered mass under boundary (initial) conditions by analogy with information from section 2.1 for homogenous medium without taking into consideration a stope advance.

Similar shot was taken by us in a paper [100]. Initial differential equation (2.6) was solved under following boundary conditions:

$$f(x)=\begin{cases} 0, & x<0,\ x>Vt+l, \\ -h_0=-m, & 0<x<Vt, \\ -\dfrac{h_0}{l}(l+Vt-x), & Vt<x<Vt+l, \end{cases} \tag{2.44}$$

The conditions assume that main roof caving l is known; they give adequate description to the main roof break implemented under conditions close to complete undermining at rather great distance $L=Vt$ between a working face and a face entry.

These very conditions are of interest from the viewpoint of identifying factors of earth's surface strain state if mining takes place under protected objects.

On the other hand it is of interest to calculate caving step of a stope roof. To do that, it is required to see about rock changes in the neighbourhood of a stope in an initial stage of mining to find out convergence dependence $h(x,y)$ within the main roof on the most important influencing factors. Hence, it is essential to develop analytical solution encompassing the whole period of mining – from the very beginning up to complete undermining.

The theoretical research and field studies show that $L=Vt$ (dimension of a stope) as well as maximum closure rate $U_{max\,кр}$ - a stope advance ratio are the determinants in a displacement process.

The factors should be reflected in boundary conditions to obtain target analytic expressions for strain state factors providing their determination in any point of rock strata and earth's surface at any stage of mining.

If we assume in this context that rock fault in a face subjects to exponential law depending upon maximum closure rate in a face-its advance and distance between a stope and a face entry ratio, write it down as:

$$h(x,y)\big|_{y=0}=f(x)=\begin{cases} 0 \quad , & x<0, \quad x>L \\ -h_0(1-exp(-aL)), & 0<x<L \end{cases} \tag{2.45}$$

Origin of coordinates aligns with the extreme left section of a stope (Fig. 2.7).

Parameter a being a part of (2.45) conditions is a function of maximum speed of rock fault U_{max} in a longwall – rate of advance V ratio being determined in accordance with underground investigations data.

The paper uses data of instrumental measurements in the process of layer C_6 mining by 117th longwall of "Stepnaia" mine of "Pavlogradugol" OJSC over the July to December 2002 period.

While mining, rate of advance during investigation varied within 40-60 m par month, and measured background values of rock fault speed in a midsection of the longwall were within 0.02-0.06 mm per minute. In this context, if rock fault speed is U=0.03 mm per minute, and rate of advance is V=40 m per month, then a parameter was 0.038, and if U=0.03 mm par minute and V=60 m per month, then a=0.03 [86].

Partial solution of differential equation (2.6) matching boundary conditions (2.45) is developed from general solution (2.18) being:

$$h(x,y) = -\frac{h_0}{2\sqrt{p\,j(y)}}\int_0^L (1-exp(-aL))exp\left(-\frac{(x-x)^2}{4j(y)}\right)dx = \left\{\frac{x-x}{2\sqrt{j(y)}} = z\right\} =$$

$$= -\frac{h_0}{2\sqrt{p\,j(y)}} 2\sqrt{j(y)} \int_{-\frac{x}{2\sqrt{j(y)}}}^{\frac{L-x}{2\sqrt{j(y)}}} exp(-z^2)dz =$$

$$= -\frac{h_0}{2}(1-exp(-aL))\left[\Phi\left(\frac{L-x}{2\sqrt{j(y)}}\right) + \Phi\left(\frac{x}{2\sqrt{j(y)}}\right)\right], \qquad (2.46)$$

Where $$\Phi(z) = \frac{2}{\sqrt{p}}\int_0^z exp(-t^2)dt \qquad (2.47)$$

$j(y)$ function in expression (2.46) is determined with the help of (2.32) formulae.

Abscissa of a point with maximum convergence is determined from a condition of equality to zero of (2.46) derivative in this way:

$$\frac{\partial h}{\partial x} = 0 \Rightarrow -\frac{h_0}{2}(1-exp(-aL))\frac{2}{\sqrt{p}}\left[exp\left(-\frac{(L-x)^2}{4j(y)}\right)\cdot\left(-\frac{1}{2\sqrt{j(y)}}\right) + \right.$$

$$\left. + exp\left(-\frac{x^2}{4j(y)}\right)\cdot\frac{1}{2\sqrt{j(y)}}\right] = 0 \Rightarrow exp\left(-\frac{(L-x)^2}{4j(y)}\right) - exp\left(-\frac{x^2}{4j(y)}\right) = 0 \Rightarrow$$

$$exp\left(-\frac{x^2}{4j(y)}\right)\cdot\left[exp\left(-\frac{(L^2-2Lx)}{4j(y)}\right) - 1\right] = 0 \Rightarrow$$

$$exp\left(-\frac{(L^2-2Lx)}{4j(y)}\right) = 1 \Rightarrow -\frac{(L^2-2Lx)}{4j(y)} = 0 \Rightarrow x = \frac{L}{2}$$

Substituting $x = \frac{L}{2}$ and $y = H$ to (2.46) expression we obtain a formula to determine a value of maximum convergence at the earth's surface in the form of

$$h_{max} = -h_0(1-exp(-aL))\cdot\Phi\left(\frac{L}{4\sqrt{j(H)}}\right) \qquad (2.48)$$

If one knows deflection function (2.46), then known differential relations help to obtain easily falls and degrees of convergence curves within mass taking into account advance rate.

Adequate analytical expressions are:

$$i(x,y)=\frac{\partial h}{\partial x}=\frac{h_0(1-exp(-aL))}{2\sqrt{pj(y)}}\left[exp\left(-\frac{(L-x)^2}{4j(y)}\right)-exp\left(-\frac{x^2}{4j(y)}\right)\right] \quad (2.49)$$

$$k(x,y)=\frac{\partial^2 h}{\partial x^2}=\frac{h_0(1-exp(-aL))}{4\sqrt{pj(y)}}\left[(L-x)exp\left(-\frac{(L-x)^2}{4j(y)}\right)+x\cdot exp\left(-\frac{x^2}{4j(y)}\right)\right] \quad (2.50)$$

$$x(x,y)=-K(y)\frac{\partial h}{\partial x}=\frac{-K(y)(1-exp(-aL))}{2\sqrt{pj(y)}}\left[exp\left(-\frac{(L-x)^2}{4j(y)}\right)-exp\left(-\frac{x^2}{4j(y)}\right)\right] \quad (2.51)$$

Formulae for maximum falls, curvatures and horizontal displacements at the earth's surface are obtained by analogy with those made in the process of deflection function analysis. Only equations used to determine coordinates of possible extermum points (conditions of equality to zero of adequate derivatives) for those factors of deformed state of mass were rather complicated; that's why they were solved numerically.

We have:

$$\frac{\partial i}{\partial x}=0\Rightarrow(L-x)exp\left(-\frac{(L-x)^2}{4j(y)}\right)+x\cdot exp\left(-\frac{x^2}{4j(y)}\right)=0\Rightarrow$$

$$(L-x)exp\left(-\frac{L^2-2Lx}{4j(y)}\right)+x=0\Rightarrow$$

$$x\cong L$$

Hence,

$$i_{max}=\frac{-h_0(1-exp(-aL))}{4\sqrt{j(H)}}\left[\Phi'\left(\frac{L}{2\sqrt{j(H)}}\right)-\Phi'(0)\right] \quad (2.52)$$

$$\frac{\partial K}{\partial x}=0\Rightarrow-exp\left(-\frac{(L-x)^2}{4j(y)}\right)+\left(\frac{(L-x)^2}{2j(y)}\right)exp\left(-\frac{(L-x)^2}{4j(y)}\right)+exp\left(-\frac{x^2}{4j(y)}\right)-$$

$$-\frac{x^2}{2j(y)}exp\left(-\frac{x^2}{4j(y)}\right)=0\Rightarrow$$

$$exp\left(-\frac{(L-x)^2}{4j(y)}\right)\left(\frac{(L-x)^2}{2j(y)}-1\right)+exp\left(-\frac{x^2}{4j(y)}\right)\left(1-\frac{x^2}{2j(y)}\right)=0\Rightarrow$$

$$exp\left(-\frac{L^2-2Lx}{4j(y)}\right)\left((L-x)^2-2j(y)\right)+\left(2j(y)-x^2\right)=0\Rightarrow$$

$$x\cong 0{,}8L$$

$$K_{max}=\frac{h_0(1-exp(-aL))}{8j(H)}\left[\Phi''\left(\frac{0{,}4L}{\sqrt{j(H)}}\right)+\Phi''\left(\frac{0{,}1L}{\sqrt{j(H)}}\right)\right] \quad (2.53)$$

Abscissa of a point in which originates x_{max}, coincides with coordinate of inclination maximum point; that is $x \cong L$.

Then,

$$x_{max} = \frac{K(H)h_0(1-exp(-aL))}{4\sqrt{j(H)}}\left[\Phi'\left(\frac{L}{2\sqrt{j(H)}}\right)-\Phi'(0)\right] \qquad (2.54)$$

Differentiating convergence function (2.46) in t time taking into consideration $L = Vt$, we develop the expression for convergence speed

$$U(x,y)=\frac{\partial h}{\partial t}=-\frac{h_0 V}{2}\left\{\begin{array}{l} a\cdot exp(-aL)\frac{2}{\sqrt{p}}\left[\Phi\left(\frac{L-x}{2\sqrt{j(y)}}\right)+\Phi\left(\frac{x}{2\sqrt{j(y)}}\right)\right]+ \\ +\frac{1}{\sqrt{pj(y)}}(1-exp(-aL))exp\left(-\frac{(L-x)^2}{4j(y)}\right) \end{array}\right\} \qquad (2.55)$$

To determine coordinates of x point in which maximum convergence at the earth's surface takes place, we have:

$$\frac{\partial U}{\partial x}=0 \Rightarrow -\frac{\partial}{\partial x}\left(\frac{\partial h}{\partial x}\right)=\left\{-\frac{h_0 V}{2}a\cdot exp(-aL)\frac{2}{\sqrt{p}}\left[-\frac{1}{2\sqrt{j(H)}}exp\left(-\frac{(L-x)^2}{4j(H)}\right)+\right.\right.$$

$$\left.\left.+\frac{1}{2\sqrt{j(H)}}exp\left(-\frac{x^2}{4j(H)}\right)\right]+\frac{1}{\sqrt{pj(H)}}(1-exp(-aL))\frac{L-x}{2j(H)}exp\left(-\frac{(L-x)^2}{4j(H)}\right)\right\}=$$

$$=\frac{h_0 V}{\sqrt{pj(H)}}\left\{2a\cdot exp(-aL)exp\left(-\frac{x^2}{4j(H)}\right)-\right.$$

$$\left.-\left[2a\,exp(-aL)-\frac{L-x}{j(H)}(1-exp(-aL))\right]\cdot exp\left(-\frac{(L-x)^2}{4j(H)}\right)\right\}=0 \Rightarrow$$

$$=2a\cdot exp(-aL)exp\left(-\frac{x^2}{4j(H)}\right)-$$

$$-\left[2a\,exp(-aL)-\frac{L-x}{j(H)}(1-exp(-aL))\right]\cdot exp\left(\frac{-L^2-2Lx-x^2}{4j(H)}\right)=0 \Rightarrow$$

$$2a-\left[2a-\frac{L-x}{j(H)}(exp(-aL)-1)\right]\cdot exp\left(\frac{-L^2-2Lx}{4j(H)}\right)=0 \qquad (2.56)$$

Numerical solution of (2.56) equation results in $x \cong L$.

Substituting $x = L$ to (2.55) expression, we get:

$$U_{max} = \frac{h_0 V}{2}\left\{a \cdot exp(-aL)\Phi\left(\frac{L}{2\sqrt{j(H)}}\right) - \frac{h_0 V}{4\sqrt{j(H)}}(1-exp(-aL))\Phi'(0)\right\} \quad (2.57)$$

To obtain maximums of earth's surface deformation in terms of complete undermining, $h_0 = m$ and $L = H$ should be inserted into (2.48), (2.52), (2.53), (2.54), and (2.57) formulae.

2.7 Results analytical determination of the earth's surface convergence, and impact assessment of determinants

The dependences obtained for mining and geological conditions of mines in Western Donbass, displacement curves, curves of displacement velocities, curves of falls and curvatures of a convergence curves at the earth's surface of two-layered mass under various values of determinants have been described. Analyze main results.

Fig. 2.11 gives graphic pictures of dependences of maximum convergences in a basin at the earth's surface of h/H ratio if L=200 m for various mining depths.

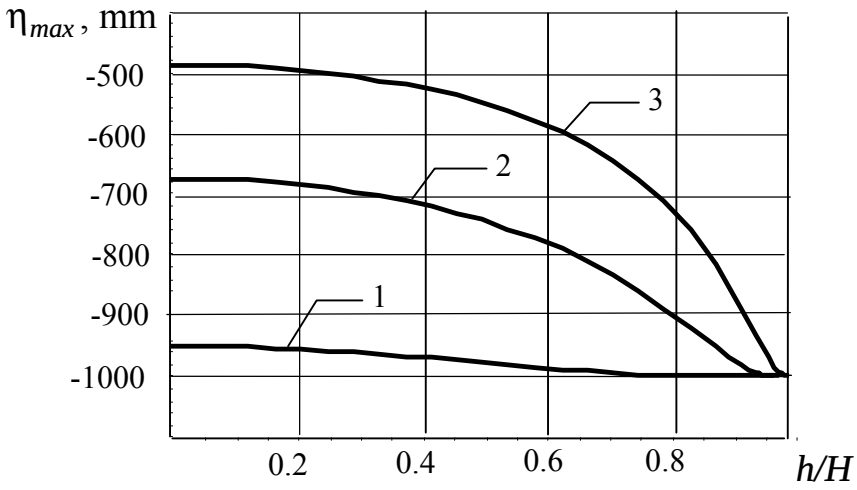

Fig. 2.11 Maximum convergences in a basin at the earth's surface depending on h/H parameter if L=200 m, and on various mining depths: 1 – H = 200 m; 2 – H = 400 m; and 3 – H =600 m.

As expected, h_{max} decreases if H depth deepens. Among other things, under similar ratio (h/H = 0.35 and L= 200 m, h_{max}= 700 mm, if H=400 m and h_{max}= 520 mm if H=600 m) that is in terms of partial undermining, h_{max} becomes 1.35 times less if mining depth deepens.

To a smaller degree, capping thickness affects h_{max} value of partial undermining. Hence, if capping thickness is h=140 m, L=200 m, and mining depth is H= 400 m (h/H=0.35) h_{max}=700 mm, and if h=250 m, L=200 m, and

H=400 m (h/H=0.63) – h_{max}=800 mm; that is 1.78 increase in capping thickness results in 1.14 times increase of h_{max}.

Figs 2.12, 2.13, and 2.14 represent settling curves in a basin at the surface for such L parameters as 50, 100, and 200 m accordingly if capping thickness is h=140 m, H=400 m and values of a stope advance rate are similar; it is obvious that V influences settling values greatly at initial mining stage only. If L=50 m, then settling curves going with various rates of advance differ drastically. That is: in this context 1.3 to 2.7 times increase of V results in 1.2 to 1.5 times decrease of h_{max} (Fig. 2.12). Under L=100 m and similar advance rate h_{max} becomes 1.09 to 1.1 times less (Fig. 2.13); if L=200 m, then curves are practically merged (Fig. 2.14).

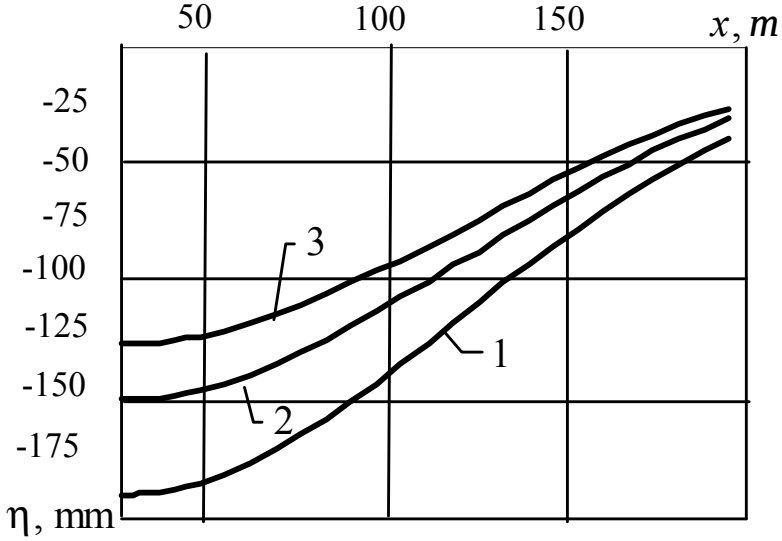

Fig. 2.12. Surface convergence in a basin if $L=50$ m under various rates of advance: 1 – $V=30$ m per second; 2 – $V=60$ m per second; 3 – $V=80$ m per second.

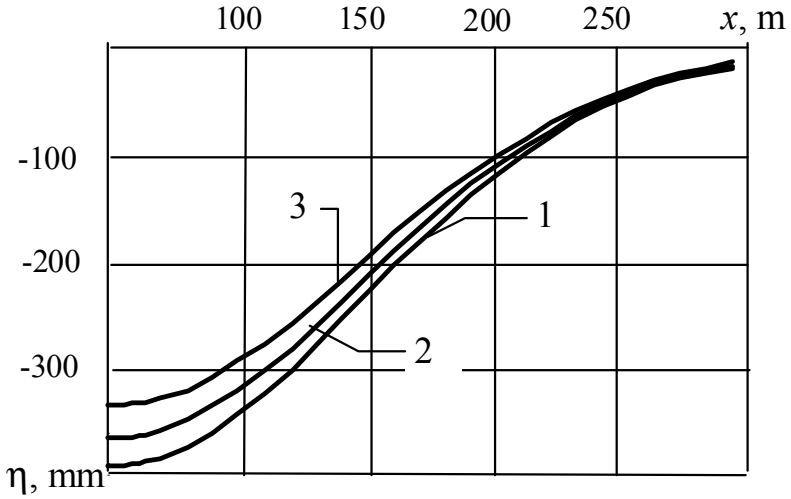

Fig. 2.13. Surface convergence in a basin if $L=100$ m under various rates of advance: 1 – $V=30$ m per month; 2 – $V=60$ m per month; 3 – $V=80$ m per month.

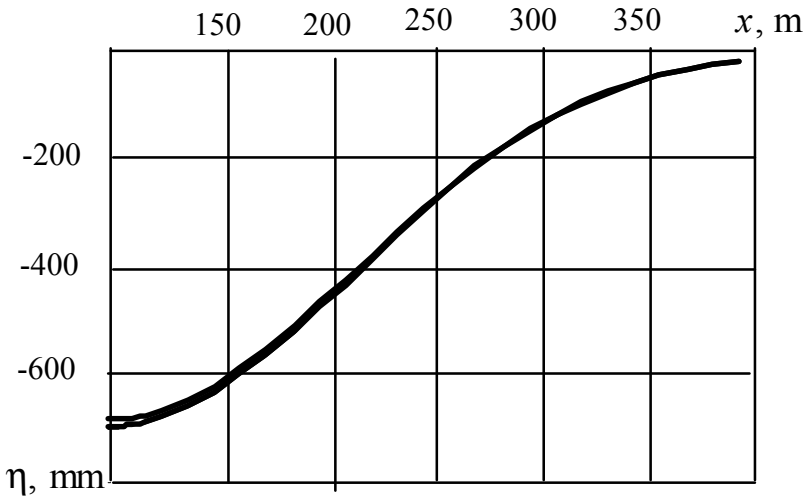

Fig. 2.14. Surface convergence in a basin if $L = 200$ m under various rates of advance.

Fig. 2.15 shows that assigned mining depth H under the conditions of incomplete undermining results in increase of maximum convergence if capping thickness h increases. Moreover, the less L is the greater changes are. If L=50 m, then 1.3 times increase of h ($0.6H$ to $0.8H$), and h_{max} experiences 1.23 times increase. If L=200 m, such and increase of h can not involve drastical changes of h_{max}.

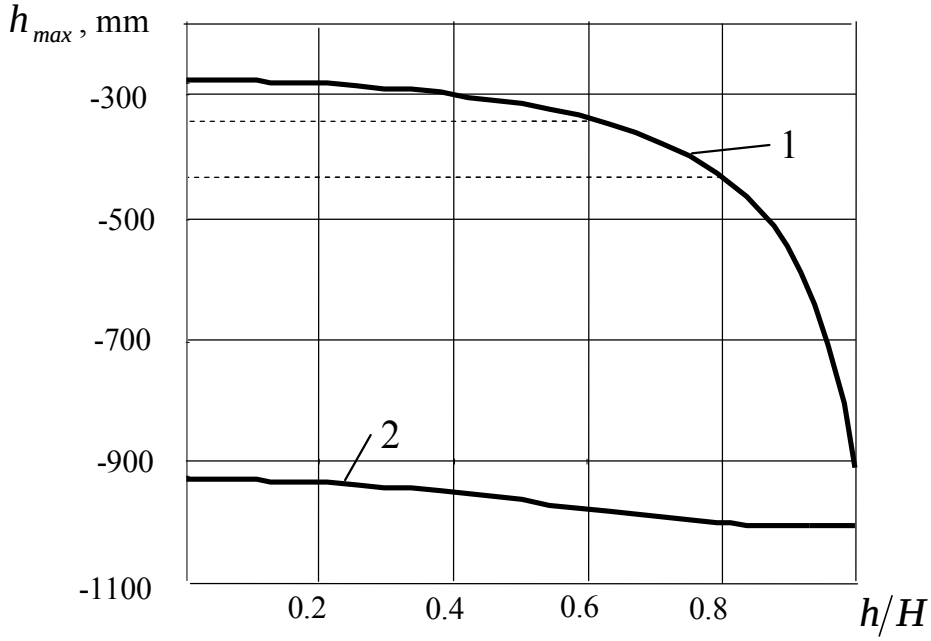

Fig. 2.15. Dependence of maximum convergence on h/H parameter under H =400 m and various parameters of L: 1 - $L = 50$ m; and 2 - $L = 200$ m.

As the results of performed calculations show, under the conditions of complete undermining (H=400 m, and $L=500$ m), cappings can not affect h_{max} value. In this context h/H h_{max} = 1.000 mm under any parameter.

Convergence curves $h(x)$ of earth's surface for L=400 m, V=60 m per month, and h=140 m if mining depth H is different (Fig. 2.16) imply the fact that in terms of complete undermining (curve 1) each bottom point of a basin formed convergences are maximum. The value is equal to thickness m of a seam being mined.

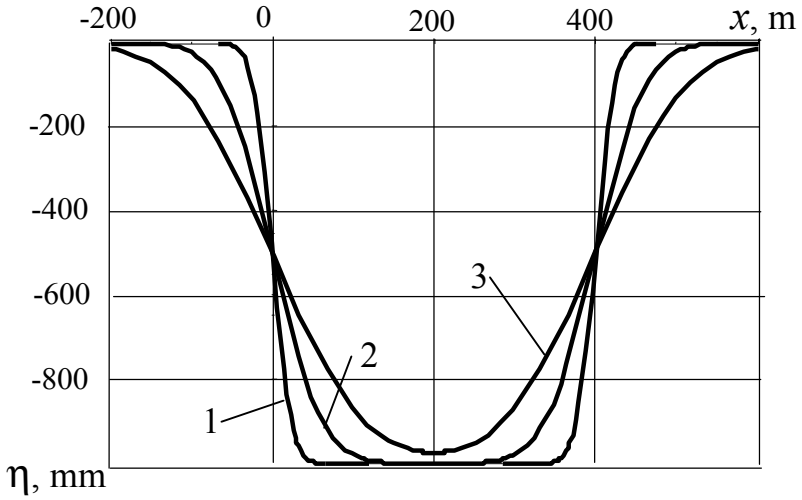

Fig. 2.16. Convergences at the earth's surface under various mining depths: 1 – $H=200$ m; 2 – $H=400$ m; and 3 – $H=600$ m.

Fig. 2.17 gives graphical picture of maximum horizontal displacements on h/H ratio in a basin at the earth's surface (within $x=L$ point) if V=60 m per month under the conditions of complete undermining (H=400 m, and L=500 m). It is seen that despite maximum convergence, horizontal displacement decreases greatly depending on increase in capping thickness h: if h increases 1.7 times (0.35H to 0.6H) x_{max} decreases 1.4 times.

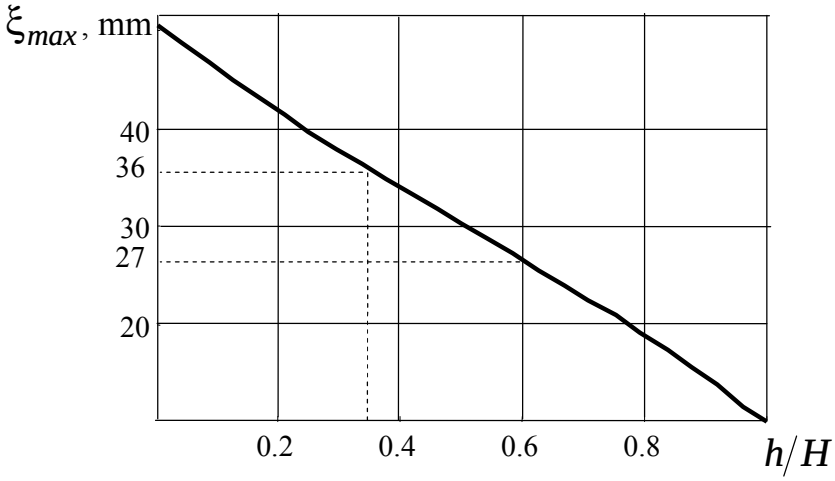

Fig. 2.17. Maximum horizontal displacements in a basin at the earth's surface in terms of complete undermining.

Fig. 2.18 shows curves of maximum horizontal displacement of both h/H parameter at H=400 m mining depth, and V=60 m per month advance rate for the two values of a stope dimensions being L=100 m and L=200 m. It follows that x_{max} increase with increase of a stope dimensions, and decreases with increase of capping thickness in both cases. 1.3 times h increase ($0.6H$ to $0.8H$) involves 1.33 times decrease of x_{max}.

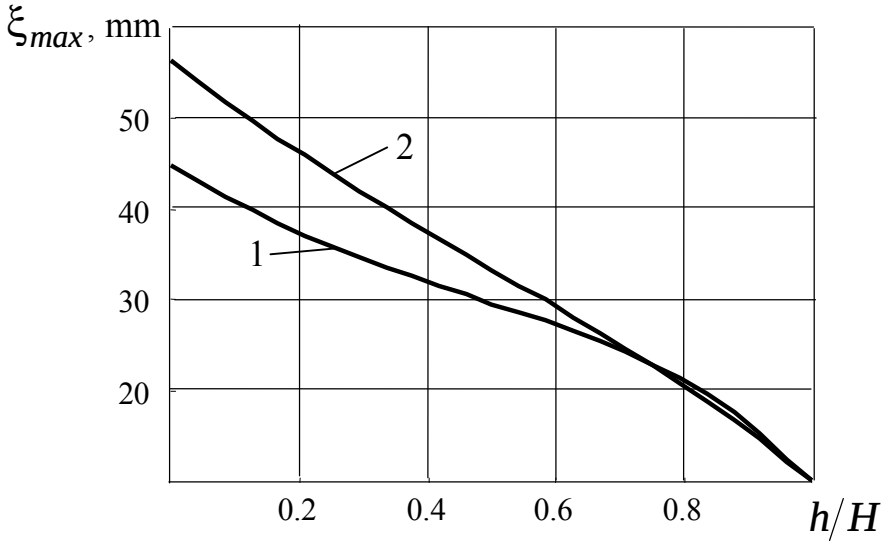

Fig. 2.18. Maximum horizontal displacements within a basin at the earth's surface in terms of incomplete undermining: 1 – $L=100$ m; and 2 – $L=200$ m.

Calculations show that when a stope dimension is L=250 m, then maximum horizontal displacements $x_{max}(h/H)$ become invariable. Proper values are kept up to complete undermining.

Hence, in terms of conditions concerned x_{max} is 40 mm under complete undermining (H=400 m, h=140 m, L=500 m, and V=60 m per month).

Calculations neglecting creeping were also performed to assess the effect of rheological properties of rocks. Similar qualitative situation shaped, and values of horizontal displacements proved to be 1.5 to 1.53 times less.

Fig. 2.19 shows curves of horizontal displacements along x coordinate. The calculations were performed by (2.51) formula if h = 140 m, L= 200 m, V=60 m per month when mining depth was H=200, 400, and 600 m.

As the Fig. shows, the curves shape stays invariable despite depth variation, and displacement values x_{max} decrease with H increase: if H=200 m they are 1.6 times more than if H=600 m.

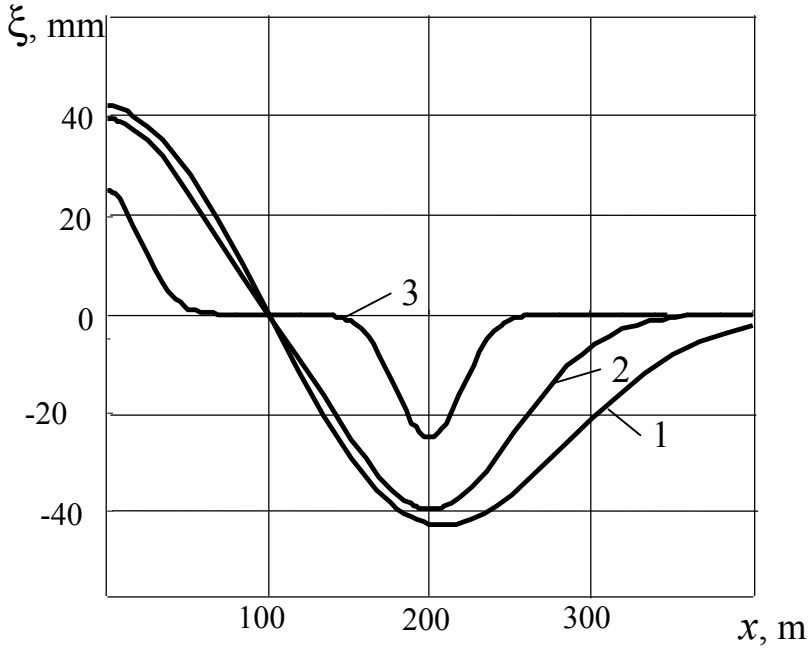

Fig. 2.19. Horizontal displacements of the earth's surface points at various values of mining depth: 1 – $H = 200$ m; 2 – $H = 400$ m; and 3 – $H = 600$ m.

Fig. 2.20 shows changes in horizontal displacements depending upon x coordinates at different values of L if H =400 m and h=140 m.

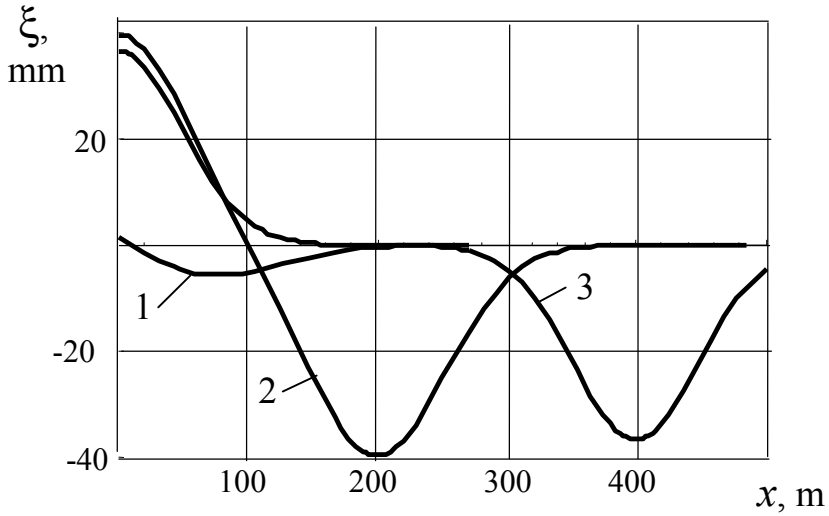

Fig. 2.20.Horizontal displacements within a basin at the earth's surface depending upon x coordinate: 1 - $L = 20$ m; 2 - $L = 200$ m; and 3 - $L = 400$ m.

As the Fig. shows that while qualitative picture stays stable, displacement values and x coordinates of the earth's surface points in which x is equal to zero differ greatly.

Curves in Fig. 2.21 characterize changes in the fall coordinate x within a basin at the earth's surface at different L values and fixed ratio h/H (H =400 m and h=140 m) if V =60 m per month. At such initial data under the conditions of complete

undermining when L=500 m, maximum value of i_{max} fall within a principal profile of a basin is 85 mm per minute.

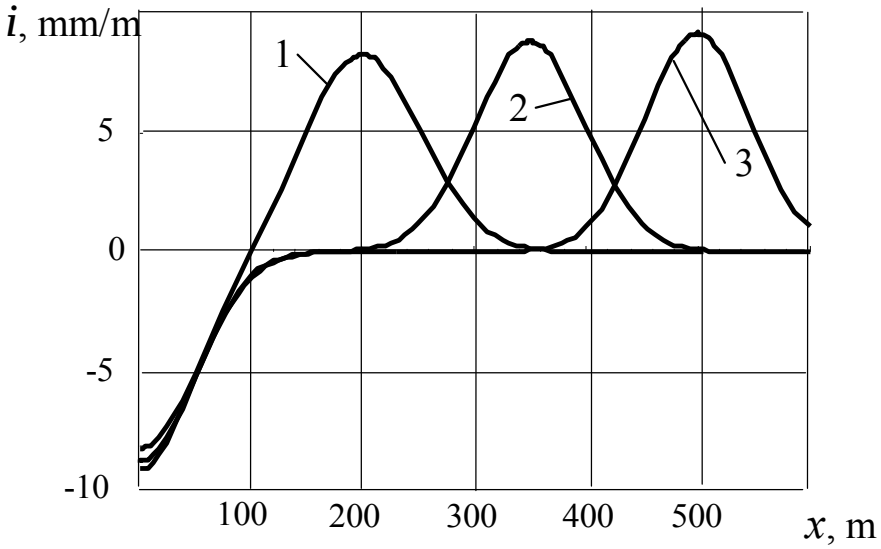

Fig. 2.21. Falls in a basin at the earth's surface depending upon x coordinate if $H = 400$ m, $h = 140$ m: 1 – $L = 200$ m; 2 – $L = 350$ m; and 3 – $L = 500$ m.

Fig. 2.22 shows curves of falls to a settling curve in terms of complete undermining built according to the calculation results on (2.49) dependence taking into account rheological properties of rocks (curve 1), and without taking them into account (curve 2). Their comparison illustrates that due to rock, creeping maximum fall experiences 2.1 times increase.

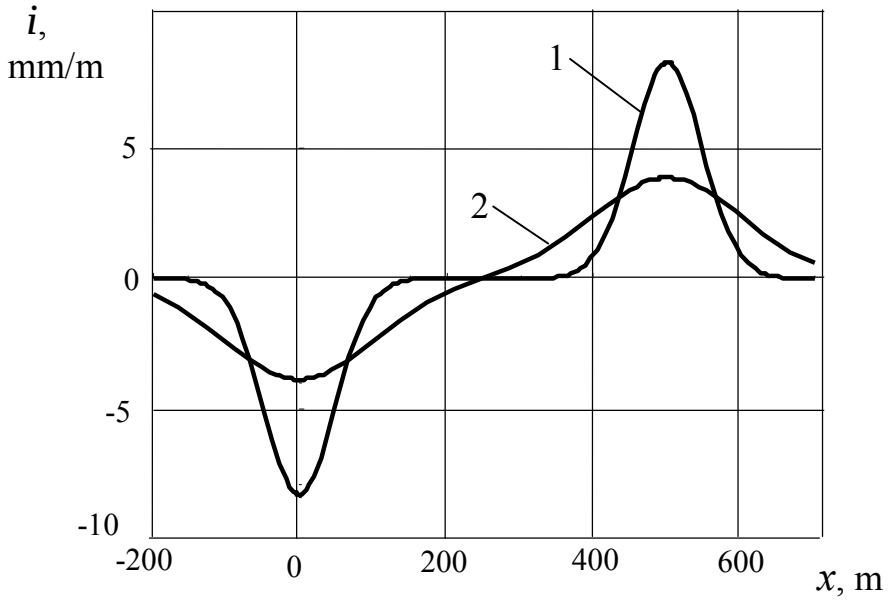

Fig. 2.22. Falls to a settlement curve in terms of complete undermining ($H = 400$ m, $h = 140$ m, $L = 500$ m, and $V = 60$ m per month)

Fig. 2.23 shows variations of maximum falls originating in $x = L$ section, in a basin at the earth's surface depending upon h/H parameter if L=100 m, and L=500 m if $H = 400$ m, and $V = 60$ m per month. In terms of incomplete undermining (L=100 m), 1.3 times increase of h ($0.6H$ to $0.8H$) results in 1.5 times increase of i_{max}, and double in the case of complete undermining (L=500 m).

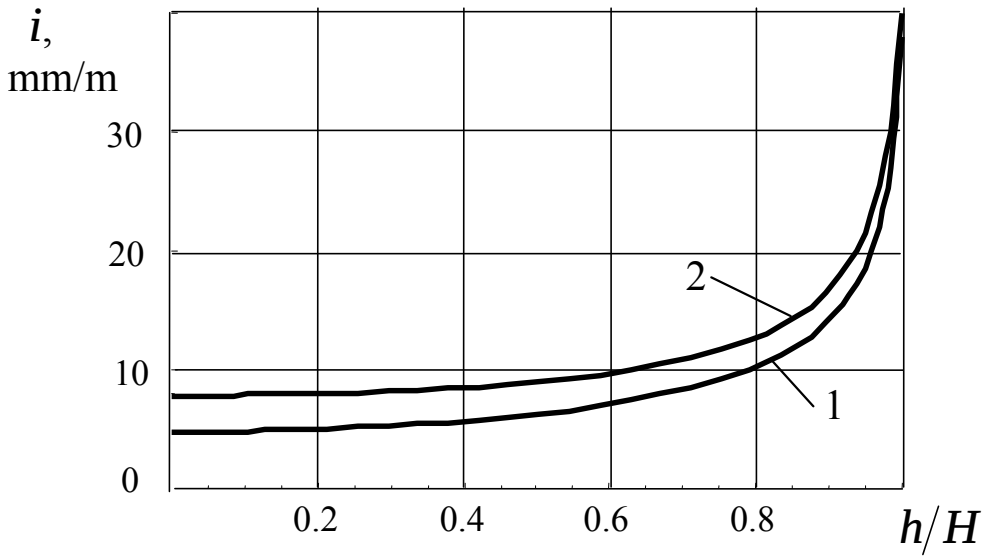

Fig. 2.23. Maximum falls in a basin at the earth's surface depending upon h/H parameter: *1 -* $L = 100$ *m, 2 -* $L = 500$ *m*

If $L > 500$ m, calculation results for i_{max} shows that resulting curves are similar to a curve 2 in a Fig. 2.23. This implies that if $L = 500$ m then complete undermining takes place, and a displacement process stabilizes.

Fig. 2.24 shows curves of the earth's surface convergence. The curves were obtained for complete undermining if $H = 400$ m, $h = 140$ m, and $L = 500$ m. Curve 1has been developed using calculation results without taking into consideration rheological properties of rocks; curve 2 takes them into account when advance rate is $V = 60$ m per month.

As the Fig. demonstrates rheological properties of rocks are rather important. Among other things, maximum curve values differ by 4.4 times: in case one K_{max} value is equal to $2.5 \cdot 10^{-5}$ 1/m; it is $11 \cdot 10^{-5}$ 1/m in case two.

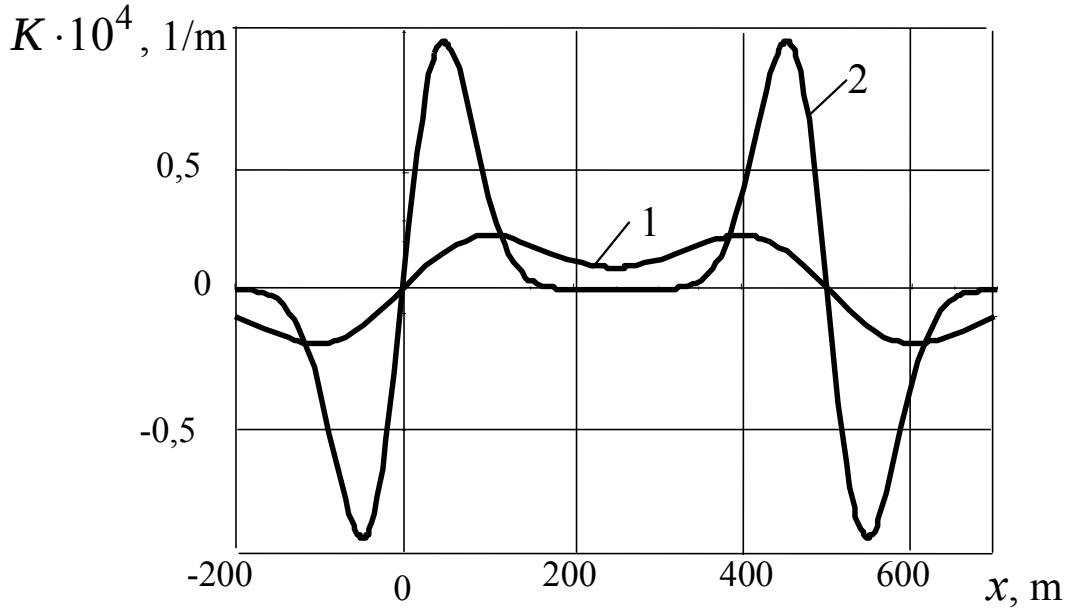

Fig. 2.24. Curves of the earth's surface curves falls in terms of complete undermining: 1 – without taking into account rheological properties of rocks; 2 – including them.

Fig. 2.25 shows dependence diagram for maximum fall curve at the earth's surface on h/H parameter in terms of complete undermining (L=500 m, H=400 m, and V=60 m per month). It follows that if H has fixed value, then 1.7 times increase in capping thickness (0.35 H to 0.6 H) results in 1.25 times increase in maximum fall curve ($11 \cdot 10^{-5}$ to $13.75 \cdot 10^{-5}$ 1/m).

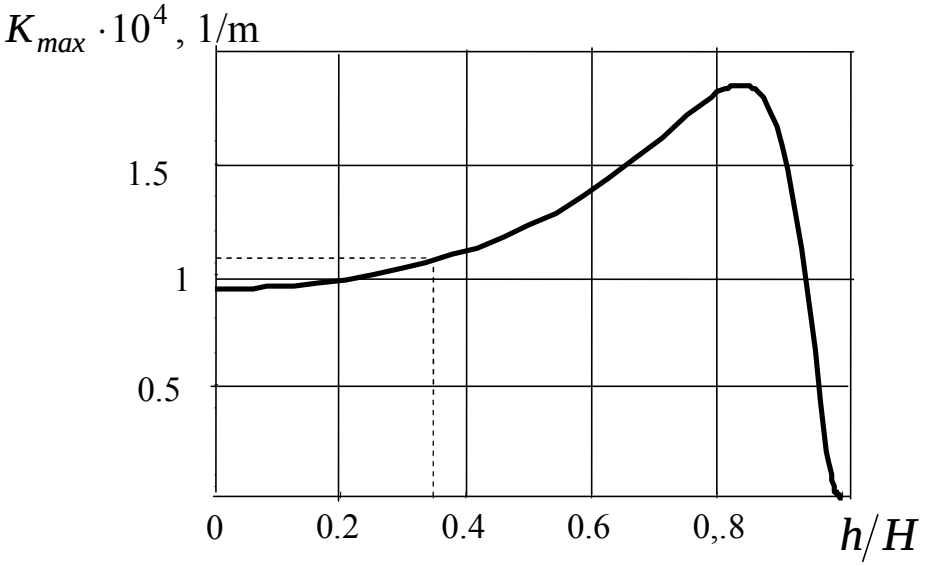

Fig. 2.25.Dependence of $K_{max}(h/H)$ within a basin at the earth's surface in terms of complete undermining.

Fig. 2.26 shows curves of settling rates of the earth's surface points developed on (2.55) for h=140 m, L=400 m, and V=30 m per month at different values of mining depth H.

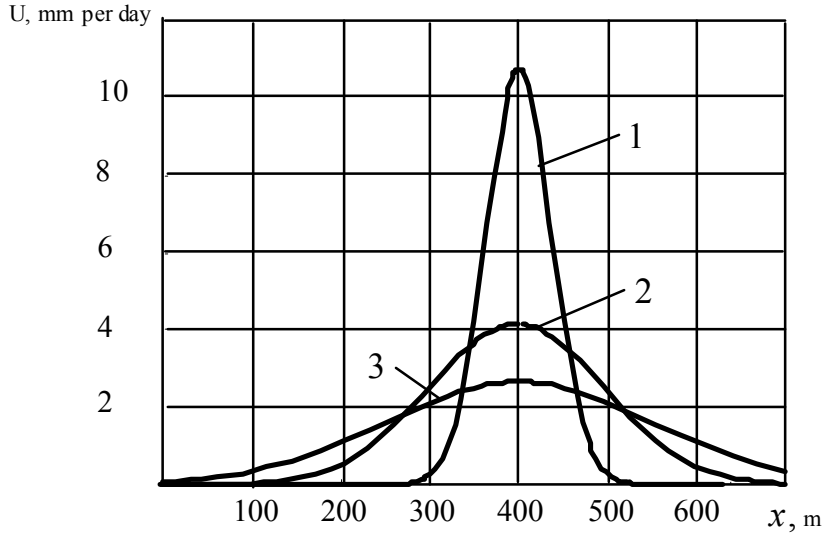

Fig. 2.26. Curves of rates of the earth's surface points fall if $L = 400$ m: 1 – $H = 200$ m; 2 – $H = 400$ m; and 3 – $H = 600$ m.

It follows that when mining deepens, curves, retaining their shape, become more low-angle, and maximums of rates decrease: 1.5 times mining deepen increase (400 m to 600 m) results in 1.6 times decrease of U_{max} (4 mm per day to 2.5 mm per day).

Fig. 2.27 gives information concerning quantitative changes of the earth's surface convergence rate when advance rate varies. The curves also use (2.55) dependence. They characterize the state of complete undermining (L=500 m, H=400 m) if h=140 m.

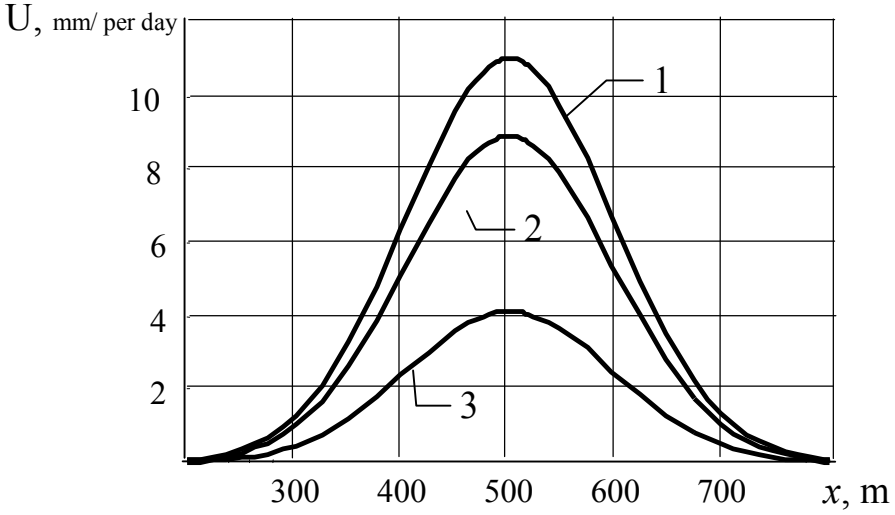

Fig. 2.27. The earth's surface points convergence in the process of complete undermining: 1 – $V = 80$ m per month; 2 – $V = 60$ m per month; 3 – $V = 30$ m per month.

The graphs demonstrate that convergence rate increases as a result of advance rate increase. In particular, 2.7 times increase in advance rate involves 2.75 times maximum rate increase (if V=30 m per month U_{max}=4 mm per day, and if V=80 m per month U_{max}=11 mm per day).

Fig. 2.28 demonstrates similar situation in term of incomplete undermining when L=300 m. It has not any qualitative variations. Maximums of convergence rates stay unchangeable too as it is under the conditions of complete undermining. However, an area in the line of axis OX within which qualitative changes in rates take place are less important to compare with those when L=500 m.

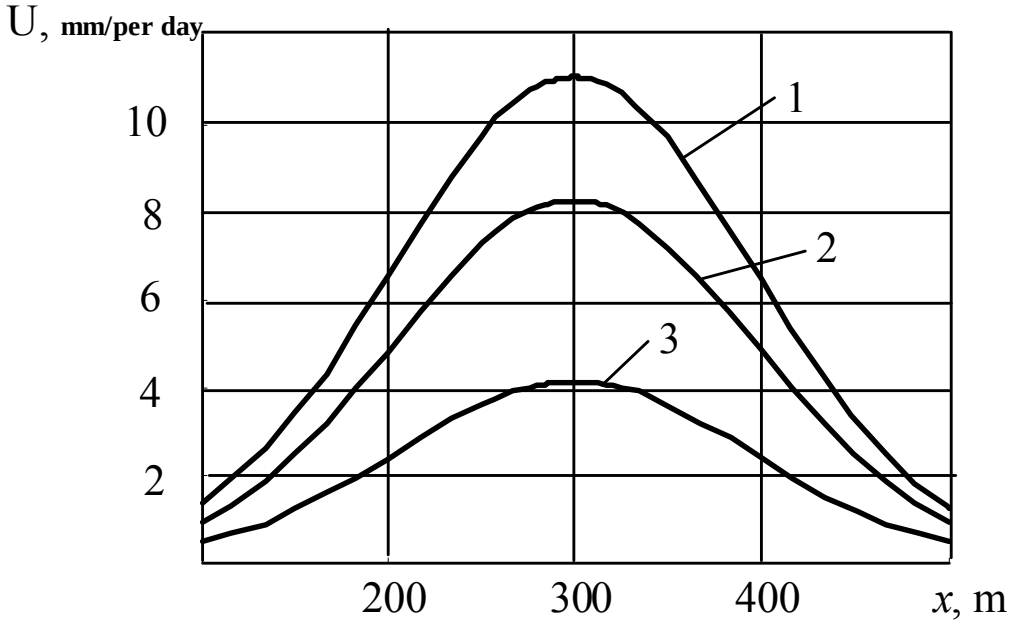

Fig. 2.28. Rate of the earth's surface points convergence in terms of incomplete undermining: 1 – $V = 80$ m per month; 2 – $V = 60$ m per month; 3 – $V = 30$ m per month.

Curves in Fig. 2.29 are curves of the earth's surface points convergence if H=400 m, L=500 m, and V=30 m per month at various values of capping thickness h.

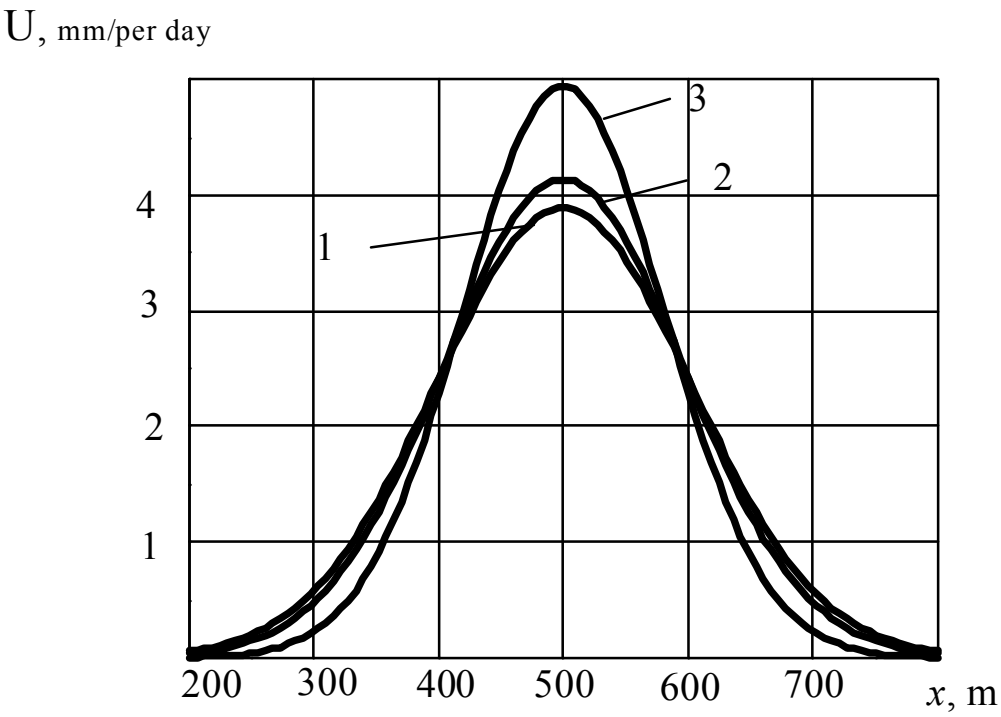

Fig. 2.29. Convergence rate of the earth's surface points depending upon capping thickness values: 1 – $h = 0$ m; 2 – $h = 140$ m; 3 – $h = 250$ m.

That means that in fact h parameter effects convergence rate maximum only. The more thickness of cappings is, the higher is maximum convergence rate. Hence, if h=140 m U_{max}= 4 mm per day, and h=250 m U_{max}= 11 mm per day, then 1.78 times increase of h makes U_{max} 1.2 times increase.

Generalizing results of capping effect quantitative assessment on deformation indices of the earth's surface should take into account that their thickness exercises a significant influence not only on U_{max} value but also on maximums of horizontal displacements, falls, and convergence curves in terms of complete undermining. In terms of incomplete undermining, as it is demonstrated above, the factor effect convergence value too.

Fig. 2.30 shows curves of the earth's surface convergence points as a function of x coordinate for various values of L if H=400 m, and h=140 m. The Fig. demonstrates that under considered conditions, maximum convergence of rate starting from L=100 m arises in $x \cong L$ point being 4 mm per day.

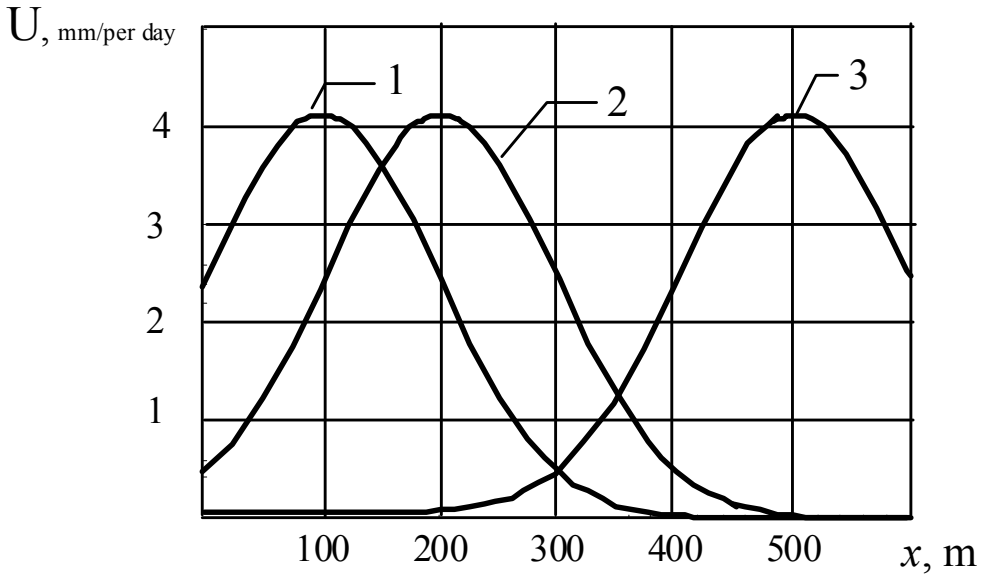

Fig. 2.30. Convergence rate for the earth's surface points at various values of L parameter: 1 – L = 100 m; 2 – L = 200 m; and 3 – L = 500 m.

Fig. 2.31 shows curves of maximum rates of the earth's surface points convergence as a function of h/H parameter for various values of mining depth if advance rate is V=30 m per month. They appear that maximum convergence rate decreases when mining deepens. Hence, if h/H =0.4 then U_{max}=8.2 mm per day; and if H=400 m, and U_{max}=3 mm per day, if H =600 m.

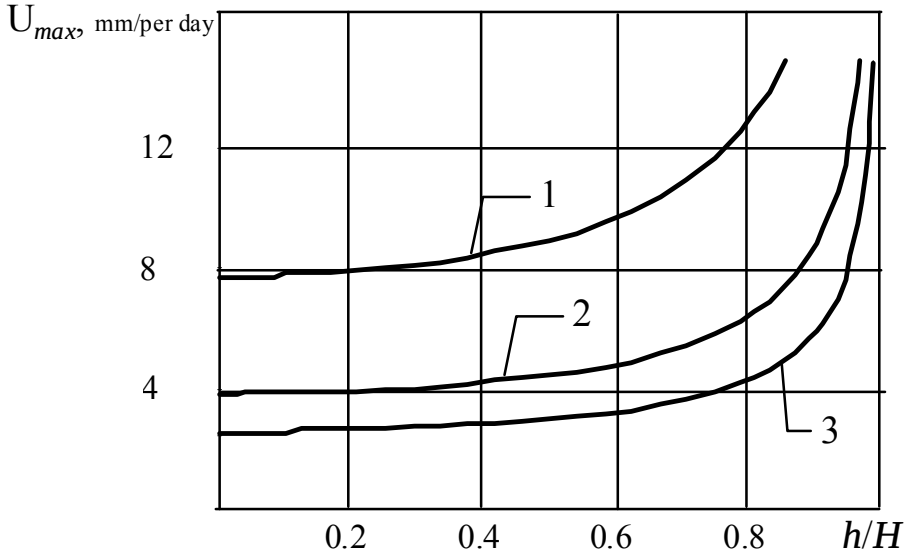

Fig. 2.31.Maximum rate of the earth's surface points convergence depending upon various mining depth values: 1 – H = 200 m; 2 – H = 400 m; and 3 – H = 600 m.

Curves in Fig. 2.32 show U_{max} alternations depending upon L if H=400 m, h=140 m, and various values of V. Increase in maximum convergence rates at any advance rate takes place up to L=100 m value; then U_{max} stays to be constant being equal to 4 mm per day if V=30 m per month, 9mm per day if V=60 m per month, and 11 mm per day if V=80 m per month.

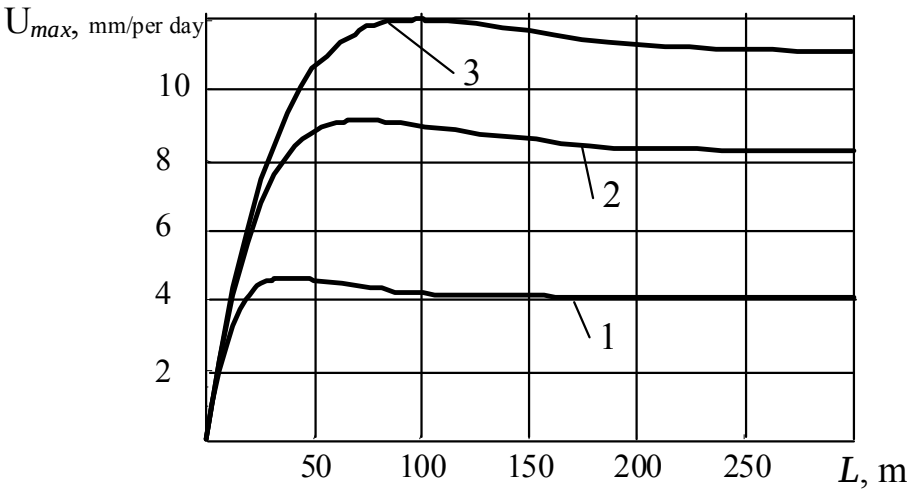

Fig. 2.32. $U_{max}(L)$ curves at different values of advance rate: 1 – $V = 30$ m per month; 2 – $V = 60$ m per month; and 3 – $V = 80$ m per month.

Process time of the earth's surface displacement has also been determined.

In accordance with normative technique [13], a value of maximum convergence h_{max}=1000 mm within a midsection of a basin $x = 250$ m in terms of complete undermining when a stope dimension is L=500 m is taken as a basis.

In contrast to technique [13], specifying h convergences within noted base point at various time moments by means of instrumental observation; the paper identifies adequate values used to determine duration of various stages of displacement process with the help of formula (2.46).

Calculations have been performed for: $h = 140$ m, $V = 80$ m per month, and $L_1 = 1000$ m (extraction pillar length).

According to standard technique, displacement process starts at the moment when convergence takes place within a considered point h=15 mm. By the moment of a $L = 50$ m stope formation, h =$0.03h_{max}$ within the point, and if $L = 150$ m, then convergence is $0.19h_{max}$ in it; that means that initial convergence stage is over. According to calculations, its duration is t=3.75 months.

Active stage starts when a stope is right behind the considered point of the earth's surface $x = 250$ m. At the moment, the earth's surface convergence is $h = 0.47h_{max}$. According to calculations active stage lasts t=5 months; during active stage, convergence within basic point of the earth's surface reaches $h = 0.75h_{max}$.

Like initial stage, dying-out stage lasts during 3.75 months. It is over when a distance between the stope and considered point is $L = (1.2\ldots1.25)H$.

In this context, within the point $x = 250$ m convergence varies from $0.85 h_{max}$ to $0.95 h_{max}$. When the mining process of $L_1 = 1000$ m pillar is over, then $h = 0.998 h_{max}$ within the considered point.

Total duration of displacement process after a longwall had been mined on C_6 seam was 14 months.

Curves shown in this chapter characterize displacements, falls, and convergence curves at the earth's surface; however, such analytical expressions as (2.46), (2.49), (2.50), (2.51), and (2.55) can help to develop them for any level.

Hence, analytical solution for plane problem of rock mechanics has been identified. As a result, ratios to determine displacements, convergence rates, falls, and convergence curves within a point of a mass being undermined have been at any mining stage. Rheological properties of rocks, advance rate, mining depth, and stope parameters have been taken into account.

The solution is based upon a model of two-layer "cappings-carbon" linear and congenital structure with creep kernel of Abel type which hardness is broken-line function vertical coordinate y. Besides, it is based upon an assumption that roof fault in a longwall with advance rate takes place in accordance with exponential law depending on maximum rate of roof fault in a longwall-advance rate ratio, and distance between a stope and face entry.

Works [94-99] picture basic content of the chapter as well as results mentioned.

Hence, the analytical solution gives complete explanation of strained state of the whole mass being undermined giving ability to develop required factors of the earth's surface deformations to compare them with accepted values by Ukrainian branch standards.

However, problems of coal-mining rational parameters identification under protected objects involves analysis of both strained and stressed state of mass being undermined. Therefore, the displacements obtained should be correlated with adequate stresses. Following section considers the problem.

Conclusions

1. Taking into account available mathematical analogy between rock displacements and thermal conductivity, analytical solution of plane geomechanical problem for two-layer “cappings-carbon” mass has been obtained with the help of Fourier method for differential equation of thermal conductivity equation type. In contrast to the known, the solution takes into account rheological properties of rocks and advance rate. Thereby, it helps to identify deformations of rock and the earth’s surface at any stage of coal mining.

2. Overall analytical ratios are applied to develop formulae for calculating maximums of the earth’s surface deformations to compare with industrial standards for various protected objects.

3. Boundary-element method is used to develop an algorithm of numerical solution for plane geomechanical problem for laminary linear and congenital medium with creep cernel of Abel type.

The algorithm advantage is that it uses ratios of S. Crouch problem for semiplane. That provides automated execution of boundary conditions within outer contour of a mass under consideration; only internal contours are discretized.

The algorithm developed for mines in Western Donbass, identifies stiffening parameters of “washes-carbon” two-layer mass required for the problem solving; besides basins of the earth’s surface displacements depending upon various locations of a stope have been formed.

4. Following rules of the earth’s surface deformation have been identified for mining and geological conditions with the help of the analytical solution:

- Similar distance between L slope and face entry results in decrease of maximum convergence with depth increase; the higher capping thickness h is, the greater h_{max} value is at given depth H.

- At fixed values of mining depth H, maximum horizontal displacements taken place under the conditions of incomplete undermining increase depending upon a stope L dimensions decreasing with capping thickness h increase.

- At fixed values of mining depth H and capping thickness h, advance rate has a pronounced effect on h convergences at initial stage of mining only (up to reaching L=50 m); moreover, the greater V is, the smaller is h.

-In terms of complete undermining, maximum convergence h_{max} is of common value at any capping thickness h, and maximum falls i_{max} as well as maximum curves of K_{max} convergence depends on capping thickness. In contrast to them maximum horizontal displacement x_{max} decreases depending upon capping thickness increase.

- The higher thickness of cappings h is, the quicker is convergence maximum.

- Convergence rate increases depending upon advance rate increase.

- Mining depth H increase results in convergence U_{max} maximum decrease.

- At fixed values of mining depth H and capping thickness h maximum convergence rate U_{max} increases up to L=100 m at any advance rate V; then,

U_{max} stays to be constant being 4 mm per day if $V=30$ m per month, 9 mm per day if $V=60$ m per month, and 11 mm per day if $V=80$ m per month.

- In terms of complete undermining in the context of considered mining and geological conditions (L=400…500 m, H=400 m, and h=140 m), maximums of the earth's surface (if $V=60$ m per month) are: convergence is h_{max}=1000 mm, horizontal displacement is x_{max}=40 mm, curve is $K_{max}=11\cdot10^{-5}$ 1/м, fall is i_{max}=8.5 mm per meter, and U_{max}= 9 mm per day.

5. There was performed the assessment of rheological properties of rocks on factors of the earth's surface deformation. It is shown that in terms of complete undermining there values calculated with regard to rock creep are greater than those determined without the factor consideration, s.s.: owing to creep, $h(x,H,L)$ convergences increase by 10 to 25 %, maximum horizontal displacement experiences 1.5 to 1.53 increase, maximum convergence curve – 2.5 times increase, and maximum falls – 2.1 times.

6. Duration of the earth's surface displacement is determined: if $V=80$ m per month, then initial displacement stage is 3.75 months; active stage is 5 months, and attenuation stage is 3.75; total duration of displacement process after the longwall within C_6 stratum has been mined is 14 months.

CHAPTER 3. STRESS CONDITION OF UNDERMINED TWO-LAYER "WASHES-CARBON" MASS

3.1 Relation between displacement and deformations

Previous chapter describes analytical solution in displacements of plane geomechanical problem; as a result, among other things, there are developed analytical expressions for $h(x,y)$ falls (2.46) and horizontal displacements $x(x,y)$ (2.51) within undermined two-layer mass.

As it is known, deformations are connected with displacements by means of Cauchy equations

$$\begin{aligned} e_x &= \frac{\partial x}{\partial x}; \\ e_x &= \frac{\partial h}{\partial y}; \\ g_{xy} &= \frac{\partial x}{\partial y} + \frac{\partial h}{\partial x}. \end{aligned} \tag{3.1}$$

Taking into account initial differential equation of (2.6) considered problem as well as conditions of deformation discontinuity (2.26), expressions for deformations (3.1) may be shown as follows:

$$e_x = -K(y)\frac{\partial^2 h}{\partial x^2};$$

$$e_y = -e_x = K(y)\frac{\partial^2 h}{\partial x^2};$$

$$g_{xy} = -\frac{dK(y)}{dy}\cdot\frac{\partial h}{\partial x} - K(y)\frac{\partial^2 h}{\partial x \partial y} + \frac{\partial h}{\partial x} = \left(1 - \frac{dK(y)}{dy}\right)\frac{\partial h}{\partial x} - K(y)\frac{\partial^2 h}{\partial x \partial y}.$$

Expressions for convergence derivatives $h(x,y)$, being a part of (3.2) ratios, are:

$$\frac{\partial h}{\partial x} = -\frac{h_0(1-exp(-aL))}{\sqrt{2pj(y)}}\left[exp\left(-\frac{(L-x)^2}{4j(y)}\right) - exp\left(-\frac{x^2}{4j(y)}\right)\right];$$

$$\frac{\partial^2 h}{\partial x^2} = -\frac{h_0(1-exp(-aL))}{4\sqrt{pj(y)}}\left[(L-x)exp\left(-\frac{(L-x)^2}{4j(y)}\right) + x\,exp\left(-\frac{x^2}{4j(y)}\right)\right];$$

$$\frac{\partial^2 h}{\partial x \partial y} = \frac{\left(1-\frac{dK(y)}{dy}\right)h_0(1-exp(-aL))}{2\sqrt{pj(y)}}\left[exp\left(-\frac{(L-x)^2}{4j(y)}\right) - exp\left(-\frac{x^2}{4j(y)}\right)\right] -$$

$$-\frac{h_0(1-exp(-aL))j'(y)}{8j^2(y)\sqrt{pj(y)}}\left\{\left[\left(L-x^2\right) - 2j(y)\right]exp\left(-\frac{(L-x)^2}{4j(y)}\right) -\right.$$

$$-\left(x^2-2j(y)\right)exp\left(-\frac{x^2}{4j(y)}\right)\Bigg\} \tag{3.3}$$

$j(y)$ function, characterizing two-layer mass inelasticity, is identified with the help of (2.32) expressions.

3.2 Stress identification

To identify stresses apply formulae of well-known Hooke law; it is required to replace elasticity modulus E with a modulus determined by (1.2) formula:

$$t_{xy}=\frac{E_t}{2(1+n)}g_{xy} \tag{3.4}$$

Formulae for such standard stresses as s_x and s_y of Hooke law should be given taking into account deformation continuity conditions (medium incompressibility):

$$e_x+e_y=0.$$

For s_x stress we obtain

$$s_x=\frac{E_t}{(1+n)(1-2n)}\left[e_x(1-n)+ne_y\right]=-\frac{Ee_y}{1+n} \tag{3.5}$$

According to (3.2) when e_y expression is taken into account, formula (3.5) is:

$$s_x=-\frac{E_t}{1+n}K(y)\frac{\partial^2 h}{\partial x^2} \tag{3.6}$$

Analogously a formula for s_y stresses is developed:

$$s_y=\frac{E_t}{1+n}K(y)\frac{\partial^2 h}{\partial x^2}. \tag{3.7}$$

After expression for displacement deformation g_{xy} from (3.2) has been substituted for a formula for shear stresses t_{xy}, the latter is:

$$t_{xy}=\frac{E_t}{2(1+n)}\left[\left(1-\frac{dK(y)}{dy}\right)\frac{\partial h}{\partial x}-K(y)\frac{\partial^2 h}{\partial x\partial y}\right]. \tag{3.8}$$

(3.6), (3.7), and (3.8) formulae are applied to identify stresses in weightless. Using superposition principle we add to them adequate components of natural stress field we obtain formulae for stresses with allowance for rock weight:

$$s_x = -\frac{E_t K(y)}{1+n}\frac{\partial^2 h}{\partial x^2} - lg(H-h);$$

$$s_y = \frac{E_t K(y)}{1+n}\frac{\partial^2 h}{\partial x^2} - g(H-h);$$

$$t_{xy} = \frac{E_t}{2(1+n)}\left[\left(1-\frac{dK(y)}{dy}\right)\frac{\partial h}{\partial x} - K(y)\frac{\partial^2 h}{\partial x \partial y}\right] + \frac{1-2n}{2(1-n)}g(H-y), \quad (3.9)$$

where $K(y)$ is described with the help of (2.31) equations;

E_t is elasticity modulus identified with allowance of time factor using (1.2) formula;

n is the Poisson ratio of the rock;

g is specific weight of rocks, t per м^3; and

$l = \frac{n}{1-n}$ is a side bearing reaction factor.

(3.3) expressions determine derivatives of convergence function $h(x,y)$ being a part of (3.9) formulae.

Hence, formulae for stresses at any point of considered two-layer mass are obtained for any stage of coal mining.

As formulae (3.3) and (3.9) demonstrate, stress state within selected point depends on such its coordinates as x and y, mining depth H, a stope dimension L by t time at certain advance rate V, and $j(y)$ function.

In turn, as previous chapter shows, $j(y)$ function depends on capping thickness h and stiffening parameters of carbon c_k and cappings $c_н$.

Considering stress and strain state of mass in terms of complete undermining, c_k and $c_н$ parameters should involve time factor t as 2.4 describes; the matter is that the condition is the result of rather long deformation process.

3.3 Analysis of stress and strained conditions within a neighbourhood of a stope

To have graphic representation of advance rate and mining depth effect on a stress state of rocks within a neighbourhood of a stope, to identify zonal boundary of their potential fall, to determine possible caving step for immediate roof and main roof, and to classify a load acting on roof support canopy for the most dangerous load situations, calculate stresses in terms of the mining and geological conditions.

To do that use calculation model shown by Fig. 3.1 and 3.9 formulae.

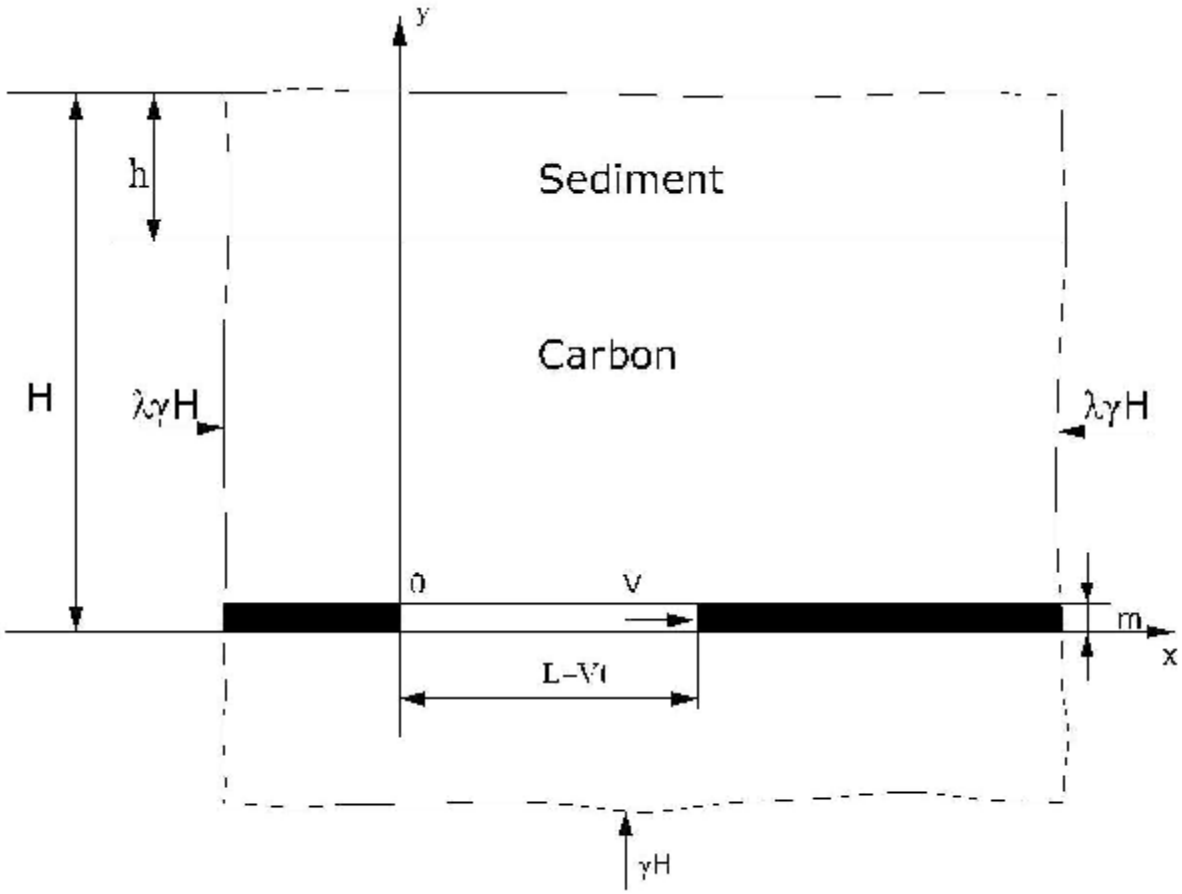

Fig. 3.1.Calculation model

Assume g , E, and n values for carbon and washes (Fig.2.2), and compression strength of enclosing rocks s_c (Table 1.2) as basic data.

Take into consideration, that thickness of immediate rock is 4 to 5 m; moreover, it consists of aleurites and argillites for which s_c=20…25 MPa. Argillites, aleurites, and sandstones are deposited in the main roof which thickness is up to 15 m. Weighted average value s_c of the main roof rocks is 30 MPa.

To identify caving pitch of the main roof, let's assume that the caving is possible when according to (1.4) restriction, limit stresses cover its total thickness.

However if limit stresses s_{eq} affect not only immediate roof but also third of the main roof thickness at least, then the main roof caving may take place.

Section 2.4 determines parameters of carbon hardness (c_k=0.275) and washes ($c_н$=0.033).

Geometry of considered are as follows: mining depth is H=200, 400, and 600 m; capping thickness is h=140 m; and the stope dimension is L=5, 10, 15, 20 and 22 m. Advance rate is V=30, 60, 80 m per month; consequently, parameter a=0.04; 0.03; and 0.019.

Technical characteristic of specified powered support

Power parameters are as follows:

resistance of element is $\sum_j R_j$ =1560 кН; specific resistance per 1 square meter of supported area is R=400 kN/m^2; and maximum bearing capacity of hydraulic prop is R_j=650 kN.

The element dimensions are as follows:

Length is 3 m;

Width is 1 m;

Length of front mounting base is 1.1 m;

Length of rare mounting base is 0.8 m; distance between hydraulic props is 1.1 m; and

Height is $h_{min} - h_{max}$=0.64 m.

Analyze the results.

Fig. 3.2, 3.3, 3.4, and 3.5 demonstrate the nature of stresses s_x, s_y, t_{xy}, and s_{eq} change according to x coordinate within the main roof of the stope if y=10 m, H=400 m, and L=5 m at such three advance rates as V=30, 60 and 80 m per month.

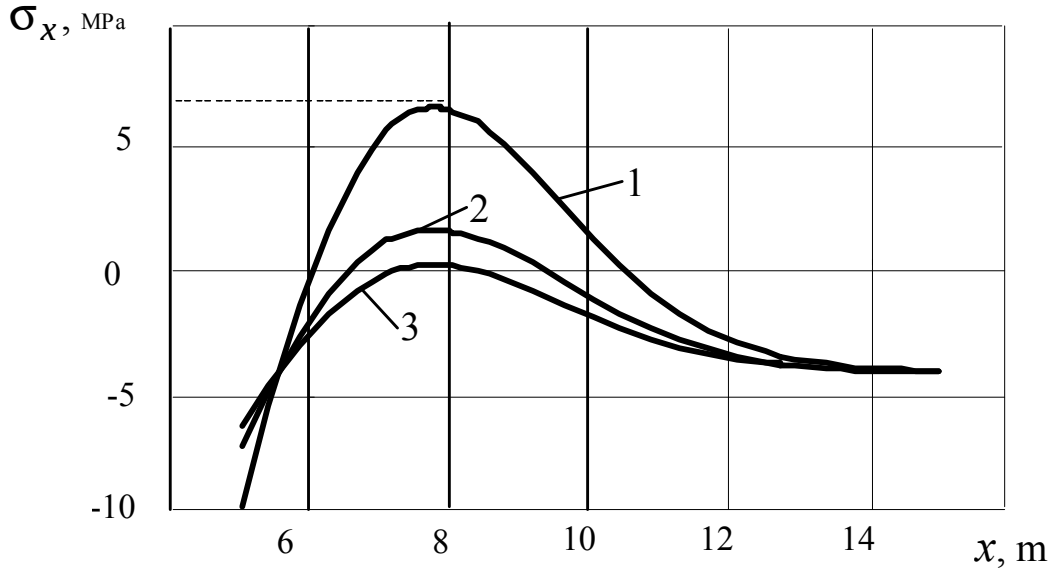

Fig. 3.2.Stresses s_x within the roof (y =10 m) at H =400 m, L =5 м, and various advance rates: 1 - V =30 m per month; 2 - V =60 m per month; and 3 - V =80 m per month .

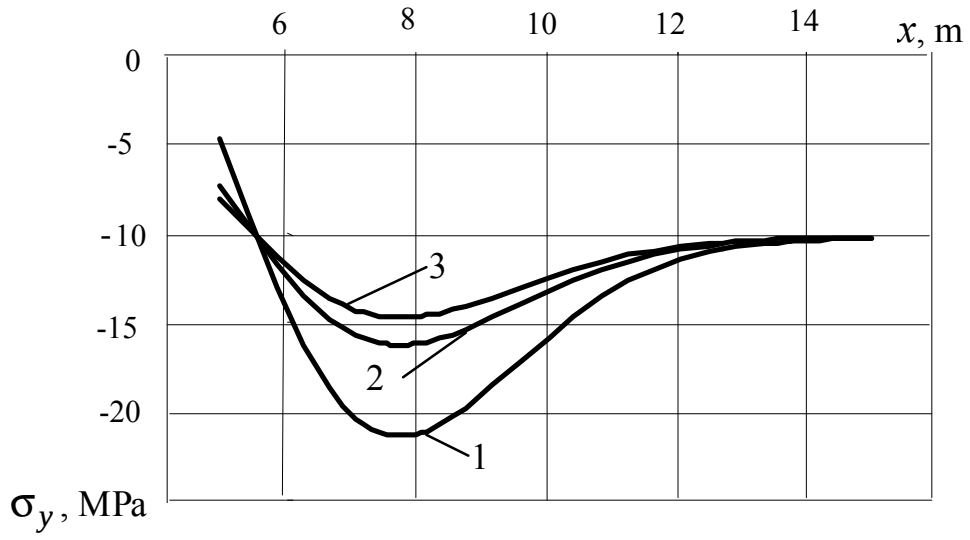

Fig. 3.3. Stresses s_y within a roof (y =10 m) at H =400 m, L =5 m, various advance rates: 1 - V =30 m per month; 2 - V =60 m per month; 3 - V =80 m per month.

The curves demonstrate that stress level height depends on lesser advance rate.

Fig. 3.2 shows that within a point with x =7.5 m coordinate (at the distance of 2.5 m from the stope line) dangerous tension stresses originate at considered level y: s_x= 6.5 MPa if V = 30 m per month, and s_x= 1.5 MPa if V = 60 m per month.

Moreover, within x=6 m point (a meter away from the stope line) available tangential stresses t_{xy} are much higher than acceptable values at the same y=10 m level t_{xy} (Fig. 3.4).

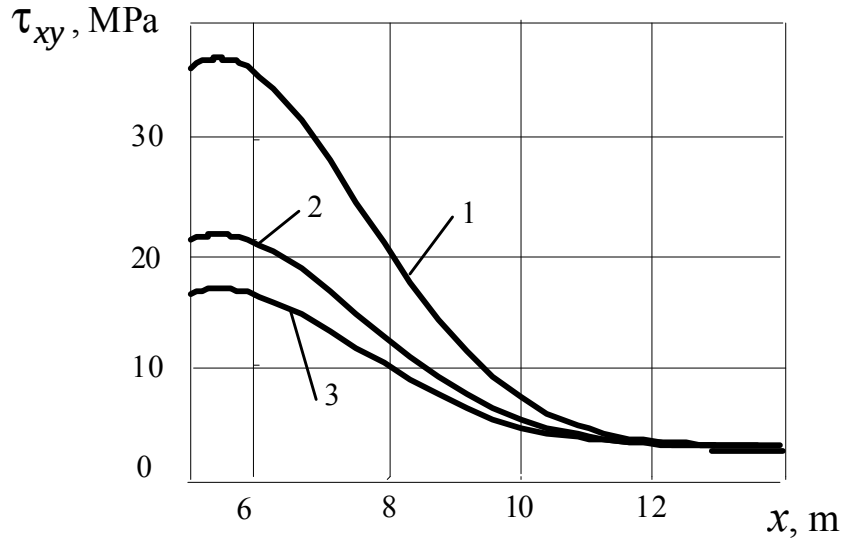

Fig. 3.4. Stresses t_{xy} within a roof (y =10 m) at H =400 m, L =5 m, and various advance rates: 1 - V =30 m per month; 2 - V =60 m per month; 3 - V =80 m per month.

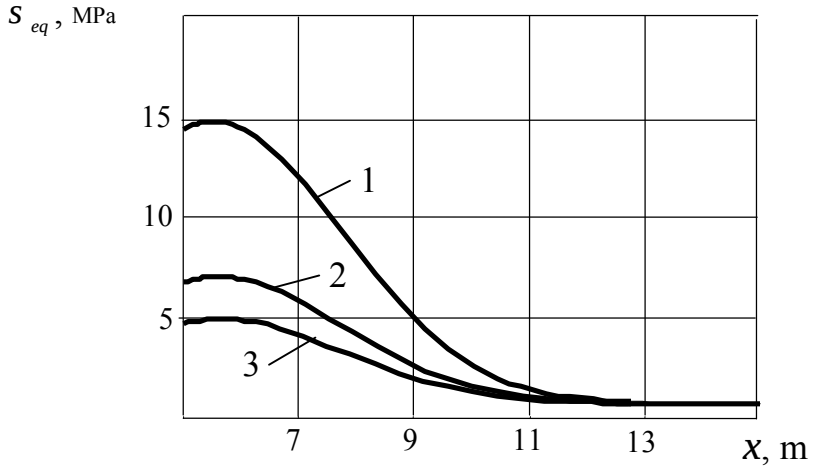

Fig. 3.5. Equivalent stresses within a roof (y =10m) at H =400 m, L =5m, and various advance rates: 1 - V =30 m per month; 2 - V =60 m per month; 3 - V =80 m per month.

Hence, under these conditions crack initiation and rock foliation of the main roof are potential. However, as far as s_y stresses are less then rock stress s_c=30 MPa (Fig. 3.3), and equivalent stresses are in excess of it if only V=30 m per month (Fig. 3.5), then, according to strength criterion (1.4), if H=400 m and L=5 m, rational value of advance rate is within 60 to 80 m per month.

Identical conclusion is drawn upon the study of stress pattern within the roof at y=10 m level. The pattern is obtained from formulae of analytical solution for H=400 m if L=10 m.

Fig. 3.6, 3.7, 3.8, and 3.9 demonstrate adequate stress curves.

In this context, within x=12.5 m point (over the same distance from the stope x=2.5 m as at L=5 m), if y=10 m, then stresses s_x rank over limit stress s_p at each considered values V of advance rate (Fig. 3.6).

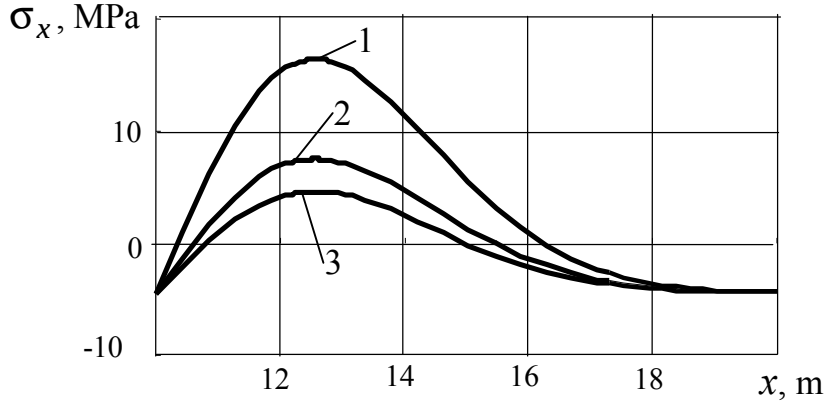

Fig. 3.6. Stresses s_x within the roof (y =10m) at H =400 m, L =10m, and various advance rates: 1 - V =30 m per month; 2 - V =60 m per month; 3 - V = 80 m per month.

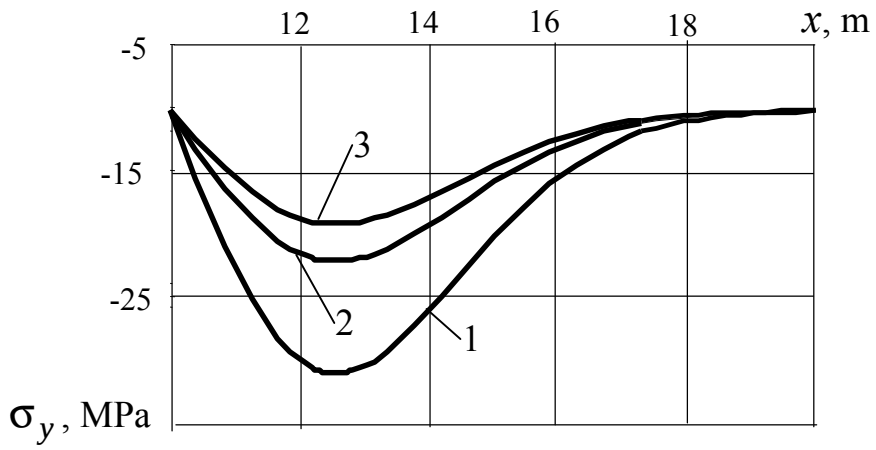

Fig. 3.7. Stresses s_y within the roof (y =10 m) at H =400 m, L =10 m and various advance rates: 1 - V =30 m per month; 2 - V =60 m per month; 3 - V =80 m per month.

Fig. 3.7 demonstrate that within the point, compression stresses s_y rank over limit value s_c if V =30 m per month. The same is also true concerning shear stress t_{xy} (Fig. 3.8).

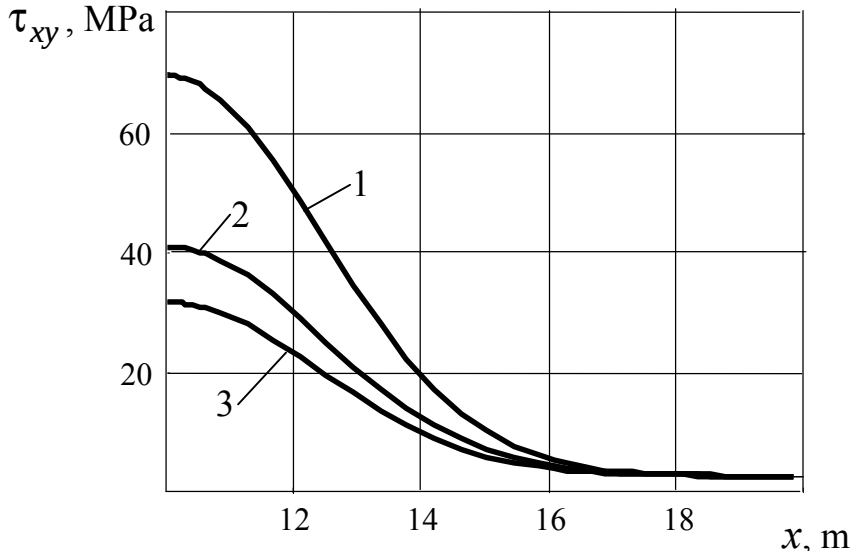

Fig. 3.8. Stresses t_{xy} within the roof (y =10 m) at H =400 m, L =10 m, and various advance rates: 1 - V =30 m per month; 2 - V =60 m per month; 3 - V = 80 m per month.

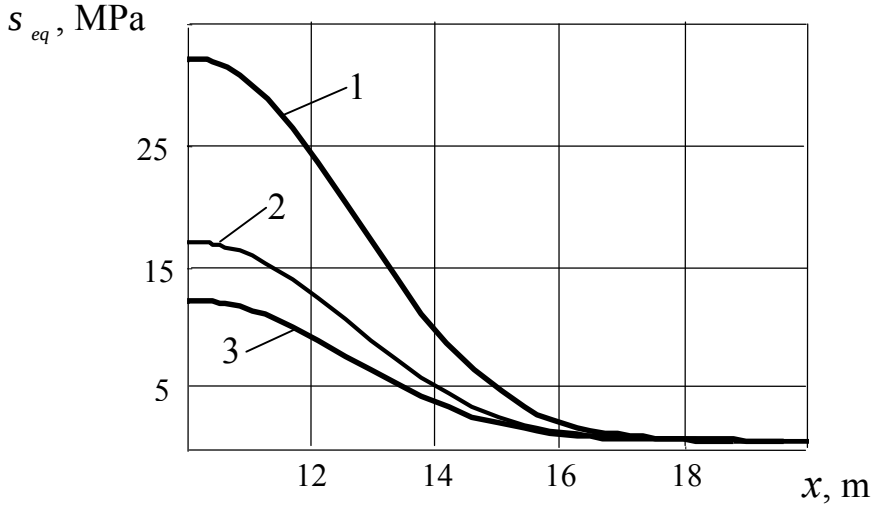

Fig. 3.9. Equivalent stresses within the roof (y =10 m) at H =400 m, L = 10 m, and various advance rates: 1 - V =30 m per month; 2 - V =60 m per month; 3 - V =80 m per month.

However, equivalent stresses rank over s_c if only V=30 m per month (Fig. 3.9); hence, at L=10 m along with L=5 m, rational on mining pressure factor advance rate V is within 60 to 80 m per month.

Curves in Fig. 3.10, 3.11 and 3.12 help to consider efficiency of L in stress distribution within immediate roof at H=400 m, and V=30, 60 and 80 m per month. They are curves of equivalent stress alternation in the x coordinate at y=5 m obtained for such three L parameters as 5, 10 and 15 m.

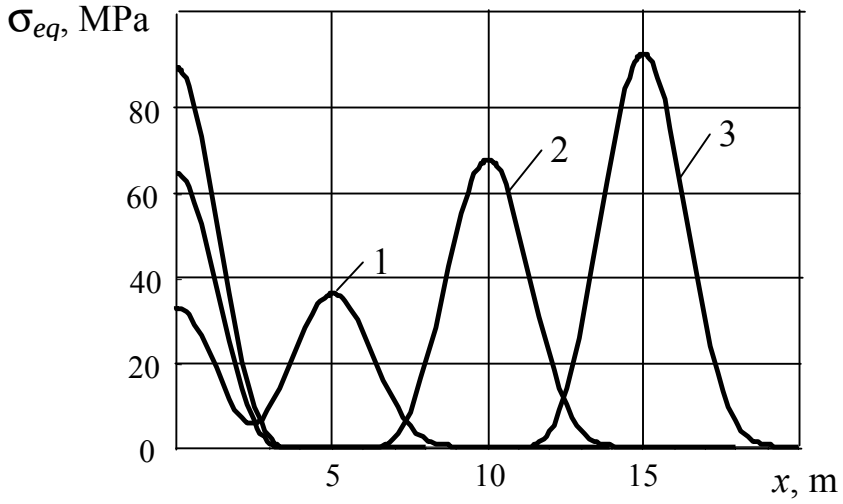

Fig. 3.10. s_{eq} curves if y =5 m at V = 30 m per month and various stope dimensions: 1 - L =5 m; 2 - L =10 m; and 3 - L =15 m.

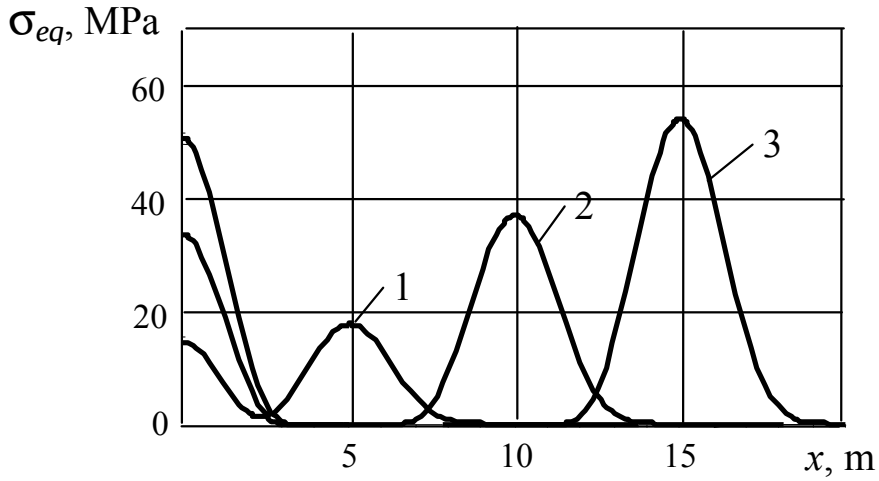

Fig. 3.11. s_{eq} curves if y =5 m at V = 60 m per month and various dimensions of the stope: 1 - L =5 m; 2 - L =10 m; and 3 - L =15 m.

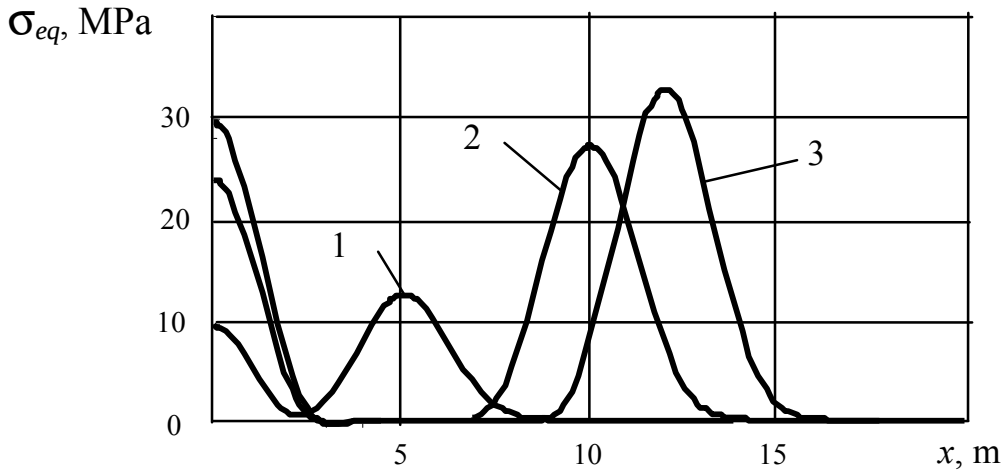

Fig. 3.12. s_{eq} curves if y =5 m at V = 80 m per month and various dimensions of the stope: 1 - L =5 m; 2 - L =10 m; and 3 - L =15 m.

As the curves demonstrate, s_{eq} level is in direct ratio with L being in inverse ratio with V. Thus, if V =30 m per month, s_{eq} stresses within considered section of immediate roof rank over rock compression strength s_c =30 MPa when L =5 m.

To determine caving step of both immediate roof and main one with allowance for advance rate, it is required to know the distribution of equivalent stresses throughout the height.

To that effect, curves of stress variation s_{eq} in the y coordinate within dangerous section $x = L$ (over the stope line) have been developed for various L values, and V =30, 60, and 80 m per month (Fig. 3.13, 3.14 and 3.15).

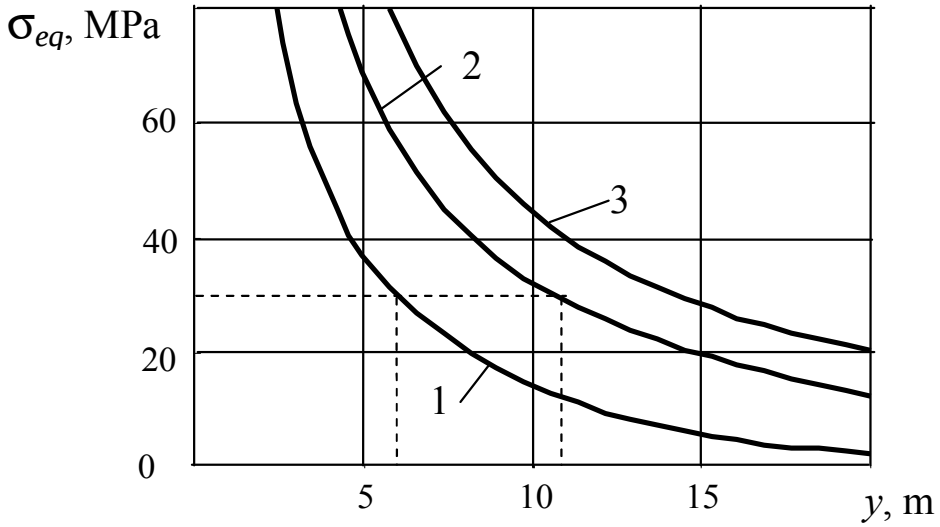

Fig. 3.13. s_{eq} curves within dangerous section $x = L$ m at V = 30 m per month and various stope dimensions: 1 - L =5 m; 2 - L =10 m; and 3 - L =15 m.

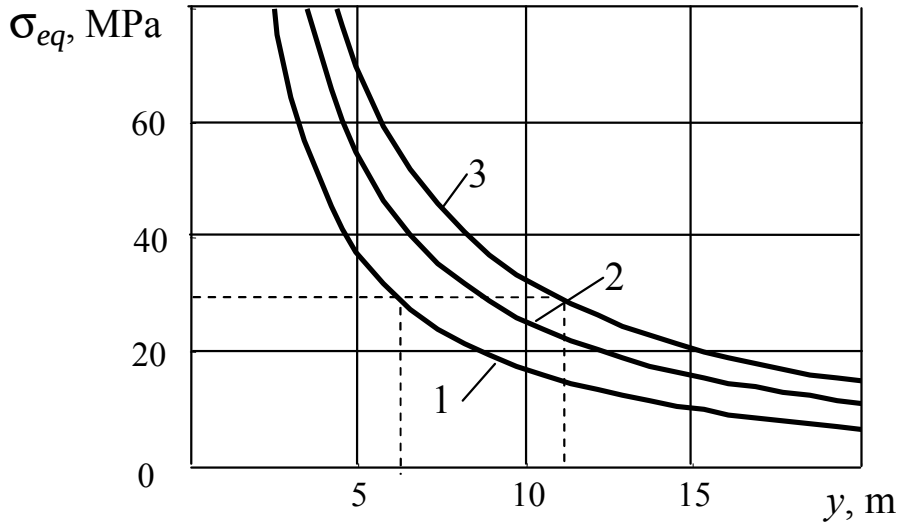

Fig. 3.14. s_{eq} curves within dangerous section $x = L$ m at V = 60 m per month and various stope dimensions: 1 - L =10 m; 2 - L =15 m; and 3 - L =20 m.

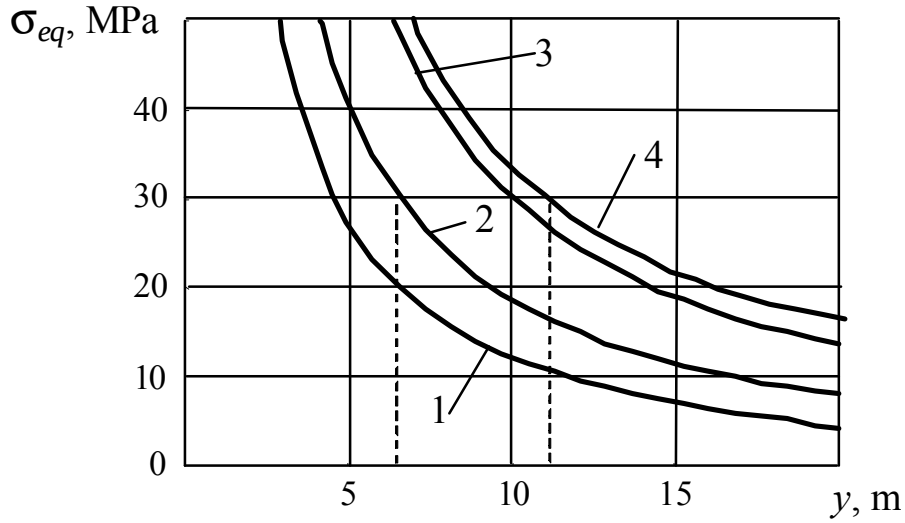

Fig. 3.15. s_{eq} curves within dangerous section $x = L$ m at V = 80 m per month and various stope dimensions: 1 - L =10 m; 2 - L =15 m; 3 - L =20 m; and 4 - L = 22 m.

Fig. 3.13 demonstrates that if V=30 m per month and L=5 m, entire immediate roof (about 7 m) is within stresses ranking over s_c=30 MPa. Hence, expected caving step of immediate roof $l_н$ is 5 m when V=30 m per month.

If V=60 m per month (Fig. 3.14), then the situation takes place at L=10 m; therefore, expected caving step of immediate roof is $l_н$=10 m.

If V=80 m per month, then $l_н$=15 m caving step is expect (Fig. 3.15).

The same Figures help to identify the main roof caving.

If V=30 m per month, then limit stresses extend over OY axis to 12 m when L=10 m involving 7 m of the main roof (curve 2 in Fig. 3.13); hence the main roof caving may have l_o=10 m step.

If V=60 m per month, then l_o=20 m according to curve 3 in Fig. 3.14, and if V=80 m per month, then expected caving step of the main roof l_o is 22 m according to curve 4 in Fig. 3.15.

Estimated values of the main roof caving step at V=30 m per month and V= 60 m per month are not in contrast with mine observations. While seam C_6 mining in "Stepnaia" mine ("Pavlogradugol"OJSC), proper values were l_o=16…17 m at V=30 m per month, and l_o=20…21 m at V=60 m per month [86].

To calculate load acting on powered support during the most dangerous loading period when the main roof is possible, stress condition of the roof in the neighbourhood of the stope was examined.

Load on a ceiling of powered support unit was determined on rock weight within a zone of limit stress conditions; (1.4) criterion was applied to define its borders.

On the assumption of equal distribution of acting load along the horizontal of the unit ceiling, reactions in hydraulic props were calculated on the pattern of two-point bearer with two mountain bases.

Table 3.1 demonstrates the calculation results for H=200, 400, and 600 m values at V=60 m per month, and a=0.03.

Table 3.1

Calculations of load on powered support

Mining depth H, m	Maximum length of limit stress condition zone, m		Load on a ceiling		Reactions in hydraulic props, kN	
	OX-direction	OY-direction	Total R, kN	Specific q, kN/m^2	Within a front R_1	Within an end R_2
200	1.2	7.0	210	70	76	134
400	2.1	12	627	209	228	399
600	2.7	15	1005	335	366	639

The tabulated data shows that three-times increase in mining depth (from 200 m to 600 m), maximum length of limit stress condition zone along OX axis experiences 2.25 times increase; along OY axis the increase is 2.14 times. Total R load acting on the support ceiling experiences 4.77 times increase. Moreover, the calculation shows that when longwall advance V is constant and depths H vary, then expected caving step of the main roof l_o is 0.05 of adequate depth. Thus, if V=60 m per month and a=0.03, then l_o=10 m at H=200 m; l_o=20 m if H=400 m, and l_o=30 m if H=600 m.

Fig. 3.16, 3.17, and 3.18 demonstrate contour lines of equivalent stresses within the stope roof and mass in front of the stope. The contour lines have been developed for V=60 m per month, a=0.04 and H=200, 400, and 600 m values if L=10, 20, and 30 m correspondingly.

To make the results comparable, in each accounting variant L is 0.05 of adequate depth H.

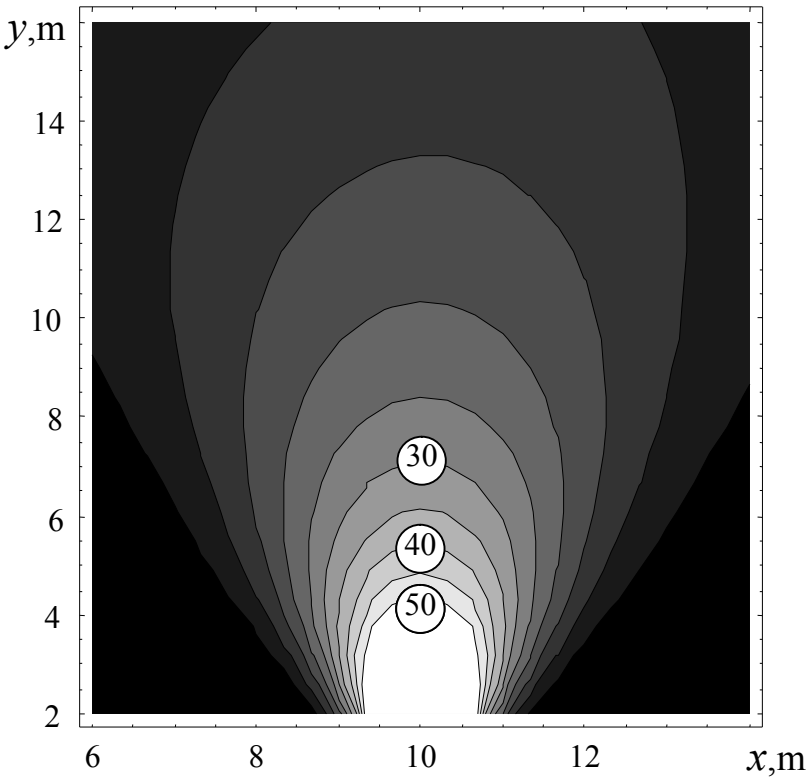

Fig. 3.16. Contour lines of stresses s_{eq} within neighbourhood of the stope (H =200 m, L =10 m, and V =60 m per month).

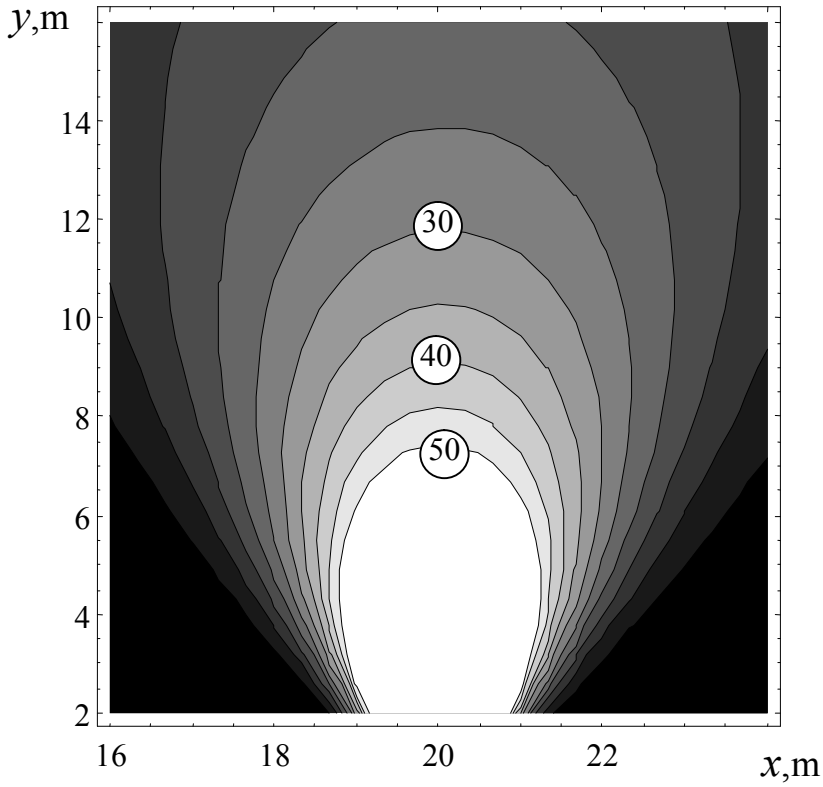

Fig. 3.17. Contour lines of stresses s_{eq} within neighbourhood of the stope (H =400 m, L =20 m, and V =60 m per month).

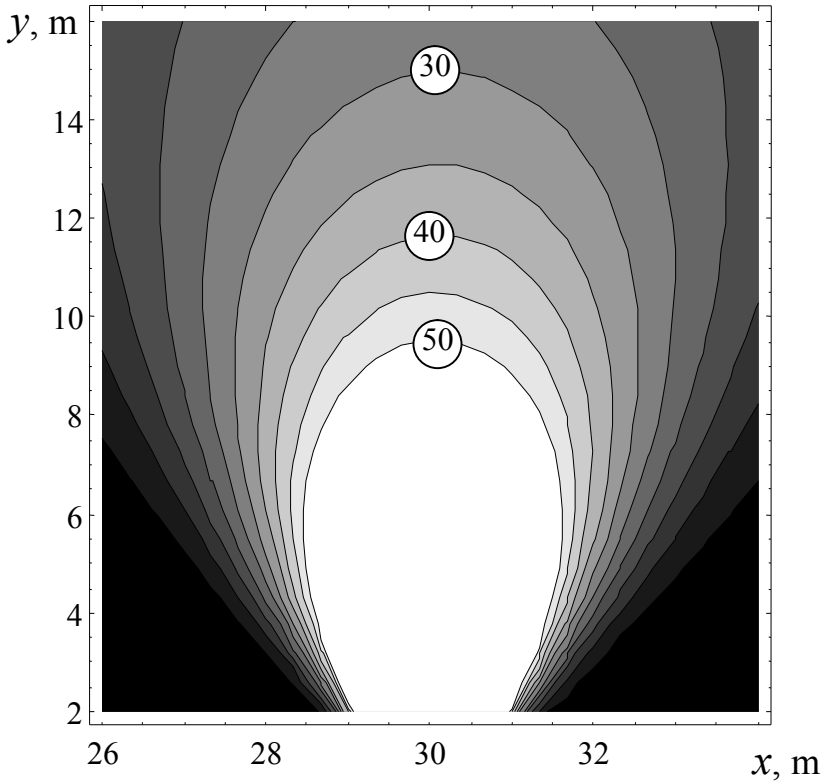

Fig. 3.18. Contour lines of stresses s_{eq} within neighbourhood of the stope (H =600 m, L =30 m, and V =60 m per month).

The Figures give well-defined contours of stressed limit condition where level is s_{eq}=30 MPa. Rock weight within these very zones helps to identify loads R, acting on the ceiling of powered support unit which values are in Table 3.1.

According to specification of powered support used, tolerable value is $[R]$= 400 kN/m^2. Hence, required for normal support work condition $R \le [R]$ is met at each considered H value as well as $R_{\max} \le [R_j]$=650 kN condition.

Main roof fault $h_{\max}$, computed using (2.48) formula in which $j(H)$ is replaced with $j(y) = j(5)$ at H=200, 400, and 600 m being 0.252, 0.440, and 0.580 m correspondingly.

If acceptable value is $[\Delta h] = 0.64$ m, then one may certify that $h_{\max} \le [\Delta h] = 0.64$ is not violated either.

Hence, under the mining and geological conditions, powered support operates properly at H=400 m depth and V=60 m per month. Mine observations [86] confirm that.

Thereby, analytical solution of geomechanical problem for two-layer undermined mass "washes-carbon" has been indentified. The solution helps to obtain both assessment and visualization of stress-strain state of the whole rock mass up to the earth's surface at each stage of coal mining. That is very important to explain parameters of coal seam mining under protected objects and to protect the latter against harmful effect of mining.

Conclusions

1. A relationship between rock faults and deformations in two-layer undermined mass has been identified.

Contrary to known expressions, the analytical ones take into consideration rheological properties of rocks and convergence changes by exponential law depending upon a stope dimension and roof rocks subsidence rate-advance rate ratio.

2. With the help of Hooke's law and deformation consistency condition, analytical expressions for stress tensor components at any point of undermined mass have been obtained. On the superposition principle, they cover components of natural field stresses.

The analytical expressions are subsidence function $h(x,y)$ and its derivatives which depend on mining depth H, stope dimension L, its velocity V to considered time t, and stiffening parameters of seams determined inclusive of rheological properties of rocks.

That makes it possible to identify stress-strain condition of the mass at any mining stage.

3. P.P.Balandin's criterion has been applied to determine both a shape and boundaries of a zone of limit stress condition of rocks within neighbourhood of the stope to be required to find probable caving step of roof and to calculate load acting on the powered support unit ceiling.

4. It is specified that depending upon 3 times increase in H depth (from 200 m to 600 m), maximum length of limit stress condition zones experiences 2.14 times increase in the direction of vertical axis OY and 2.25 times increase in the direction of horizontal axis OX.

5. Weight of rocks within a zone of limit stress condition around the stope made it possible to identify load acting on the powered support ceiling at the moment of the most dangerous stress.

It is 627 kN under the mining and geological conditions when H=400 m, L=20 m, V=60 m per month, and a=0.03.

It is determined that in terms of such stress, power parameters and stiffening parameters of the support provide standard functioning: estimated values of resistivity per 1 m^2 of supported are q=209 kN/m^2, stress in the most loaded hydraulic prop R_1=399 kN and yield of hydraulic props $Dh_{max} = 0.5$ m are less than acceptable values of the support specifications.

6. The analytical expressions for stresses make it possible to identify probable caving step of both immediate and main roof.

Under mining and geological conditions of Western Donbass, at H=400 m, V=30 m per month, and a=0.04, probable caving step of immediate roof is $l_н = 5$ m, and $l_o = 10$ m for the main one; if V=60 m per month and a=0.03 $l_н = 10$ m, and $l_o = 20$ м; if V=80 m per month and a=0.019 $l_н = 15$ m, and $l_o = 22$ m.

CHAPTER 4. VALIDATION OF THEORETICAL RESEARCH

The chapter performs comparative analysis of theoretical research and experiments.

Moreover, results of the geomechanical problem analytical solution are compared with proper data obtained with the help of normative technique and according to worked out algorithm of numerical solution.

4.1. Comparing results of numerical solution and analytical one

Compare relative maximum convergences within a basin at the earth's surface $\frac{h_{max}(z)}{h_0}$, obtained for different parameters of value $z = L / H$, characterizing distance between a stope and a face entry through boundary-element method described in Chapter 2 with those calculated on analytical dependence (2.57).

Numerical solution was based on calculation model shown in Fig. 2.8, and analytical one – on the pattern in Fig. 4.1.

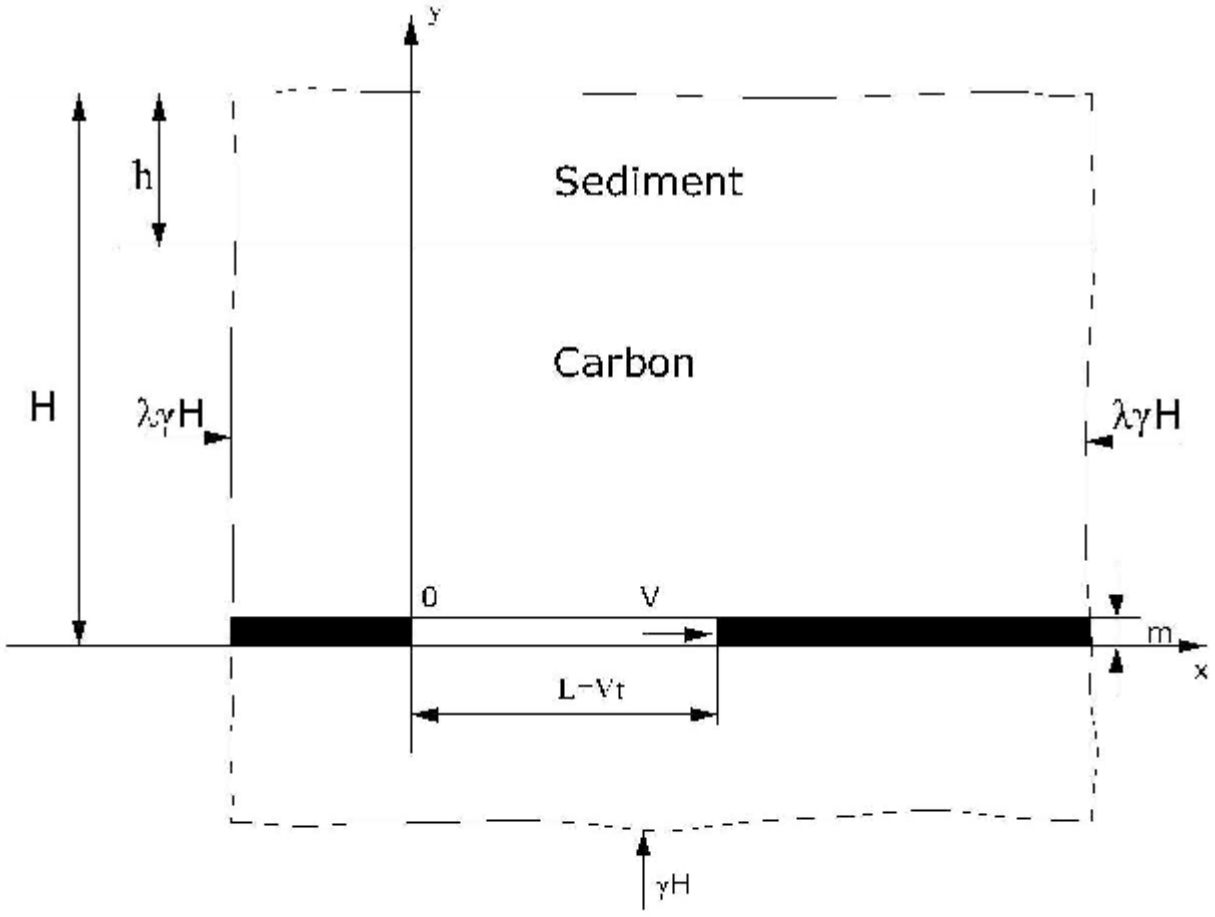

Fig. 4.1. Calculation model used in analytical solution

Table 2.2 describes data on properties of coal, carbon, and washes typical for considered conditions of mines in Western Donbass. Stiffening parameters of washes and carbons are: $C_{tн}$ =0.0249 and $C_{tк}$ =0.137.

Fig. 4.2 demonstrate curves obtained for H =400 m, h=140 m, m=1.0 m, and V =60 m per month. Curve 1 has been developed according to correlation dependence (2.43), and curve 2 – according to results of the analytical solution.

As it is mentioned, (2.43) dependence has been obtained with the help of least square method on the results of a number of numerical solutions for different values of influencing parameters.

As the Figure demonstrates, difference between compared values is 15 to 20%, and maximums of relative convergence at $x = H$ are in line independent of a method applied. The differences can be explained by the fact that numerical solution makes more precise consideration of the rock weight; in addition, calculation model of numerical solution covers breccia.

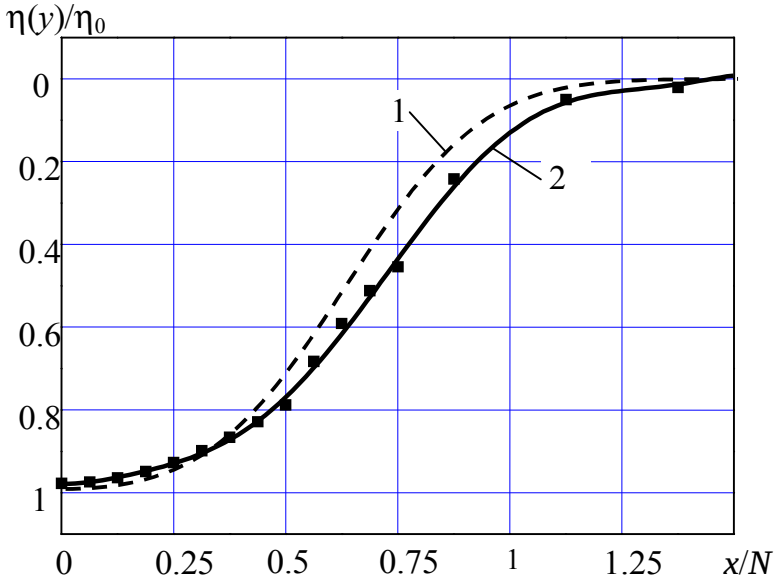

Fig 4.2. Relative maximum convergences in a basin at the earth's surface over going stope: 1 – numerical solution; 2 – analytical solution.

4.2 Comparing results of the analytical solution with calculations on normative technique

To make proper analysis and choose adequate protective measures for objects entering affected zone of mining of 100-bis and 102-bis longwalls of C_6 seam of "Stepnaia" mine ("Pavlogradugol" OJSC), in 2001 "Dneprogiproshakht" Institute performed analysis of probable displacements and deformations of the earth's surface according to "Norms of protecting buildings and natural objects against harmful effect of underground coal mining" 14].

Within undermining, such enclosing rocks as unstable and midstable argillites, aleurites, and sandstones, being typical for Western Donbass mines, are available. Table 2.1 demonstrates proper average characteristics.

Mining is performed by means of longwalls to the rise. Wall length is 200 m. Length of extraction pillars is 1100 m. Powered facilities of KMK – 97M types are applied. Average advance rate is 70 m per month. Complete caving is the roof control.

Compare theoretical values and expected values of displacements and deformations in a basin at the earth's surface within high-pressure gas pipeline undermining. The values have been calculated according to analytical ratios and normative technique [14] under following basic data:

Amount of inclination is 4°;

Mining height is $m = 0.95$ m;

Seam depth is $H = 350$ m;

Capping thickness is $h = 56$ m; and

Relative value of maximum convergence is $\frac{h_{max}}{h_0} = 0.8$.

Fig. 4.3 demonstrates curves of convergence in a basin at the earth's surface while mining $L = 300$ m pillar. Curve 1 is obtained according to analytical ratio (2.47), and curve 2 is a result of normative technique. The Figure explains that average differences are 18 % (6% at the centre of the basin, and up to 30 % on each side). Obviously, it depends on the lack of rheological properties of rocks omitted by normative technique.

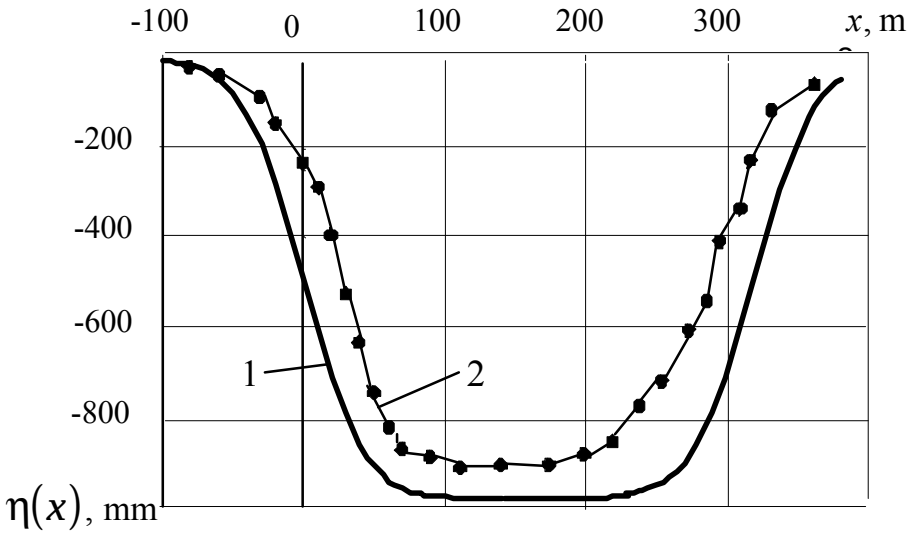

Fig. 4.3.Convergences in a basin at the earth's surface after $L = 300$ m pillar has been mined: 1 – analytical solution; 2 – calculations on the "Norms of protecting buildings and natural objects against harmful effect of underground coal mining" [14]

Fig. 4.4 demonstrates curves developed without rheological properties of rocks when $L = 490$ m. As it is understood, the curves are of similar shape, and their values differ in 5…10 %.

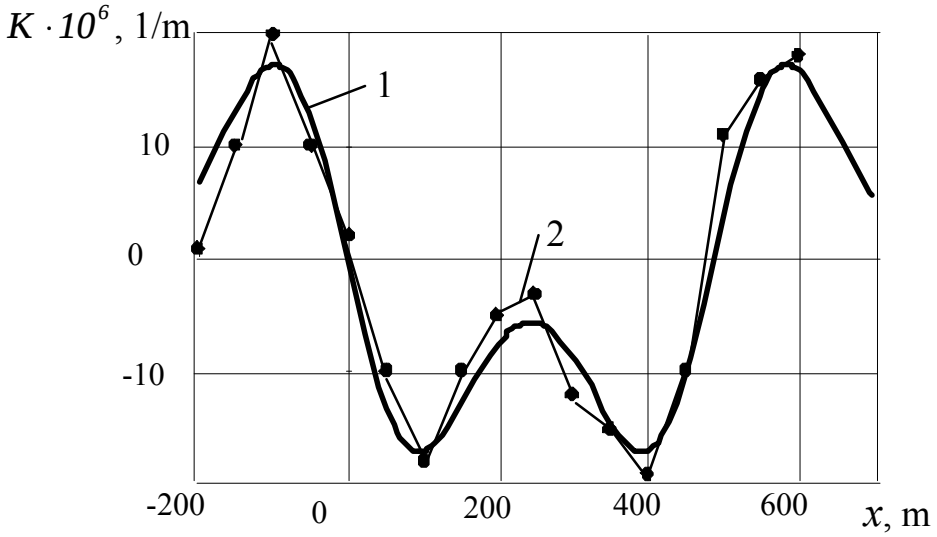

Fig. 4.4. Convergences in a basin at the earth's surface after $L = 490$ m pillar has been mined: 1 – analytical solution; 2 – calculations on the "Norms of protecting buildings and natural objects against harmful effect of underground coal mining" [14]

Curves in Fig. 4.5 confirm that slope curves are of similar shape too, and maximums differ in 6% (obtained on (2.52) formula without rheological properties of rocks $i_{max} = 3 \cdot 10^{-3}$, and $i_{max} = 2.8 \cdot 10^{-3}$ on a normative technique). Other values have 5…12% differences.

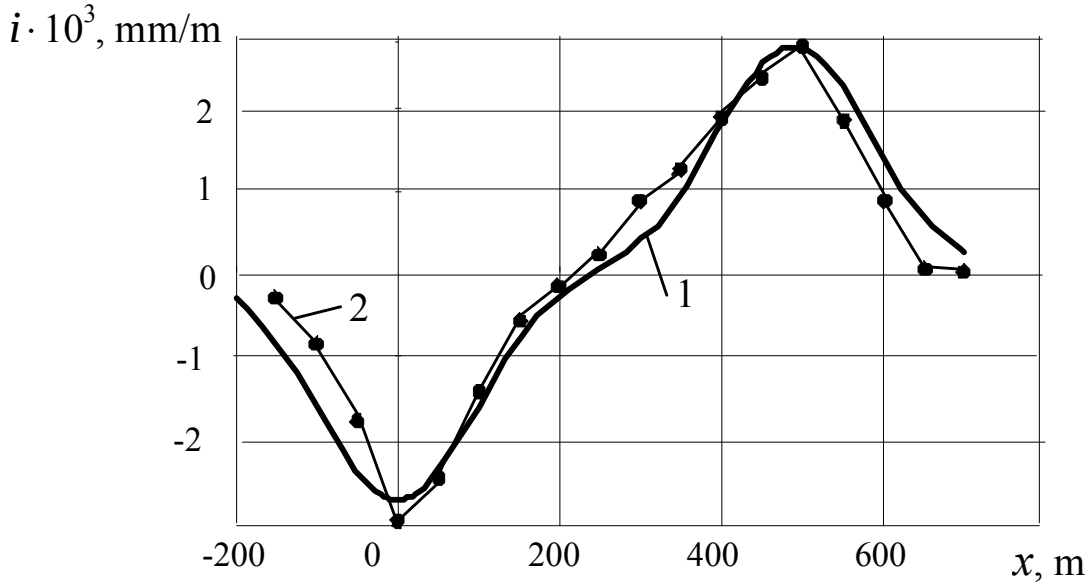

Fig. 4.5. Slopes in a basin of the earth's surface if $L = 490$ m:
1 – analytical solution; 2 – calculations on the "Norms of protecting buildings and natural objects against harmful effect of underground coal mining" [14]

Hence, in terms of complete undermining, convergences, curves, and slopes in a basin at the earth's surface, obtained for identical conditions on normative technique and on analytical ratios have 5 to 10% of differences.

4.3 Comparing results of theoretical studies and experiments

The section compares the earth's surface deformation values calculated by the analytical solution formulae with adequate results of instrumental measurements performed in 1971-1974 at on observation stations 8, 10, and 13 established by members of Mine Surveying Department of the National Mining University above mining operations of "Stepnaia" and "Yubileinaia" mines.

In the area of the stations mining depth of C_6 and C_6^1 seams was 120 to 190 m. Mining height was 0.9 to 1 m. Bedding was flat-lying with a =3…4° slope angle. Lithology and properties of carbon rocks were typical for Western Donbass mines. Capping thickness was 50 to 70 m. Pillar mining to the rise was applied. Wall length was 180 to 200 m. Advance rate was 30 to 60 m per month. Rock pressure was controlled with the help of complete caving.

Benchmarks were put at the earth's surface above mid longitudinal section of mined pillar with 10-m step.

Fig. 4.6 shows combined plan of mining and observation station 10 located over longwall 530 of "Yubileinaia" mine. Mining depth is $H = 150$ m, capping thickness is $h = 60$ m, mined C_6 seam thickness is $m = 1.0$ m, and average advance rate is $V = 30$ m per month. 350 m of the pillar were mined from October, 1971 till October, 1972.

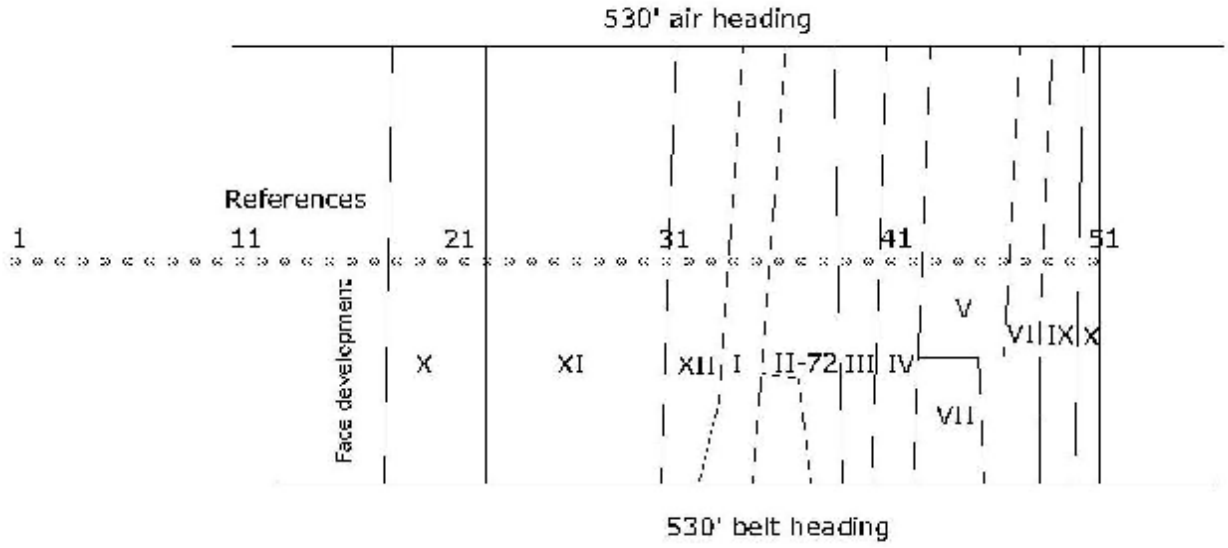

Fig. 4.6. Plan of observation station 10 ("Yubileinaia" mine)

Fig. 4.7 demonstrates both experimental and theoretical settling curves in a basin at the earth's surface if $L = 300$ m.

As the Figure shows, h_m maximums coincide, and other values differences are not more than 6%.

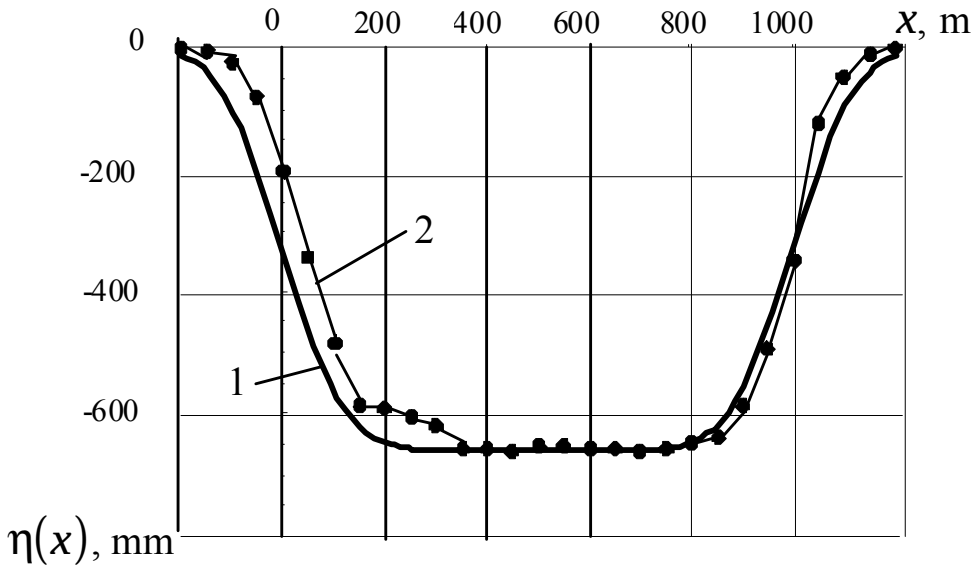

Fig. 4.7. Settling curves in a basin at the earth's surface (station 10) if $L = 300$ m: 1 - theoretical; 2 - experimental

Fig. 4.8 demonstrates integrated mining plan on C_6^1 seam and observation station 8 located on double 713 and 715 longwalls of "Stepnaia" mines.
Mining depth of working seam is $H = 190$ m, and capping thickness is $h =$ 70 m. Average advance rate is $V = 40$ m per month. Period under study is September, 1971 – April, 1972. Thickness of mined seam is $m = 0.7$ m.

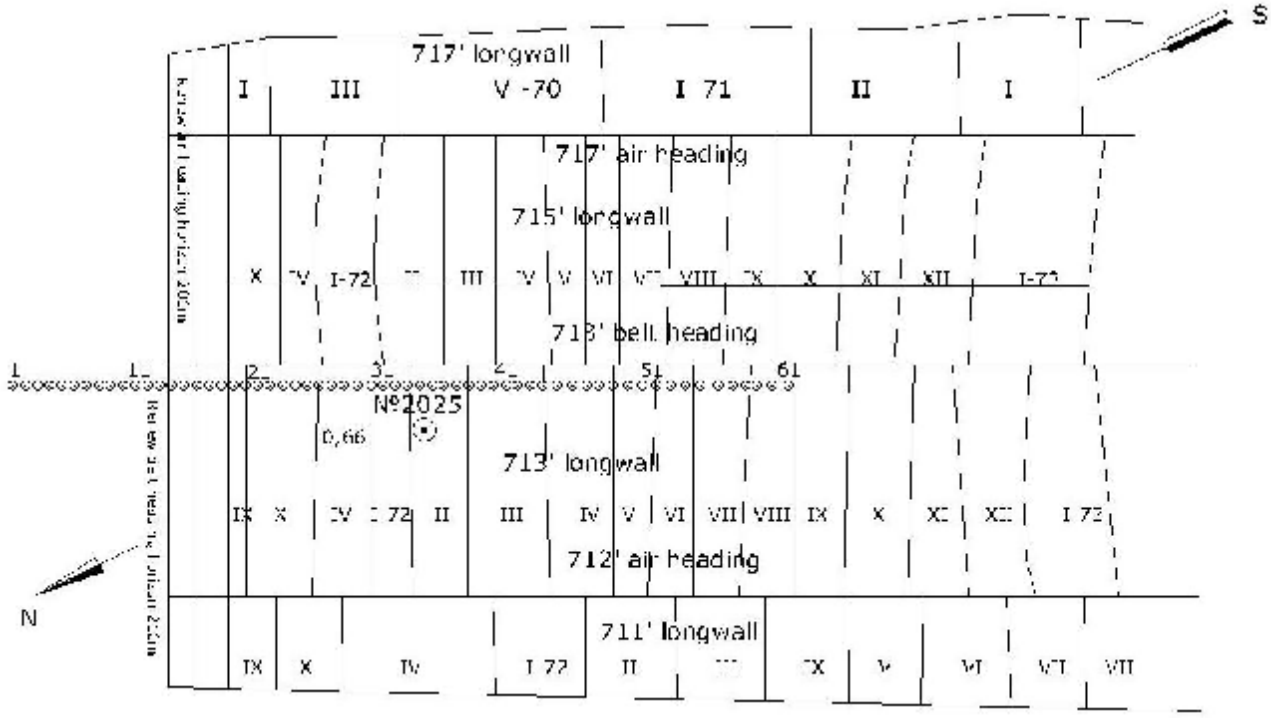

Fig. 4.8. Plan of observation station 8 ("Stepnaia" mine)

Fig. 4.9 demonstrates settling curves within principal section of the earth's surface basin above $L = 300$ m stope, and Fig. 4.10 – inclinations to the settling curves. In these Figures, makers label experimental curves, and full lines show theoretical curves. In this context, h_m difference is 14%, and i_{max} – 12%.

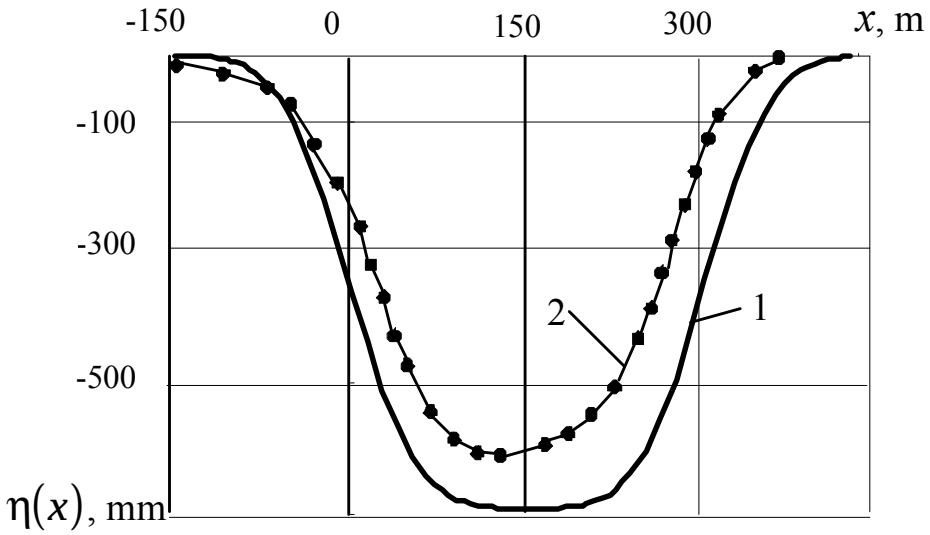

Fig. 4.9. Settling curves in the earth's surface basin (station 8) if $L=300$ m: 1 – theoretical; 2 - experimental

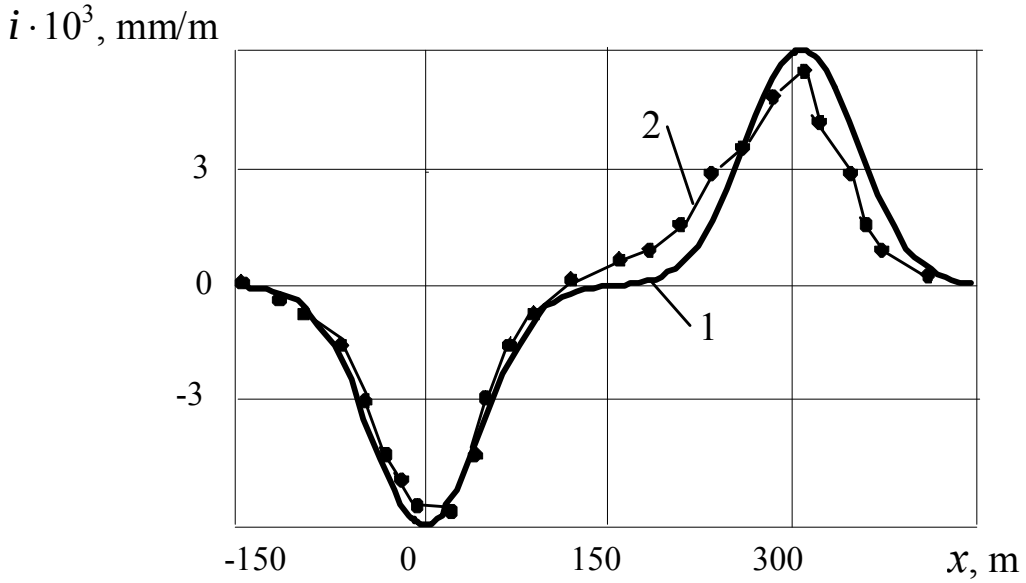

Fig. 4.10. Inclinations in the earth's surface basin (station 8) if $L=300$ m: 1 – experimental solution; 2 – experimental curve

Fig. 4.11 demonstrates integrated mining plan and observation station 13, located above longwall 604 of "Stepnaia" mine. Within the territory, mining depth is $H=120$ m, and mined seam thickness is $m=1$ m. Capping thickness is $h=50$ m; advance rate is 60 m per month, and observation period is from April, 1974 to September, 1974.

Fig. 4.12 and 4.13 demonstrate results of observations and calculations concerning the analytical solution ratios. They are shown as settling curves and

inclination curves within principal section of the earth's surface basin above $L = 300$ m stope.

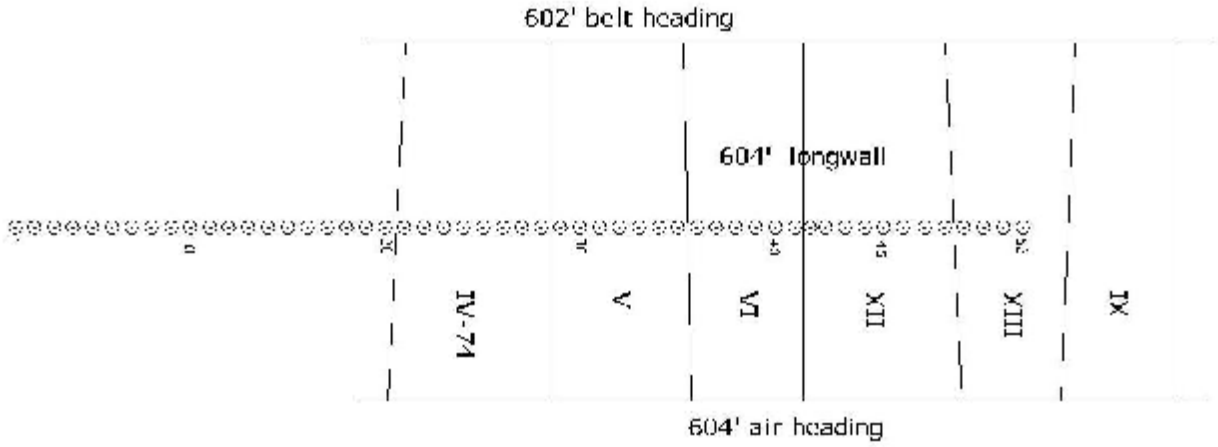

Fig. 4.11. Plan of observation station 13 ("Stepnaia" mine)

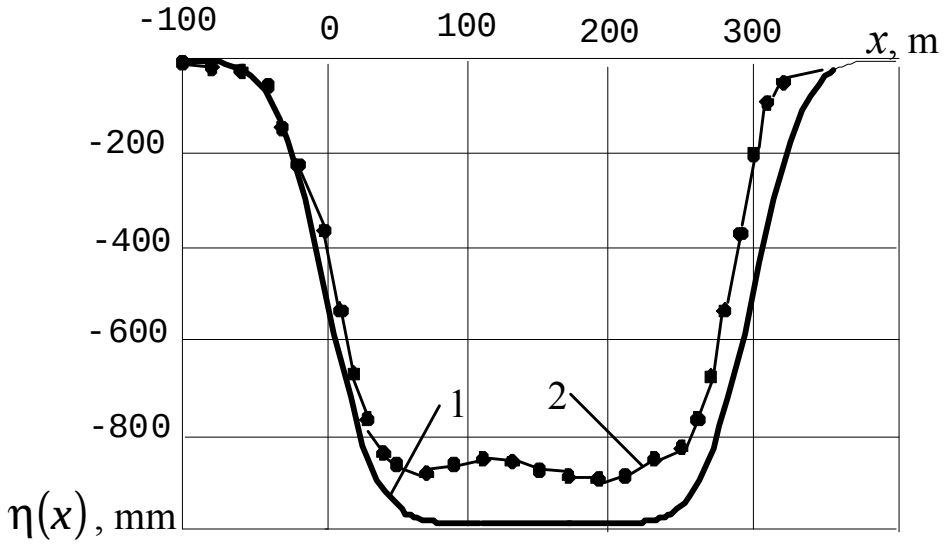

Fig. 4.12. Settling curves in the earth's surface basin (station 13) if $L = 300$ m: 1 – theoretical; 2 – experimental

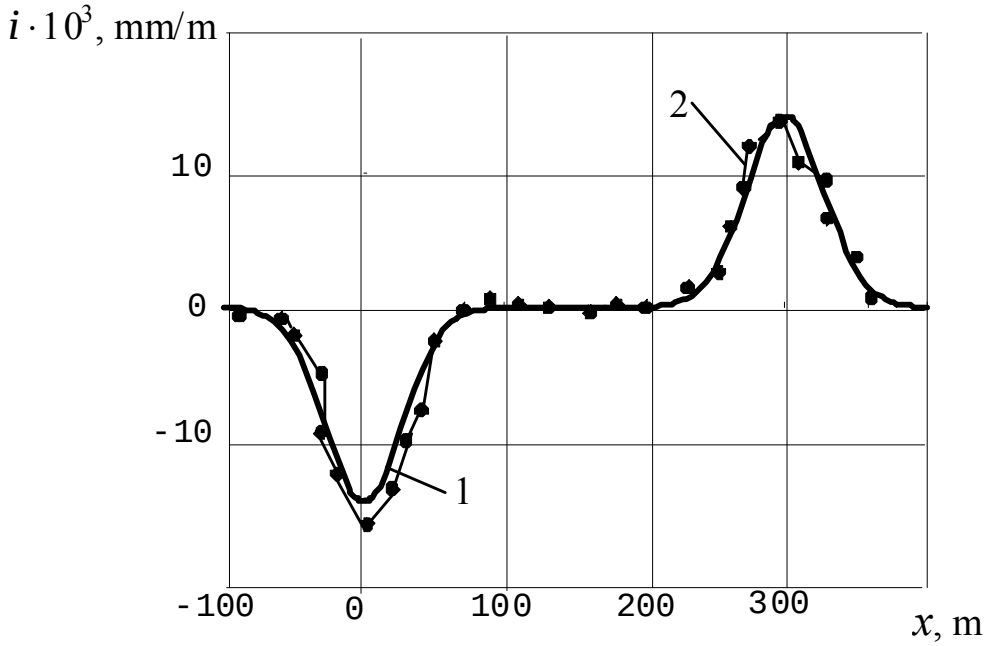

Fig. 4.13. Inclinations in the earth's surface basin station 13) if $L = 300$ m: 1 – theoretical curve; 2 – experimental curve

Similar situation is observed. Practically, all curves are of the same shape. In this context, convergence maximums difference is 17% and inclinations' ones is 8%.

Hence, when qualitative changes in convergences and inclinations in the earth's surface basin are similar, then quantitative differences are 12 to 17% on settling curves, and 6 to 14% on inclinations to them.

To evaluate results of the theoretical research according to the analytical solution formulae, deformation maximums in the earth's surface basin were determined in terms of complete undermining for mining and geological conditions of a 630-m underworking unit of electric railway "Krasnoarmeisk-Pavlograd". 622 and 624 double longwalls of "Stepnaia" mine C_6 seam performed the undermining. Each longwall length was 180 m; extracting seam thickness was 1.0 m; mining depth was $H = 190$ m; capping thickness was $h = 55$ m; and average advance was $V = 50$ m per month.

The deformation values were compared with those determined by the branch standard [14]. The comparison results are in Table 4.1.

Table 4.1 demonstrates the fact that calculated maximums of curves, the earth's surface convergence curves, and settling rates are greater than accepted ones; hence, they may cause damages of the electric railway undermining unit.

Table 4.1

Comparison of calculated parameters with those allowable for second-category railways

Deformation factors	Calculated	Calculated inclusive of overload factor according to category four	Allowable	Calculated-allowable ratio
Tension stress (compression) $(e_x)max$	$1 \cdot 10^{-3}$	$1.4 \cdot 10^{-3}$	$4 \cdot 10^{-3}$	0.35
Curvature K_{max}, 1/m	$1.1 \cdot 10^{-4}$	$1.98 \cdot 10^{-4}$	$1.5 \cdot 10^{-4}$	1.32
Inclinations i_{max}, mm/m	$8.5 \cdot 10^{-3}$	$11.9 \cdot 10^{-3}$	$6.0 \cdot 10^{-3}$	1.98
Subsidence rate U_{max}, mm/day	14.2	17	4.0	4.25

Relaying the departmental out-of-order parallel track to “Pavlogradugol” OJSC mirrors real situation with deformation in the earth’s surface basin.

Comparable situation within restricted area of active railway was avoided thanks to special activities proposed by the Department of Mine Surveying of the NMU and “Dneprogiproshakht” Institute [85]. In addition to continuous welded rail replacing by jointed track they involved tighten control over the railway (instrumental observations after 5-7 days rather than after 15-20 days as it is recommended by the “Norms of protecting buildings and natural objects against harmful effect of underground coal mining” [14]), regular track repair within undermined area, and replacing concrete sleepers by timber ones.

Conclusions

1. The results of numerical evaluations of relative maximum convergences of the earth's surface $\frac{h_{max}}{h_0}$ in a basin above working stope have 15 to 20% difference to compare with the analytical solution ratios depending upon actual relative dimension of the stope $\frac{h_{max}}{h_0}$.

2. In terms of complete undermining, convergences within various points of the earth's surface basin obtained for identical conditions according to normative technique, and those obtained according to analytical ratios have 6 to 30% difference; as for curvature and inclinations, difference is 5 to 12%.

3. Comparison of theoretical settling curves and inclinations at the earth's surface with those obtained experimentally shows that if qualitative factors coincide, then quantitative ones have 12 to 17% difference on settling curves, and 6 to 14 % on inclinations.

4. Maximums of curvature, inclinations, and subsidence rate at the earth's surface basin obtained within 622 and 624 longwalls of C_6 seam of railway of "Stepnaia" mines rank over allowable ones. That can explain replacing in 1977 replacing driveway rails to "Pavlogradugol" OJSC mines railed in parallel to the controlled area. Analogous situation was avoided owing to replacing substitution continuous welded rail by jointed one.

CHAPTER 5. DEFINING RATIONAL PARAMETERS OF COAL MINING UNDER PROTECTED OBJECTS FOR MINING AND GEOLOGICAL CONDITIONS OF WESTERN DONBASS MINES

Chapters two and three detail ratios of analytical solution which help to analyze stress and strained state of undermined mass. That makes it possible to identify certain laws of enclosing rocks deformation and failure formulated in conclusions of those chapters.

"Practice of coal-mining rational parameters defining under protected objects" has been developed using the laws.

The question is advance rate and powered support parameters.

The parameters may be considered as rational if mining equipment is efficient providing labour safety of workers in a longwall. In this context, the earth's surface deformation should not rank over acceptable values of "Norms of protecting buildings and natural objects against harmful effect of underground coal mining" [14].

If acceptable values are ranked over, then measures concerning buildings and other object protection should be adequate and economically viable.

Therefore, the chapter provides formulae to calculate maximums of parameters characterizing deformations in the earth's surface basin in terms of complete undermining and to calculate stresses in a stope roof developing maximum load on the power support ceiling.

5.1 Formulae to determine maximums of the earth's surface deformation in terms of complete undermining

To calculate maximums of convergence, falls, curves, and subsidence rate in the earth's surface basin in terms of complete undermining, give short description of (2.48), (2.52), (2.53), and (2.57) formulae without breaking down expressions for defining function (2.47) and its derivatives.

As chapter 2 shows, all deformation factors are expressed through convergence function

$$h(x,y,L) = -\frac{h_0}{2}(1-exp(-aL))\left[\Phi\left(\frac{L-x}{2\sqrt{j(y)}}\right)+\Phi\left(\frac{x}{2\sqrt{j(y)}}\right)\right] \qquad (5.1)$$

Convergence maximum is determined by

$$h_{max} = h(x,y,L)\Big|_{\substack{x=\frac{L}{2}\\ y=H}} = h_0(1-exp(-aL))\cdot\Phi\left(\frac{L}{4\sqrt{j(H)}}\right) \qquad (5.2)$$

Settling curves are determined by

$$i(x,y,L) = \frac{\partial h}{\partial x} = -\frac{h_0(1-exp(-aL))}{2}\left[\Phi'\left(\frac{L-x}{2\sqrt{j(y)}}\right)\left(\frac{1}{2\sqrt{j(y)}}\right)-\Phi'\left(\frac{x}{2\sqrt{j(y)}}\right)\frac{1}{2\sqrt{j(y)}}\right] =$$

$$= \frac{h_0(1-exp(-aL))}{2 \cdot 2\sqrt{j(y)}} \left[\Phi'\left(\frac{x}{2\sqrt{j(y)}} \right) - \Phi'\left(\frac{L-x}{2\sqrt{j(y)}} \right) \right] \quad (5.3)$$

Correspondingly, maximum is

$$i_{max} = i(x,y,L)\big|_{\substack{x=L \\ y=H}} = -\frac{h_0(1-exp(-aL))}{4\sqrt{j(H)}} \left[\Phi'\left(\frac{L}{2\sqrt{j(H)}} \right) - \Phi'(0) \right] \quad (5.4)$$

Settling curve is

$$k(x,y,L) = \frac{\partial^2 h}{\partial x^2} = \frac{h_0(1-exp(-aL))}{4\sqrt{j(y)}} \left[\Phi''\left(\frac{x}{2\sqrt{j(y)}} \right) \frac{1}{2\sqrt{j(y)}} - \Phi''\left(\frac{L-x}{2\sqrt{j(y)}} \right) \left(-\frac{1}{2\sqrt{j(y)}} \right) \right] =$$

$$= \frac{h_0(1-exp(-aL))}{8j(y)} \left[\Phi''\left(\frac{x}{2\sqrt{j(y)}} \right) + \Phi''\left(\frac{L-x}{2\sqrt{j(y)}} \right) \right] \quad (5.5)$$

$$k_{max} = k(x,y,L)\big|_{\substack{x \cong 0,8L \\ y=H}} = \frac{h_0(1-exp(-aL))}{8j(H)} \left[\Phi''\left(\frac{0,4L}{\sqrt{j(H)}} \right) + \Phi''\left(\frac{0,1L}{\sqrt{j(H)}} \right) \right] \quad (5.6)$$

Horizontal displacements are

$$x(x,y,L) = -K(y)\frac{\partial h}{\partial x} = \frac{K(y)h_0(1-exp(-aL))}{4\sqrt{j(y)}} \left[\Phi'\left(\frac{x}{2\sqrt{j(y)}} \right) - \Phi'\left(\frac{L-x}{2\sqrt{j(y)}} \right) \right] \quad (5.7)$$

Maximum horizontal displacement is

$$x_{max} = x(x,y,L)\big|_{\substack{x \cong L \\ y=H}} = \frac{K(H)h_0(1-exp(-aL))}{4\sqrt{j(H)}} \left[\Phi'_x\left(\frac{L}{2\sqrt{j(H)}} \right) - \Phi'_x(0) \right] \quad (5.8)$$

To identify subsidence rate at any point as a function of variables x, y, and t, insert $L = Vt$ into (5.1).

We get

$$h(x,y,t) = -\frac{h_0}{2}(1-exp(-aVt)) \left[\Phi\left(\frac{Vt-x}{2\sqrt{j(y)}} \right) + \Phi\left(\frac{x}{2\sqrt{j(y)}} \right) \right] \quad (5.9)$$

Differentiating (5.9) function, we obtain expression for subsidence rate as follows

$$U(x,y,t) = \frac{\partial h}{\partial t} = \frac{h_0}{2} aV\, exp(-aVt) \left[\Phi\left(\frac{Vt-x}{2\sqrt{j(y)}} \right) + \Phi\left(\frac{x}{2\sqrt{j(y)}} \right) \right] - \frac{h_0}{2}(1-exp(-aVt)) \times$$

$$\times \frac{V}{2\sqrt{j(y)}} \cdot \Phi'\left(\frac{Vt-x}{2\sqrt{j(y)}} \right) \quad (5.10)$$

Then

$$U_{max} = U(x,y,L)\big|_{\substack{x\cong L \\ y=H}} = \frac{h_0}{2} aV\, exp(-aVt)\Phi\left(\frac{L}{2\sqrt{j(H)}}\right) - \\ - \frac{h_0 V}{4\sqrt{j(H)}}\left(1 - exp(-aVt)\right)\cdot\Phi'(0) \qquad (5.11)$$

As Chapter 2 shows, in terms of considered mining and geological conditions, complete undermining takes place when $\frac{L}{H}$ ratio is equal to unit. Thereby, maximum subsidence reaches value, equal to m thickness of mined bed. Hence, in terms of complete undermining, formulae for maximum deformation h_{max}, i_{max}, K_{max}, x_{max}, and U_{max} are

$$h_{max} = m(1 - exp(-aH))\cdot\Phi\left(\frac{H}{4\sqrt{j(H)}}\right) \qquad (5.12)$$

$$i_{max} = -\frac{m(1-exp(-aH))}{4\sqrt{j(H)}}\left[\Phi'\left(\frac{H}{2\sqrt{j(H)}}\right) - \Phi'(0)\right] \qquad (5.13)$$

$$k_{max} = \frac{m(1-exp(-aH))}{8j(H)}\left[\Phi''\left(\frac{0{,}4H}{\sqrt{j(H)}}\right) + \Phi''\left(\frac{0{,}1H}{\sqrt{j(H)}}\right)\right] \qquad (5.14)$$

$$x_{max} = \frac{K(H)m(1-exp(-aH))}{4\sqrt{j(H)}}\left[\Phi'\left(\frac{H}{2\sqrt{j(H)}}\right) - \Phi'(0)\right] \qquad (5.15)$$

$$U_{max} = \frac{m}{2} aV\, exp(-aH)\Phi\left(\frac{H}{2\sqrt{j(H)}}\right) - \frac{mV}{4\sqrt{j(H)}}\left(1 - exp(-aH)\right)\cdot\Phi'(0) \qquad (5.16)$$

$K(H)$ parameter, being a part of (5.15), is obtained from equation 2 of (2.31), if inserting $y = H$ and $y_1 = H - h$ into it.

Adequate formula is

$$K(H) = c_{tH}^2 H + \left(c_{t\kappa}^2 - c_{tH}^2\right)(H - h) \qquad (5.17)$$

Analogously, equation 2 from (2.32) is applied if we insert $y = H$ into it, obtaining formula for $j(H)$ in view of

$$j(H)=\frac{c_{tн}^2 H^2}{2}+\frac{c_{tк}^2-c_{tн}^2}{2}\left(H^2-h^2\right) \qquad (5.18)$$

According to formula (2.8), dimensionless stiffening parameters c_t^2 of carbon and washes, are identified using following ratio

$$c_t^2=\frac{c^2 E_t}{E}, \qquad (5.19)$$

Being a part of ratio (5.19), c^2 parameter for $c_к^2$=0.075 is a mean of enclosing rocks c_i demonstrated in Table 2.1; it is $c_н^2$=0.0011 for cappings. Section 2.4 describes the technique with the help of developed algorithm.

According to assumed model of linear and congenital creep, elasticity modulus E_t is determined on the formula

$$E_t=\frac{E}{1+\Phi(t)},$$

where $\Phi(t)=\frac{d}{1-a}t^{1-a}$ is a creep function.

Table 2.2 demonstrates values of elasticity moduli E, and creep parameters a and d for carbon and cappings.

Time t, for which elasticity moduli E_t are identified, depends on V and L. $L=H$ in terms of complete undermining, then $t=\frac{H}{V}$.

5.2 Calculating maximum expected values of the earth's surface deformation in terms of complete undermining

Calculation data for mining depth H varying within 200…700 m and capping thickness h varying within 50…240 m (if h/H ratio is 0.25 or 0.4) are of interest for Western Donbass mines. Today average advance rate V is 90…95 m per month, and maximum one reaches 150 m per month.

Table 5.1 demonstrates results of $c_{tн}$, $c_{tк}$, $j(H)$parameter calculation for complete undermining in terms of H,h, and Vvalues varying within indicated values. They are a source material to calculate i_{max}, K_{max}, x_{max}, and U_{max} on formulae (5.13 – 5.16) accordingly.

Tables, mentioned in monograph [64], contain values of function $\Phi(x)$ and its derivatives Φ' and Φ'', being a part of the formulae.

Table 5.1

Source data to calculate deformation factors within the earth's surface basin in terms of complete undermining

H, m	h, m	$j(H)$, m^2				c_{tH}				c_{tK}			
		V, m per month				V, m per month				V, m per month			
		40	80	120	150	40	80	120	150	40	80	120	150
200	50	327.5	384.2	422.7	439.8	0.0251	0.0256	0.0259	0.0261	0.132	0.143	0.150	0.153
	70	307.3	360.5	396.5	412.5								
300	80	665.6	786.6	856.9	905.4	0.0248	0.0253	0.0256	0.0258	0.126	0.137	0.143	0.147
	120	604.5	714.1	777.7	821.6								
400	100	1119.3	1309.9	1452.3	1515.6	0.0246	0.0251	0.0254	0.0256	0.122	0.132	0.139	0.142
	140	1050.8	1229.3	1362.7	1421.9								
500	120	1672.4	1964.8	2151.5	2280.7	0.0244	0.0249	0.0252	0.0254	0.119	0.129	0.135	0.139
	180	1550.4	1820.6	1993.2	2112.6								
600	150	2277.3	2685.9	2947.4	3128.4	0.0243	0.0248	0.0251	0.0253	0.116	0.126	0.132	0.136
	240	2051.6	2418.2	2652.7	2815.0								
700	150	3044.4	3601.0	3957.4	4204.4	00241	0.0247	0.0250	0.0252	0.114	0.124	0.130	0.134
	240	2826.5	3341.9	3671.8	3900.4								

Exponential function $exp(-aH)$ is a part of calculated values too. Any directory on higher mathematics contains the function values table, and Table 5.2 contains values of parameter a for different V rates.

Table 5.2

Values of parameter a

V, m per month	40	80	120	150
a, 1/m	0.038	0.019	0.013	0.010

Tables 5.3 and 5.4 demonstrate calculation results in the form of the earth's surface deformation maximums in terms of complete undermining, responding to the source data. In addition to U_{max} values, Table 5.4 shows maximums of horizontal deformations of tensile (compression) e_x, being essential if mining takes place under various pipelines.

Table 5.3

Maximums of falls and curves within the earth's basin in terms of complete undermining

H, m	h, m	$i_{max} \cdot 10^3$, mm per month				$K_{max} \cdot 10^3$, 1/m			
		V, m per month				V, m per month			
		40	80	120	150	40	80	120	150
200	50	15.59	14.24	13.11	12.23	0.368	0.306	0.245	0.241
	70	16.09	14.70	13.54	12.63	0.393	0.328	0.285	0.259
300	80	10.93	10.05	9.55	9.12	0.182	0.152	0.137	0.127
	120	11.47	10.55	10.02	9.57	0.200	0.169	0.153	0.141
400	100	8.43	7.79	7.39	7.19	0.108	0.0920	0.0821	0.0778
	140	8.70	8.04	7.63	7.42	0.115	0.0983	0.0880	0.0835
500	120	6.90	6.36	6.08	5.89	0.0722	0.0615	0.0558	0.0522
	180	7.16	6.61	6.32	6.12	0.0776	0.0665	0.0605	0.0568
600	150	5.91	5.44	5.20	5.04	0.0529	0.0450	0.0409	0.0383
	240	6.23	5.74	5.48	5.31	0.0581	0.0500	0.0456	0.0429
700	150	5.11	4.70	4.48	4.35	0.0395	0.0336	0.0305	0.0286
	240	5.31	4.88	4.66	4.52	0.0422	0.0362	0.0329	0.0309

Table 5.4

Maximums of deformations e_x and subsidence rates within the earth's surface basin in terms of complete undermining

H, m	h, m	$(e_x)_{max}$, mm per month				U_{max}, mm per day			
		V, mm per month				V, m per month			
		40	80	120	150	40	80	120	150
200	50	0.973	0.945	0.903	0.853	20.78	38.24	53.61	63.43
	70	0.908	0.888	0.847	0.801	21.46	39.47	55.31	65.42
300	80	0.644	0.637	0.625	0.609	14.58	26.82	38.43	46.28
	120	0.580	0.583	0.575	0.561	15.30	28.15	40.33	48.55
400	100	0.489	0.487	0.481	0.476	11.24	20.78	29.60	36.14
	140	0.454	0.454	0.450	0.446	11.60	21.46	30.56	37.30
500	120	0.394	0.393	0.391	0.388	9.20	16.97	24.33	29.52
	180	0.360	0.361	0.360	0.358	9.55	17.63	25.27	30.67
600	150	0.325	0.326	0.324	0.323	7.88	14.51	20.78	25.22
	240	0.290	0.293	0.293	0.292	8.30	15.30	21.91	26.58
700	150	0.286	0.287	0.286	0.285	6.82	12.54	17.94	21.75
	240	0.258	0.261	0.261	0.260	7.07	13.01	18.62	22.59

As Table 5.1 demonstrates, $j(H)$ values depend greatly not only on mining depth H, but also on capping thickness h. As for c_{tH} and c_{tK} parameters, H variation is negligible, and h variation can not be manifested. However, when 1.4 to 1.6 capping thickness increase takes place, maximum falls increase is 4…10%, maximum curve increase is 13…20 %. Data of Table 5.3 confirm that. At such an increase in h, maximum subsidence rate experiences 7 to 10% increase, and as Table 5.4 demonstrates, maximum deformations of tensile (compression) e_x, experience 7 to 12% decrease.

It points to the fact, that availability of washes can not be forgotten while identifying factors of the earth's surface deformation.

Mining depth is very important for deformation factor. Thus, if 3.5 times increase of H (200 to 700 m) takes place, depending upon advance rate maximum falls i_{max} experience 2.8 to 3 times decrease, maximum curve – 8.4 to 9.3 times decrease, deformations of tensile (compression) $(e_x)_{max}$ – 3.2 to 3.4 times decrease, and maximum subsidence rate experiences 2.9 to 3.0 times decrease.

In terms of advance rate V 3.75 times increase (40 m per month to 150 m per month), i_{max} experiences 1.2 to 1.27 times decrease depending upon mining depth H, K_{max} experiences 1.4 to 1.53 times decrease, and $(e_x)_{max}$ experiences 1.02 to 1.14 times decrease; at such an increase of advance rate, maximum subsidence rate experiences 3.05 to 3.2 increase.

According to "Undermining rules…" [13], calculated displacements and deformations of the earth's surface are obtained by means of multiplying maximum predicted displacements and deformations by overload factor having following values: 1.2 for falls; 1.4 for horizontal deformations and falls; and 1.8 for curves.

Undermining building and structures is performed without protective measures if it meets the requirements of rational coal mining.

Table 5.5 demonstrates environment for rational coal mining typical for area of interest. Also, this very Table lists normative tolerable factors of the earth's surface deformations specified by "Undermining rules…" [13].

Table 5.5

Environment for rational coal mining

Undermined structures	Rational mining environment	normative tolerable factors of the earth's surface deformations	Units
1. Transmission towers a) 220 - 400 kV b) 6 - 110 kV			
	$i \le [i]$	$[i]=12\cdot10^{-3}$	-
	$i \le [i]$	$[i]=15\cdot10^{-3}$	-
2. Surface gas pipelines	$e \le [e]$	$[e]=8\cdot10^{-3}$	mm/m
Approach lines	$e \le [e]$	$[e]=8\cdot10^{-3}$	mm/m
	$i \le [i]$	$[i]=10\cdot10^{-3}$	-
	$K \le [K]$	$[K]=5\cdot10^{-4}$	1/m
	$U \le [U]$	$[U]=10$	mm/day

If rated factors of deformations or daily subsidence rates of the earth's surface go beyond proper tolerable values, then undermining structures should include protective measures.

Hence, while coal mining in terms of considered mining and geological conditions takes place under power transmission towers of 10 kV at the mining depth of 200 m and V = 40…150 m per month, expected falls are more than allowable standard values. Therefore, such a case needs involving certain protective measures, for example, matching towers, bypassing overhead conductors, resetting damaged areas of conductors etc.

Mining at the depth of 300…400 m is possible without involving protective measures, if $V \ge 80$ m per month as in this context $i = i_{max} \cdot 1.4 = 8.04\cdot10^{-3}\cdot1.4=11.26\cdot10^{-3}<12\cdot10^{-3}$. When mining depth is $H \ge$ 500 m, the requirement is met at $V \ge 40$ m per month.

In the case of surface gas pipeline undermining calculation of deformation of tensile (compression) $e_x = (e_x)_{max}\cdot1.4$ assumes such values as $e_x = 0.36…1.36$ depending upon advance rate V and mining depth H. The values rank over allowable $[e]=0.008$. Hence, any H and V values falling into considered intervals of the parameters variation should involve these or those protective measures.

If approach lines are undermined, then the condition of rational mining at the depth of H =400 m is met on falls if advance rate is; it is true at the depth of $H \geq$500 m if $V \geq$40 m per month. However, estimated deformations e_x as well as subsidence rate U rank over allowable ones at any values of $H \in$ [200…700] m and $V \in$ [40…150] m per month. Thus, undermining approach lines under considered mining and geological conditions require protective measures by specialized Ukrainian Institute of Mine Surveying.

5.3 Calculating a load acting on a ceiling of powered support unit

To identify load acting on a ceiling of powered support unit against mining pressure and calculate reaction of hydraulic props, it is required to determine and analyze stress-strain state of a stope roof rocks.

For this purpose use following analytical expressions of stress tensor

$$s_x = -\frac{EK(y)}{1+n}\frac{\partial^2 h}{\partial x^2} - lg(H-y) \tag{5.21}$$

$$s_y = \frac{EK(y)}{1+n}\frac{\partial^2 h}{\partial x^2} - g(H-y) \tag{5.22}$$

$$t_{xy} = \frac{E}{2(1+n)}\left[\left(1-\frac{dK(y)}{dy}\right)\frac{\partial h}{\partial x} - K(y)\frac{\partial^2 h}{\partial x \partial y}\right] + \frac{1-2n}{2(1-n)}g(H-y) \tag{5.23}$$

Derived functions $h(x,y,L)$ from (5.21 - 5.23) formulae expressed through derived functions $\Phi(x)$, are identified by the ratios

$$\begin{aligned}
\frac{\partial h}{\partial x} &= -\frac{h_0(1-exp(-aL))}{2}\left[\Phi'\left(-\frac{L-x}{2\sqrt{j(y)}}\right) + \Phi'\left(\frac{x}{2\sqrt{j(y)}}\right)\right];\\
\frac{\partial^2 h}{\partial x^2} &= -\frac{h_0(1-exp(-aL))}{4\sqrt{j(y)}}\left[\Phi'\left(\frac{x}{2\sqrt{j(y)}}\right) - \Phi'\left(\frac{L-x}{2\sqrt{j(y)}}\right)\right];\\
\frac{\partial^2 h}{\partial x \partial y} &= -\frac{h_0(1-exp(-aL))}{8j(y)\sqrt{j(y)}}\left[(L-x)\cdot\Phi'\left(\frac{L-x}{2\sqrt{j(y)}}\right) + x\cdot\Phi'\left(\frac{x}{2\sqrt{j(y)}}\right)\right],
\end{aligned} \tag{5.24}$$

Where e $j(y)$ is described with the help of equation one of (2.32) being in the form of

$$j(y) = \frac{c_{tk}^2 y^2}{2} \tag{5.25}$$

Accordingly, $K(y)$ function, effecting (5.21 - 5.22) stresses is

$$K(y) = c_{tk}^2 y \tag{5.26}$$

As it is shown above, load, acting on power support, depends on weight of rocks within boundary state of stress in the neighbourhood the stope. Criterion (1.4) identifies the zone boundaries.

The greatest pressure power support experiences while main roof caving;

hence, time t helping to determine $c_{t\kappa}^2$ parameter with the use of (5.18) ratio is identified by the formula $t = \frac{l_0}{V}$,

where l_0=0.05 H is a caving step of the main roof.

Table 5.6 demonstrates initial data and calculation results for maximum load, acting on power support ceiling.

Table 5.6

Results of calculating load, acting on powered support

Mining depth H, m	Stiffening parameter $c_{t\kappa}$	Maximum length of boundary state of stress zone, m		Load, acting of the section unit		Reactions in hydraulic props, kN	
		OX-direction	OY-direction	Total, kN	Specific q, kN/m^2	In front R_1	In rear R_2
V=40 m per month							
200	0.182	1.6	13.9	552	184	200	352
300	0.176	2.4	19	1139	380	412	727
400	0.171	2.6	23.4	1494	498	541	953
500	0.168	2.8	26.8	1864	621	675	1189
600	0.165	3	30	2272	757	822	1450
700	0.163	3.3	31.2	2558	853	926	1632
V=80 m per month							
200	0.193	1.9	7.1	159	53	58	101
300	0.186	1.22	10.4	315	105	114	201
400	0.182	1.5	13	484	162	175	309
500	0.179	1.8	15.4	689	230	249	440
600	0.176	2.0	17.5	870	290	315	555
700	0.174	2.2	19.4	1060	353	384	676
V=120 m per month							
200	0.198	0.62	4.9	75	25	27	48
300	0.193	0.9	7.1	158	53	57	101
400	0.188	1.1	9.1	249	83	90	159
500	0.185	1.3	11	466	118	129	227
600	0.182	1.5	12.5	870	155	169	297
700	0.180	1.6	14	564	188	204	360
V=150 m per month							
200	0.201	0.5	3.8	47	16	17	30
300	0.196	0.72	5.5	99	33	36	63
400	0.192	0.85	7.1	149	50	54	95
500	0.188	1.0	8.6	224	75	81	143
600	0.186	1.2	10	298	99	108	190
700	0.183	1.3	11	358	120	130	228

Following requirements should be met for adequate operation of the powered support according to its specifications noted above:

$R \le \sum_j R_j$ =1560 kN according to total load on the ceiling;

$q \le [q]$ =400 kN/m^2 according to specific total load on the ceiling;

$R_{j\,max} \le [R_j]$ =650 kN according to maximum load on the hydraulic prop.

Comparing specified values (Table 5.6) with allowable ones helps to come to conclusion that under considered mining and geological conditions the support is efficient at $H = 200 \ldots 700$ m, if $V = 80$, 120, and 150 m per month; if $V = 40$ m per month only at 200 m.

Interpolation of data, showed in Table 5.6 for $V = 40$ m per month and $V = 80$ m per month, can demonstrate that the support operates efficiently at 200…700 m depth even if $V = 70$ m per month.

5.4 Determining rational advance rate and power support parameters for certain mining and geological conditions

According to advanced development program of mining in "Stepnaia" mine for 2007-2010, mine seam C_6^1 will be mined by longwalls No.202-bis and No.204-bis.

In 2001-2002 longwalls No. 100-bis and 102-bis mined C_6 seam. Mining depth H was 350, capping thickness was h=80 m, mined thickness was m=1.0 m, and average advance rate was $V = 70$ m per month.

Overhead line of 10 kV was within a mining affected zone; it was mined again by such longwalls as No.104-bis and No. 106- bis within the area of about 1.45 km.

While mining C_6^1 seam at the depth of H =330 m, a site having 1.1 km length will be undermined again.

According to conditions of rational mining under power transmission towers of 10 kV (Table 5.5), expected falls should not be more than $15 \cdot 10^{-3}$ values.

Let's check, if the requirement is met. In this context we consider each undermining as it is required by design norms of meaningful protective measures.

Using interpolation and data of Table 5, we determine calculated value $i = i_{max} \cdot 1.4 = 8.69 \cdot 10^{-3} \cdot 1.4 = 12.2 \cdot 10^{-3}$ in the process of primary undermining by such longwalls as No. 100-bis and No. 102-bis for H =350, h=80 m, and V = 70 m per month $i_{max} = 8.69 \cdot 10^{-3}$.

As in this context $i < 15 \cdot 10^{-3}$, then protective measures are not provided. During next stage (operations of 104-bis and 106-bis longwalls) we have $i_{max} = 8.69 \cdot 10^{-3}$ and $i = 12.2 \cdot 10^{-3}$, and total fall $i_{max} = 17.4 \cdot 10^{-3}$ and $i = 24.3 \cdot 10^{-3}$ for similar values of H =350 m, h=80 m, and $V = 70$ m per month. As $i > 15 \cdot 10^{-3}$, then corrective maintenance took place at the stage. The maintenance was required to get undermined object under a state meeting the requirements of its normal operation.

Finally, using data by Table 5.3, determine i_{max}=9.17·10^{-3} under the conditions of 202-bis and 204-bis longwalls operation at the depth of H=330 m, at h=80 m, and V = 70 m per month.

It follows that at the stage of such longwalls as 202-bis and 204-bis operation, calculated value of falls is 2.48 times more than allowable standard one. Hence, the stage should provide corrective maintenance of specific area of electric power line of 10 kV (support matching, line bypassing).

As for the powered support, then data by Table 5.6 are applied for interpolating H=350 and V = 70 m per month; specific pressure q on its ceiling is determined. The pressure is 206 kN/m^2. Adequate calculated value with safety factor of 1.5 is 309 kN/m^2 at allowable value of 400 kN/m^2.

Total load on the ceiling is $\sum_j R_j$=627 kN, and calculated value is $\sum_j R_j$=940 kN. The value is less than allowable $[R]$=1560 kN. Maximum load on hydraulic prop is $(R_j)_{max}$=400 kN; hence, calculated value $(R_j)_{max}$=600 kN is also within allowable value $[R_{max}]$=650 kN.

Maximum displacement of roof calculated according to formula (5.2) with 1.5 safety factor is 0.56, and allowable value 0.64 m.

Hence, at H=350 and V = 70 m per month, requirements for effectiveness of the powered support, are met.

When advance rate is V = 80…120 m per month, then safety coefficient is greater as increase in advance rate V results in decrease of load acting on the support; calculated falls also decrease. However, at V=120 m per month, i values rank over allowable ones.

Thus, operation of the powered support is efficient at such depth as 330…350 m is advance rate is $V \in$ [80…120] m per month; however, within the area of repeated undermining of 10 kV power transmission line it is required to provide certain protective measures; third undermining should involve corrective maintenance.

The recommendations were put into practice while mining C_6 seam by longwall 117, and developing measures by technical department of “Stepnaia” mine. The measures were developed to provide efficiency of equipment and protective measures for objects in the process of mining such longwalls as 202-bis and 204-bis of C_6^1 seam planned for the period of 2007-2010.

Economy of the recommendations applied in “Stepnaia” mine is 539,700 UAH.

Conclusions

1. Expected factors of the earth's surface deformation in terms of complete undermining have been calculated for mining and geological conditions of Western Donbass according to the technique.

Values of maximum falls, curves, deformations of tensile (compression), subsidence rates for H=200…700 m, such advance rates as V=40…150 m per month, and h/H=0.25 and 0.4 ratios have been rated.

2. Analysis of the calculated parameters shows the following:

- 1.4 to 1.6 times increase in capping thickness h results in 4…10% increase of maximum falls, 13…20% increase of maximum curves, 7…10% increase of maximum subsidence rate; maximum deformation of tensile (compression) experiences 7…12% decrease.

- Depending upon advance rate, 3.5 times increase in mining depth (200 to 700 m) results in i_{max} maximum falls decrease (2.8 to 3 times), maximum curves K_{max} decrease (8.4 to 9.3 times), deformation $(e_x)_{max}$ decrease (3.2 to 3.4 times), and maximum subsidence rate U_{max} decrease (2.9 to 3.0 times).

- Depending upon mining depth H, 3.75 times increase in advance rate V (40 m per month to 150 m per month) results in i_{max} decrease (1.2 to 1.27 times), decrease in K_{max} (1.4 to 1.53 times), decrease in $(e_x)_{max}$ (1.02 to 1.14 times); U_{max} experiences 3 to 3.2 times increase.

3. Basing upon the analysis of stress-strain state of rocks at the level of a mined seam load on powered support within the area of electric power line was determined taking into account the earth's surface deformation and the technique developed for mining and geological conditions of Western Donbass; besides, range of advance rate values at which the powered support operates efficiently at a given depth has been specified. It is demonstrated, that such values as V=80…120 m per month are rational for H=300…350 m. Adequate calculated maximal total load acting on the power support unit is 940 kN when allowable one is $[R]$=1560 kN; calculated value of roof caving over the ceiling of maximally loaded unit of the powered support is h_{max}=0.56 m when allowable one is h=0.64 m.

OVERALL CONCLUSIONS

The main results, generalizing conclusions, and practical recommendations amount to the following:

1. In reliance on mathematical analogy between rock displacement and thermal conductivity, Fourier method for differential equation solving is applied for two-layer "cappings-carbon" undermined mass. New analytical ratios are obtained. The ratios characterize stress-strain state in any point of rock mass and the earth's surface at any stage of coal mining.

As distinct from well-known, they take into account advance rate as well as rock rheology.

2. Boundary-element method as well as models of linear and congenital medium is applied to develop an algorithm of numerical solution for plane stress geomechanical problem; the solution is applied to identify stiffening parameters of undermined mass rocks used as initial data for the analytical solution.

The algorithm advantage is that ratios of S. Crouch problem for semiplane are applied. That provides the fulfillment of boundary conditions within outer contour of the mass's area (at the earth's surface); discretization is applied for inner contours only.

3. Minimizing general analytical ratios are used for formulae to calculate maximums of the earth's surface deformation to be compared with standard allowable values while determining rational parameters of coal mining; besides they can be functional while developing required protective measures for objects.

4. The analytical ratios obtained for mining and geological conditions of Western Donbass are applied to identify the earth's surface deformations in terms of partial and complete undermining. Following rules are made clear:

- In terms of parallel distance between the longwall and face entry L, maximum subsidence h_{max} decreases depending upon mining depth increase; the thicker cappings are (h), the greater is h_{max} value at the given depth H.

- At fixed mining depth values H and in terms of partial undermining, maximums of horizontal displacements x_{max} increase depending upon increase in the stope dimension L, decreasing with the increase of capping thickness h.

- The thicker cappings are, the greater is the maximum of subsidence rate U_{max}.

- Subsidence rate increases depending upon the increase in advance rate.

- Increase in mining depth H results in maximum of subsidence rate U_{max}.

- At fixed mining depth H and capping thickness h, maximum of subsidence rate increases (at any advance rate V) up to forming L=100 m stope; then, U_{max} remains constant being equal to 4 mm per day if V=30 m per month; 9 mm per day if V=60 m per month; and 11 mm per day if V=80 m per month.

- In terms of complete undermining (L=400 m, H=400 m, and h=140 m), maximums of the earth's surface deformation are h_{max}=1000 mm, x_{max}=40 mm, K_{max}=11·10^{-5} 1/m, i_{max}=8.5 mm per month, U_{max}=9 mm per day if V=60 m per month.

- It is illustrated that in terms of complete undermining due to creep, maximums of subsidence rates experience 1.1 to 1.25 times increase, horizontal displacements experience 1.5 to 1.53 times increase, curves experiences 2.5 times increase, and falls experience 2.1 times.

- Periods of the earth's surface displacement are determined: if V=80 m per month, then initial displacement stage is 3.75 months, active stage is 5 months, and attenuation stage is 3.75 months.

5. Resulting from the analysis of stress-strain state of rocks within undermined coal seam and with the help of obtained analytical ratios, following rock pressure manifestations are identified:

- Level of equivalent stress s_{eq} in the roof is inversely related to advance rate.

- 3 times increase in mining depth H (200 to 600 m) results in 2.14 times increase of maximum length of boundary state of stress in OY - direction (vertical), and 2.25 times increase in OX - direction (horizontal).

- If displacement rate is constant at various depths, expected caving step of the main roof is 0.05 of adequate depth.

- When mining depth is H=400 m, advance rate is V=30 m per month, and parameter a=0.04 1/m, then a step of possible caving step of immediate roof is $l_н$=5 m, and that of the main roof is l_o=10 m; if V=60 m per month, a=0.03 1/m $l_н$=10 m, and l_o=20 m; and if V=80 m per month and a=0.019 1/m $l_н$=15 m, l_o=22 m.

6. The "Technique for rational coal mining parameters under protected objects" has been developed basing upon rules of state-strain state change of mass while coal mining in terms of mining and geological conditions of Western Donbass mines. The technique was transmitted to be used by "Dneprogiproshakht" SOJSC. With the aid of it parameters of powered support are identified, and a range of rational values of advance rate under electric power line are determined: for such mining depths as H=300…350 m, values of V=80…120 m per month are rational; calculated load R falling on the powered support unit is 940 kN when allowable $[R]$=1560 kN, and calculated value of rock fault over the ceiling of maximally loaded unit of the support is h_{max}=0.56 m when allowable one is $[h]$=0.64 m . Matching power transmission towers with line bypassing are provided as protective measures for power lines if repeated undermining takes place.

7. Results of comparing calculated values of subsidence and falls at the earth's surface basin with adequate data of survey measurements confirm feasibility and validity of conclusions and recommendations (if qualitative data coincide, and then quantitatively subsidence differs by 12…17%, and falls differ by 6…14%). Comparative data obtained for similar conditions using normative technique and analytical ratios also confirm validity of the results. Subsidence in various areas of the basin at the earth's surface differ by 6…30%, and curves and falls – by 5…12%.

8. Technical department of "Stepnaia" mine applies the recommendations on determining parameters of roof fall in a longwall, stresses in hydraulic props of powered support, and advance rate while developing measures to provide efficiency of mining equipment as well as protection of objects. Economy of the recommendations applied in "Stepnaia" mine is 539,700 UAH.

REFERENCES

1. Justification of action plan to prevent harmful effect on surface due to mining by "Pavlogradugol" PA. Volume 1, Process part. – Dnipropetrovsk: "Dneprogiproshakht", 1991. – 542 p.

2. Kolokolov, O.V., Lubenets, N.A. On rational parameters of coal seam mining in Western Donbass/ Collection of scientific papers of NMU of Ukraine. – Dnipropetrovsk, 2000. – No. 10. – 5 – 12pp.

3. Kiashko, I.A., Ovchinnikov, N.P. et al. Technique of rather thin seams mining with stowing // Mining magazine "Izvestia vuzov", 1990. – No. 2. – 17-20pp.

4. Undermined coal seam augering / V. I. Bondarenko, I. A. Kovalevskaia, P. P. Korzh, G. A. Simanovich. – Dnipropetrovsk, SSPE "Sistemnye tekhnologii", 1998. – 123 c.

5. Bublik, F. P. Some problems of pillar supporting capacity determining // Manless mining. – M.: Nedra, 1965. – 39 – 45 pp.

6. Khalimendik, Y.M. Practice of mine under the conditions of complicated mining and geological conditions // Coal of Ukraine. – 1995.- No. 6. – 12 – 14pp.

7. Roof control and supports in stopes of coal seams which slope angle is up to 35º. – K.: Ministry of Fuel and Energy of Ukraine, 2002. – 142p.

8. Makarevich, Y.S., Tkachenko, A.G., Babenko, P.S. Results of underground trials of powered support for mining and stowing // Coal, 1989. - No. 7. 34-36pp.

9. Temporary guidelines for mine pressure control within seams which thickness is up to 3.5 m, and slope angle is up to 35º. L.: AUIMS, 1982. – 134p.

10. Baklashov I.V., Kartozia B.A. Mechanics of underground facilities and support structures. – M.: Nedra, 1984. – 415 p.

11. Struiev, M.I., Podgornova, N.F. Geology and coal of Western Donbass // Problems of developing coal industry of Western Donbass. – M.: Nedra, 1965. Geological and industrial outline of Western Donbass: Geological record / under the editorship of M.I. Struiev. – Kiev: Resources of UTGR. – 395 p.

12. Methodological instructive regulations on the earth's surface deformation calculating in accordance with time, and rock and geometrical forecasting plain flood protection while underground mining in Western Donbass: approved by Ministry of Industry of UkrSSR / Donetsk, 1986. 54 p.

13. Rules of undermining facilities, structures, and natural objects while underground mining / Branch standard. – K.: Ministry of Fuel and Energy of Ukraine, 2004. – 127 p.

14. Rules of protecting structures and natural objects against harmful effect within coal deposits. // – M.: Nedra, 1981. – 288 p.

15. SNiP (Construction norms and specifications)-15-74 Foundations of buildings and structures. – M.: "Stroyizdat", 1975. – 64 p.

16. Recommendations on calculating displacements of contour and loads on mine working support according to experimental factors of rock deformation beyond safety. – L.: All-Union Research Institute of Rock Mechanics and Mine Surveying, 1982. – 36 c.

17. Design, construction, and protection of buildings and structures within undermined territories. – M.: Gosgortekhizdat. – 1963. – 142 p.

18. Borisov, A.A. Mechanics of rocks and rock massifs. – M.: Nedra. 1960. – 360 p.

19. Displacement of rocks and the earth's surface in principal coal fields of the USSR. – M.: Ugletekhizdat. – 1958. – 60 c.

20. Usachenko, B.M. Rock properties and opening strength. – Kiev: Naukova dumka, 1979. – 136 p.

21. Pisarenko, G.S., Lebedev, A.L. Structural resistance to deformation and breaking in terms of combined stress. – K.: Naukova dumka, 1969. – 209 p.

22. Creep of sedimentary rocks (theory and experiment) / Z.S. Erzhanov, A.S. Saprygin, G.N. Gumeniuk et al. Alma-Ata: Nauka, 1970. – 208 p.

23. Catalog of mechanical properties of rocks when long-term trial in terms of linear compression / A.N. Stavrogin, V.S. Georgievski, E.V. Lodus. – L.: AURIMS, 1972. – 73 p.

24. Borisov, A. A. Calculating mine pressure within longwalls of flat seams. – M.: Nedra, 1964. – 277 p.

25. Ruppenneight, K.V. Certain problems of rock mechanics. M.: Ugletekhizdat, 1954. – 358 p.

26. Borshch-Komaniets, V. I., Makarov, A. V. Mine pressure in terms of mining thick flat ore deposits. – M.: Nedra, 1986. – 271 p.

27. Erzhanov, Z.S., Karimbaev, T.D. Finite-element method in problems of rock mechanics. – Alma-Ata: Nauka, 1975. – 237 p.

28. Fadeiev, A.B. Finite-element method in rock mechanics. M.: Nedra, 1987. – 236 p.

29. Komissarov, S.N. Control of rock massif in the neighbourhood of stopes. – M.: Nedra, 1981. – 237 p.

30. Crouch, S, Starfield, A. Finite-element method in solid-state mechanics. – M.: Mir, 1987. – 328 p.

31. Crouch S.L. Solution of plane elasticity problems by the displacement discontinuity method. – Int. J. Num. Methods in Engineering, 1976. – Vol. 10. –301 – 343 pp.

32. Jaswon M.A., Maiti M., Symm M. Numerical beharmonic analysis and some applications // Int. J. Solids and Structures.- 1967.- 3.- 309 - 332 pp..

33. Rizzo F.J. An integral equation approach to boundary value problems of classical elastostatics // Quart. Appl. Math.- 1967.- 25. - 83 - 95 pp.

34. Jaswon M. A., Ponter A. P. An integral equation method for a torsion problem // Proc. Roy. Soc. Sec. 4. – 1963. – 273. –237 - 246 pp.

35. Finite-element method in problems of rock mechanics / Novikova, L.V., Ponomarenko, P.I., Prikhodko, V.V., Morozov, I.T. – Dnipropetrovsk: Nauka i obrazovanie, 1977. – 304 p.

36. Shashenko, A.N., Tulub, S.B., Sdvizhkova, E.A. Some problems of statistic rock mechanics. – K.: University press "Pulsary", 2002. – 304 pp.

37. Linkov, A.M. On considering out-of-limit deformation while solving problems of rock mechanics.- L.: AURIMS, 1977.- Collected papers 103. – 71-76 pp.

38. Lieberman, Y.M., Khaimova-Malkova, R.P. Elastoplastic stress analysis of coal seam selvage stress state by finite-element method // Academic Messages / A.A. Skochinski Mining Practice Institute, 1982. – No. 204. – 34-40 pp.

39. Novikova, L.V., Sdvizhkova, E.A. Effect of mining rate on an approach rate of roof and soil of bags formed in the process of ore augering // Manganese. Abstractive collection, Tbilisi: Georgian Research Institute of Scientific and Technical Information. 1987. – 6-8 pp.

40. Novikova, L.V., Ulanova, N.P., Prikhodko, V.V. Stresses in the neighbourhood of a working within crumbling rocks massif // Izvestia vuzov. Gorny zhurnal, 1994. – No. 7. – 11-13 pp.

41. Novikova, L.V., Sdvizhkova, E.A., Kasem, Abdullah. Probabilistic assessment of rupture zone formation in the neighbourhood of interference workings // Physicotechnical application of mathematic simulation. – Kiev, 1998. – 197-199 pp.

42. Nalivaiko, Y.M. Grounding parameters of superimposed seams mining by powered systems in terms of Lvov-Volyn deposit. Synopsis of a thesis for Cand.Sc. {Engineering}: 05.15.02. – Dnipropetrovsk, 2002, - 18 p.

43. Kuzhel, S.V., Khoziaikina, N.V. Calculating parameters of steady caving step with a stratum of solid rocks in coal seam roof // "Geotehnicheskaia mehanika". Interdepartmental collection of scientific papers of Institute of Geotechnical Mechanics, Donetsk – Dnipropetrovsk, 2002, - No. 40. – 166-173.

44. Avershin, S.G. Displacing rocks while underground mining. – M.: Ugletekhizdat. – 1947. – 245 p.

45. Avershin, S.G., Kuznetsov, M.A. Calculating elements of surface displacement in terms of flat seam mining // Collected papers/ AURIMS. – L.: 1948. No. 15. – 8 – 62 pp.

46. Kazakovski, D. A. On the problem of estimating rock displacement while coal mining // Collected papers/ AURIMS. – L.: 1951. – No. 14. – 3 – 11 pp.

47. Kazakovski, D. A. A value of surface subsidence while coal seam mining // Research on the problems of mine surveying / Collected papers/ AURIMS. – L.: 1951. – No. 24. – 108 – 115 pp.

48. Kazakovski, D. A. On the study of certain problems of rock displacement in coal mines // Research on the problems of mine surveying / Collected papers/ AURIMS. – L.: 1953. – No. 27. – 68 – 89 pp.

9. Lisitsa, I.G, Petruk, E.G., Chumakov, N.I., Larchenko, V.G., Voronkin, A.I. Calculating maximums of displacements and deformations of the earth's surface as a result of mining in Western Donbass // Izvestia vuzov.– Gorny zhurnal. – 1973. – No.10. – 113 – 115 pp.

50. V.I. Miakenki. Displacing and degassing coal seams rocks in the process of mining. – K: Naukova dumka. – 1975. – 99 p.

51. Cherny, G.I. Determining values of the earth's surface subsidence and deformation in the process of rock displacement in the form of rheologic stream // Izvestia vuzov.– Gorny zhurnal. – 1966. – No. 7. – 3 – 9 pp.

52. Chetverik M.S., Androshchuk, E.V. A theory of rock massif displacement and control of deformation processes while underground coal mining. – Dnipropetrovsk, “RIA Dnepr-VAL», 2004. – 148 p.

53. Babii, E.V. Dependence of displacement process parameters on parameters of flat coal seam stope. Synopsis of a thesis for Cand.Sc. {Engineering}. – Dnipropetrovsk, 2005. – 16 p.

54. Bakka, N.T., Nazarenko, V.A., Kuchin, A.S., Kashina, N.G. Graphical and analytical characterization of maximum subsidence while displacement basin forming // Academic bulletin of the NMU, 2006. – No. 9. – 3-6 pp.

55. Muller, R.A. The earth’s surface deformations, caused by underground mining, as a factor of load on structures // Collected papers of AURIMS on the problems of mine pressure and rock displacement research. – L.: 1961. – No. XLIII. 50 – 77 pp.

56. Mediantsev, A.N., Iofis, M.A. Determining rational parameters of coal protective pillars in Donbass // Exploitation of mineral deposits. – K.: 1975. – No. 40. – 40 – 43 pp.

57. Mediantsev, A.N. Maximums of the earth’s surface deformation // Proceedings on the problems of mine pressure, rock displacement, and surveying work technique. – L.: AURIMS, 1963. - No L. – 190 – 193 pp.

58. Gvirtsman, B.Y. Determining shift angles on admissible deformations of the earth’s surface // Collected papers / AURIMS. – L.: 1972. – No. 86. – 65 – 68 pp.

59. Iofis, M.A. Preliminary calculating the earth’s surface subsidence maximums // Collected papers on the problems of mine pressure and rock displacement research. – L.: AURIMS. - 1961. – No. XLIII. 105 – 111 pp.

60. Zalepukin, A.M., Yagunov, A.S. On the determining maximum subsidence angle while underground coal mining // Collected papers of AURIMS. – L.: 1972. – No. 86. – 42 – 45 pp.

61. Crutch, G. Rock displacement and protection of undermined structures. – M.: Nedra. – 1978. – 495 c.

62. Geniev, G.A. Practice of determining the earth’s surface displacements and soil stress caused by underground workings // Structural mechanics and analysis of structures. – 1977. – No 3. , 5 p.

63. Muller, R.A. On certain differential and integral properties of settling curves and horizontals of displacement basins // The earth’s surface displacement and slope stability/ Collected papers of AURIMS. – L.: 1980. – 20– 23 pp.

64. Muller, R.A. Effect on mine workings on the earth’s surface deformation. – M.: Ugletekhizdat. – 1958. – 76 p.

65. Kolbenkov, S.P. Analytical expression of standard curves of the surface displacements // Collected papers of AURIMS on the problems of mine pressure and rock displacement research. – L.: AURIMS. – 1961. – No. XLIII. 46 – 49 pp.

66. Cherniaev, V.I. Analytical method to identify initial parameters of the process of rock mass and the earth’s surface displacement and deformation // Exploitation of mineral deposits. – 1975. – No. 40. – 51 – 57 pp.

67. Iofis, M.A., Cherniaev, V.I. Analytical and experimental calculation for displacements and deformations // Izvestia vuzov. Gorny zhurnal. – 1972. – No. 11. – 56 – 59 pp.

68. Iofis, M.A., Muller, R.A., Podakov, V.F. Calculating the earth's surface deformations while erecting structures of Leningrad tube railroad // Collected papers of AURIMS. – L. – 1972. – No. 86. – 54 – 58 pp.

69. Iofis, M.A. The earth's surface displacement and protection of structures in Lvov-Volyn coal field // Ugol Ukrainy. – 1962. – No. 12. - 22 – 24 pp.

70. Knotte, S. Equation of finally shaped profile of displacement basin // Problems of calculating the earth's surface displacements due to mining. - M.: Ugletekhizdat. – 1956. – 21 –35pp.

71. Knotte, S. Time effect on displacement basin formation // Problems of calculating the earth's surface displacements due to mining. – M.: Ugletekhizdat. – 1956. – 45 – 54 pp.

72. Litvinishin, E. Differential equation of rock displacement // Problems of calculating the earth's surface displacements due to mining. – M.: Ugletekhizdat. – 1956. – 9 –20 pp.

73. Salustovich, A. Displacement basin profile as folding of layer on elastic foundation // Problems of calculating the earth's surface displacements due to mining. – M.: Ugletekhizdat. – 1956. – 36 – 44 pp.

74. Budryk, V. Determining horizontal deformations of the earth's surface // Problems of calculating the earth's surface displacements due to mining. – M.: Ugletekhizdat. – 1956. – 55 – 64 pp.

75. Muller, R.A. Calculation of rock displacement due to underground mining if flat bedding // Research on the problems of mining and surveying / Collected papers of AURIMS. – L. – 1957. – No. XXXI.- 31 – 36 pp.

76. Muller, R.A. On statistic theory of rock displacement and the earth's surface deformation caused by mining // Research on the problems of mining and surveying / Collected papers of AURIMS. – L. – 1957. – No. XXXI.- 37 – 60 pp.

77. Muller, R.A. Certain problems of statistical mechanics of soils and rocks // Mathematical methods in mining / Conference materials, part 2. – Novosibirsk. – 1963. – 193 – 209 pp.

78. Akimov, A.G., Davydovich, A. N. Experimental and analytical technique of calculating deformations within displacement basin salvage // Collected papers of AURIMS. – L.: 1972. – No. 86. – 17 – 25 pp.

79. Bosheniatov, V.E. Rules of rock displacements and deformations if deep mining // Analysis and forecast of displacements and deformations of rock massifs and hydrogeomechanical processes while underground and open-cast mining. – L.: AURIMS. – 1991. 4 – 14 pp.

80. Trifonov, A.V. On calculation of the earth's surface horizontal deformations // Exploitation of mineral deposits. – K.: Tekhnika. – 1975. – No. 40. – 49 – 51 pp.

81. Trifonov, A.V. Effect of pillarless mining on deformations of surface and structures // Rock displacement – L.: AURIMS. – 1976. – No. 100. – 44 – 49 pp.

82. Maievski, F.M., Trifonov, A.V. On the nature of the earth's surface deformations depending upon its undermining // Ugol Ukrainy. – 1974. – No. 12. – 47 – 48 pp.

83. Shalaginov, I.F. Deformations of different layers of undermined rock mass and their dependence on the distance to a seam, the seam thickness, and the working depth // Collected papers on the problems of mine pressure and rock displacement research. – AURIMS. – L.: – 1961. – No. XLIII. – 133 – 137 pp.

84. Lobanov, A.I. Effect of mined seam thickness on rock displacement of support force // Exploitation of mineral deposits. – 1964. – No. 2. – 61 – 64 pp.

85. Developing and implementing calculating procedure for time deformation of the earth's surface to improve measures of protecting structures and natural objects in Western Donbass: Research report/ The Red Banner of Labour Dnipropetrovsk Mining Institute (DMI); under the guidance of I.G. Lisitsa. – SR. No. № 76061860.- Dnipropetrovsk, 1977. – 111 p.

86. Research of rock massif stress-strain state parameters effect on mining and first mining under the conditions of "Stepnaia" mine ("Pavlogradugol" SHC). Research report / National Mining University (NMU); under the guidance of A.G. Koshka; SR. No. 0102U004377. – Dnipropetrovsk, 2003 – 132 p.

87. Development of environmentally friendly and safe practices of coal mining: Research report / National Mining University (NMU); under the guidance of V.I. Buzilo; SR. No. 0106U001371. – Dnipropetrovsk, 2007 – 161 p.

88. Development of environmentally friendly and safe practices of coal mining: Research report (final) / National Mining University (NMU); under the guidance of V.I. Buzilo; SR. No. 0106U001371. – Dnipropetrovsk, 2007 – 157 p.

89. Creep of sedimentary rocks (theory and experiment) / Z.S. Erzhanov, A.S. Saprygin, G.N. Gumeniuk et al. Alma-Ata: Nauka, 1970. – 208 p.

90. Stavrogin, A.G., Protosenia, A.G. Rock plasticity, 1979.- 301 p.

91. Cook H.G.W., Hoek E. Rock mechanics Appyling to the Study of Kockbursts: - J. of the South A.J. of Min. and Met., 1966, p. 435 – 528.

92. Shashenko, A.N., Pustovoitenko, V.P. Rock mechanics: University textbook. – K.: Novy druk, 2004. – 400 p.

93. Smirnov, V.I. Higher mathematics course. – Vol. 2. – M.: Gostekhizdat, 1951. – 655 p.

94. L. V. Novikova, L. Zaslavskaya, A. Yavorsky. The earth's surface deformations caused by underground mining // Materials of international conference "Forum gorniakov - 2005". – D.: National Mining University, 2005. – 198 – 200pp.

95. L. Novikova, L. Zaslavskaya, A. Yavorsky Definition of stiffness coefficient of undermined non-uniform stratified mass / of NMU, 2006, № 5. – p. 32-35.

96. Novikova, L.V., L. Zaslavskaya, A. Yavorsky Stiffness assessment of stratified rock mass enclosing rocks // Scientific bulletin of the NMU. – 2006. – No. 9. – 7 – 8 pp.

97. Novikova, L.V., L. Zaslavskaya, A. Yavorsky Determining the earth's surface deformations in terms of two-layer medium model /Materials of

international conference “Forum gorniakov - 2006”. – Dnipropetrovsk: National Mining University, 2006.- 106-112 pp.

98. A. Yavorsky. Effect of advance rate on a subsidence rate of layer rock mass/ Rock mechanics: Interdepartmental collection of scientific papers/ M.S. Poliakov Institute of Rock Mechanics of the National Academy of Sciences of Ukraine. – Dnipropetrovsk, 2006. – Publ. 65. – 178 – 183 pp.

99. Novikova, L.V., L. Zaslavskaya, A. Yavorsky Identifying deformations of the earth’s surface of undermined massif by boundary-element method / Rock pressure problems. Collection of scientific papers. – Donetsk: DonNTU, 2006.- Publ. 14. –222-231 pp.

100. Novikova, L.V., L. Zaslavskaya, A. Yavorsky Analyzing stress state of undermined massif and identifying load acting on powered support // Eastern European Periodical of Advanced Technologies.-2007.-No.3/5(27).- 38-44 pp.

101. Novikova, L.V L. Zaslavskaya, A. Yavorsky Stress-strain state of two-layered undermined massif / Collection of scientific papers. International theoretical and practical conference “School of underground mining”, 17-22 September, 2007, Dnipropetrovsk, NMU, 358-368 pp.

102. Novikova, L.V L. Zaslavskaya, A. Yavorsky Determining movements of undermined massif taking into consideration advance rate / Materials of international conference “Forum gorniakov - 2007” (11 – 13 October, 2007).– Dnipropetrovsk, National Mining University, 2007. 63-67 pp.

103. Novikova, L.V., L. Zaslavskaya, A. Yavorsky Dependence of the earth’s surface subsidence and stresses in two-layered undermined massif / Abstracts of reports of International scientific and technical conference in memory of Academician of the National Academy of Sciences of Ukraine V.I. Mossakovski. – D.: Dnipropetrovsk National University, 2007.- 349-350 pp.

104. Novikova, L.V., L. Zaslavskaya, A. Yavorsky Stress-strain state of rock mass and the earth’s surface of undermined two-layered massif “capping-carbon” // Materials of international conference “Forum gorniakov - 2008". – Dnipropetrovsk: printing and publications centre of the NMU, 2008. part 2. – 119 –130 pp.

105. A. Yavorsky, E. Yavorskaya Calculation of the deformation of the earth's surface by means of an analytical solution of a plane problem of geomechanics / Rock mechanics: Interdepartmental collection of scientific papers/ M.S. Poliakov Institute of Rock Mechanics of the National Academy of Sciences of Ukraine. – Dnipropetrovsk, 2012. – Publ. 103. – 259 – 268 pp.

CONTENT

Наукове видання

Яворський Андрій Васильович
Яворська Олена Олександрівна
Кошка Олександр Григорович
Токар Лариса Олександрівна
Сердюк Володимир Петрович

НАПРУЖЕНО-ДЕФОРМОВАНИЙ СТАН ПОРОДНОГО МАСИВУ ПРИ ВІДПРАЦЮВАННІ ПОЛОГОГО ВУГІЛЬНОГО ПЛАСТА ПІД ОХОРОНЮВАНИМИ ОБ'ЄКТАМИ

Монографія

(Англійською мовою)

Друкується в редакційній обробці авторів.

Підп. до друку 25.02.2014. Формат 30х42/4.
Папір офсетний. Ризографія. Ум. друк. арк. 6,2.
Обл.-вид. арк. 6,2. Тираж 300 пр. Зам. №

Підготовлено до друку та видрукувано
у Державному ВНЗ «Національний гірничий університет».
Свідоцтво про внесення до Державного реєстру ДК № 1842 від 11.06.2004

49005, м. Дніпропетровськ, просп. К. Маркса, 19.